

ABSTRACT

Title of Dissertation: GENETIC REGULATION OF AUTOPHAGIC CELL DEATH IN
DROSOPHILA MELANOGESTER.

Sudeshna Dutta, Doctor of Philosophy, 2008

Dissertation directed by: Dr. Eric H. Baehrecke
Center for Biosystems Research
University of Maryland Biotechnology Institute
University of Maryland, College Park, MD

Department of Cancer Biology
University of Massachusetts Medical School
Worcester, MA

Apoptosis and autophagic cell death are the two most prominent morphological forms of programmed cell death that occur during animal development. While much is known about the mechanisms that regulate apoptosis, relatively little is known about autophagic cell death. The steroid hormone ecdysone coordinates

multiple cellular processes during metamorphosis in *Drosophila*, including cell differentiation, morphogenesis and death. *E93* is necessary and sufficient for larval tissue cell death during metamorphosis, including autophagic cell death of salivary glands. Here we characterize new mutant alleles of a dominant wing vein mutation *Vein-off* (*Vno*), and provide evidence that *E93* and *Vno* are related. Our data also indicate that *E93* functions in steroid regulation of both cell development and death during metamorphosis. *E93* encodes a helix-turn-helix DNA binding motif and binds to specific regions of salivary gland polytene chromosomes. We have used genetic and genomic approaches to identify downstream targets of *E93*. We have identified numerous candidate *E93* target genes using DNA microarrays, and have generated transgenic animals to identify downstream target genes of *E93* by chromatin immune precipitation. We show that one putative *E93* target gene, *hippo* (*hpo*), is required for salivary gland cell death. The *Wts/Hpo* tumor-suppressor pathway is a critical regulator of tissue growth in animals, but it is not clear how this signaling pathway controls cell growth. Our data indicate that salivary gland degradation requires genes in the *Wts/Hpo* pathway. *Wts* is required for cell growth arrest and autophagy in dying salivary glands, and regulates the degradation of this tissue in a PI3K-dependent manner.

GENETIC REGULATION OF AUTOPHAGIC CELL DEATH IN
DROSOPHILA MELANOGESTER

by

Sudeshna Dutta

Dissertation submitted to the Faculty of the Graduate School of the
University of Maryland, College Park in partial fulfillment of the
requirements for the degree of

Doctor of Philosophy

2008

Advisory Committee:

Professor Eric H. Baehrecke, Chair/Advisor

Professor Stephen M. Mount

Professor Judd O. Nelson

Professor Leslie Pick

Professor Louisa Wu

Dedication

To my parents Late Benoy Bhusan Dutta and Indira Dutta, and aunt Arati Dutta.

Acknowledgement

I would like to specially thank my advisor Dr. Eric H. Baehrecke for his support, guidance and advice throughout my graduate school years. I consider myself extremely fortunate to have him as my Ph.D mentor. I would always be grateful for what he has done for me. My cordial thank to my committee member and MOCB program director Dr. Leslie Pick for her guidance and support. I am also grateful to my other committee members: Dr. Louisa Wu for her suggestions and encouragements, Dr. Stephen Mount for his guidance and advice, and Dr. Judd Nelson for agreeing to be my Dean's representative and his support.

I am grateful to my former and current laboratory members for making the laboratory a great working environment. My special thanks go to Dr. Deb Berry, for being a constant source of encouragement as a scientist. I am grateful to her for all her advice and support. I am also thankful to Dr. Damali Martin for sharing her lab experience with me. I would also like to thank my present and former lab members for their help, support and friendship-Yakup Batlevi, Jahda Hill, Christina McPhee, Rachel Simin, Gautam Das, Bhupendra Shrivage, Tina Fortier, Kirsten Tracy, Ajjai Alva, Alvaro Godinez, Cheng-Yu Lee.

I would also like to thank our collaborators Dr. Ian Duncan, Dr. Cheng Lee and Dr. Brian Balgley, for their help with my projects. Also my special

thanks go to others that sent fly stocks and antibodies to me, including K. Irvine, G. Halder, A. Bergmann, S. Cohen, B. Edgar, M. Freeman, B. Hay, T. Neufeld, D. Pan, and the Bloomington Stock center, the VDRC Stock Center, and the Developmental Studies Hybridoma Bank for flies and antibodies. Thanks also to Tim Mangel for training me with SEM and TEM techniques.

My special thanks go to my family and friends for their constant support and encouragement. I am indebted to my parents, Late Benoy Bhusan Dutta and Indira Dutta, my aunt Arati Dutta and sister Dr. Suparna Dutta for always encouraging me for higher studies and also for installing the importance of hard work in me. I am also grateful to my friends Abbhi, Ashok, Deena, Shalini and Uma for always being there for me and making these long time an enjoyable one. Finally, thanks to my husband and best friend Amlan, for his constant support, encouragement and patience through all these years. Without his support it would not have been possible for me to complete my doctoral studies. Amlan's constant support and encouragement have made crucial years of my doctoral studies an enjoyable one.

TABLE OF CONTENTS

List of Tables	viii
List of Figures	ix
List of Abbreviations	xi
Chapter 1: Introduction	
1.1: Significance of cell growth, survival and cell death	1
1.2: Forms of programmed cell death	1
1.3: Genetic regulation of apoptosis	2
1.4: Autophagy	6
1.5: Regulation of cell growth	10
1.6 Warts/Hippo signaling pathway	13
1.7 Salivary gland model of autophagic cell death	17
Chapter 2: Characterization of the relationship between <i>E93</i> and <i>Vno</i>	
2.1 Abstract	22
2.2 Introduction	22
2.3 Results	26
Identification of new <i>Vno</i> alleles	26
<i>Vno</i> mutants influence salivary gland degradation	31
Ectopic expression of <i>Vno</i> is sufficient to induce premature salivary gland cell death	36
<i>vno</i> functions in eye cell death	38
2.4 Discussion	40

2.5 Materials and Methods	42
Chapter 3: Identification of targets of E93	44
3.1 Abstract	44
3.2 Introduction	44
3.3 Results	47
E93 encodes a conserved DNA-binding protein	47
Identification of Hpo as a E93 target that functions in salivary gland cell death	60
Development of approaches to identify E93 targets	62
3.4 Discussion	68
3.5 Materials and Methods	70
Chapter 4: Warts is required for PI3K-regulated growth arrest, autophagy and autophagic cell death in <i>Drosophila</i>	73
4.1 Abstract	73
4.2 Introduction	74
4.3 Results	77
Wts, Sav and Mats are required for salivary gland degradation	77
<i>wts</i> influences caspase activity, autophagy and cell growth	81
Expression of Bantam, but not Yki and Sd, phenocopies <i>wts</i> in salivary glands	89
PI3K signaling is required for <i>wts</i> to inhibit	

cell death	98
4.4 Discussion	103
4.5 Materials and Methods	106
Chapter 5: Conclusions and future directions	110
5.1 Revised model for genetic regulation of autophagic cell death of <i>Drosophila</i> salivary glands	115

List of Tables

Table 1: Cell death genes are conserved in diverse organisms	5
Table 2: The percent of pupae with salivary gland phenotype	35
Table 3: Candidate E93 target genes	50-56
Table 4: Candidate genes to be verified by Chromatin immunoprecipitation	57-58

List of figures

Figure 1: The apoptotic pathway is conserved in worms, flies and mammals	3
Figure 2: Genetic regulation of autophagy	9
Figure 3: Simplified model of the Insulin/PI3K pathway	12
Figure 4: Existing model of Wts/Hpo signaling pathway	16
Figure 5: Model for ecdysone regulated salivary gland responses during metamorphosis	20
Figure 6: Molecular characterization of <i>vno</i> mutants	28
Figure 7: <i>Vein-off</i> wing vein phenotypes	30
Fig 8: Trans-heterozygous <i>vno</i> mutants have salivary gland autophagic cell death defects	33
Fig 9: Ectopic-expression of <i>vno</i> is sufficient to cause premature degradation of salivary glands	37
Figure 10: <i>vno</i> causes cell death defects in developing eyes	39
Figure 11: Alignment of the putative DNA binding helix-turn-helix motif of E93	48
Figure 12: <i>hpo</i> is required for salivary gland cell death	61
Figure 13: Expression of E93 induces caspase-dependent eye cell death	64
Figure 14: Ectopic expression of Myc-tagged E93 is sufficient to induce salivary gland cell death	67
Figure 15: Wts signaling pathway is active and required for salivary gland degradation	80

Figure 16: Caspases are reduced in <i>wts</i> mutants, and DIAP1-induced inhibition of salivary gland degradation is enhanced by reduced Atg1 function	83
Figure 17: Autophagy is decreased in <i>wts</i> mutants, and expression of Atg1 rescues <i>wts</i> salivary gland persistence	85
Figure 18: <i>wts</i> mutant salivary gland cells fail to arrest growth at pupariation	87
Figure 19: Expression of Yki and Sd fail to phenocopy the <i>wts</i> salivary gland phenotype, and DIAP1 levels are not altered in <i>wts</i> mutants	91
Figure 20: Co-Expression of Yki and Sd induces premature degradation of salivary glands	93
Figure 21: <i>bantam</i> mis-expression inhibits salivary gland degradation in a PI3K-independent manner	96
Figure 22: Wts regulates growth in a PI3K pathway-dependent manner	100
Figure 23: <i>wts</i> mutants do not have altered Akt and P-Akt protein levels in salivary glands	102
Fig 24: Model for autophagic cell detach in salivary glands	117

List of Abbreviations

Ecdysone	20-Hydroxyecdysone
APF	After puparium formation
ATG	Autophagy genes
ChIP	Chromatin immunoprecipitation
Crq	Croquemort
EcR	Ecdysone Receptor
EMS	Ethane Methyl Sulfonate
Ex	Expanded
GMR	glass multimer reporter
Hid	Head involution defective
Hpo	Hippo
IAP	Inhibitor of Apoptosis
Me	Merline
PI3K	Phosphoinositide 3-kinase
Rpr	Reaper
Sav	Salvador
Sd	Scalloped
tGPH	tubulin-GFP-Pleckstrin Homology
TOR	Target of Rapamycin
TUNEL	Terminal deoxynucleotidyl transferase dUTP nick end labeling
Usp	Ultraspiracle

Vno

Vein-off

Wts

Warts

Yki

Yorkie

Chapter 1

Introduction

1.1 Significance of cell growth, survival and cell death

Cell growth, cell division and cell death are important determinants of cell and organ size and also tissue homeostasis (Conlon and Raff, 1999). Disruption in the crucial balance between cell growth, division and death can cause a variety of disorders including cancer and neurodegenerative diseases (Thompson, 1995). While the relationship between the cell cycle and cell death has been intensely studied, the relationship between cell growth and cell death is not that well characterized.

1.2 Forms of programmed cell death

Programmed cell death was initially defined as a series of events that finally leads to the death of a cell (Lockshin and Williams, 1965). This descriptive definition of programmed cell death was validated when it was shown that genes are required for this process, and that they can be placed into an order of action based on genetic epistasis analyses (Ellis and Horvitz, 1986). Morphological studies of dying cells in developing vertebrate embryos resulted in the classification of three types of physiological cell death on the basis of location, morphology and dependence on lysosomes (Schweichel and Merker, 1973). The first type is widely known as apoptosis, and usually occurs in isolated dying cells. Activation of caspases, fragmentation of DNA, cytoplasmic blebbing and engulfment of the dying cell by a phagocyte are the hallmarks of apoptotic cell death (Clarke, 1990; Kerr et al., 1972). The second morphological form of cell death

is known as autophagic cell death, and usually occurs when a group of cells or entire tissues are destroyed (Clarke, 1990). Autophagic cell death is associated with the formation of autophagosomes and self-digestion of cytoplasmic components, including organelles, in absence of phagocytes. The third morphological type is known as non-lysosomal cell death, and is characterized by swelling of cavities with membrane borders, followed by degeneration without lysosomal activity.

1.3 Genetic regulation of apoptosis

Apoptosis is a conserved process that plays an important role during animal development and tissue morphogenesis by destroying and removing unwanted cells and tissues (Baehrecke, 2002; Jacobson et al., 1997; Raff, 1992). Genetic studies of programmed cell death in the nematode *Caenorhabditis elegans* led to the discovery of the core cell death genes *ced-3*, *ced-4*, and *ced-9* (Ellis and Horvitz, 1986) (Figure 1). *Ced-3* is the homologue of mammalian caspases which are cysteine proteases (Alnemri et al., 1996; Villa et al., 1997). Proteolytic cleavage of caspases plays an important role during mammalian programmed cell death (Cryns and Yuan, 1998). *Ced-4* is the homologue of mammalian Apaf-1, which is a caspase-9 cofactor in the presence of cytochrome c and ATP, and this complex is commonly known as the apoptosome (Li et al., 1997; Rodriguez et al., 1999; Zou et al., 1997). *Ced-9* is a member of the BCL-2 family of the cell death regulators (Hengartner and Horvitz, 1994; Vaux et al., 1992). Bcl-2 family proteins were initially characterized as pro-apoptotic that impact Apaf-1 activity, but the exact mechanism of action remains unclear (Adams and Cory, 1998; Levine and Kroemer, 2008).

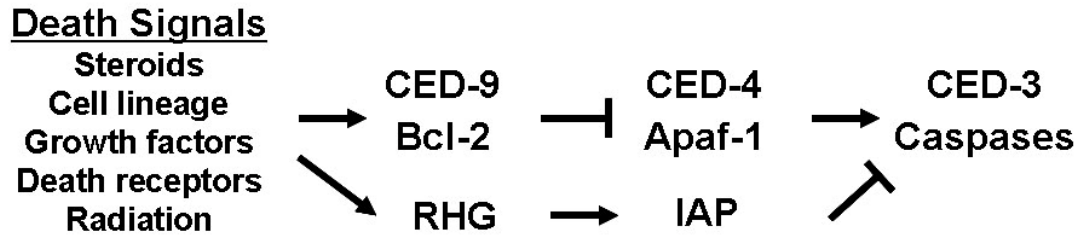





Figure 1. The apoptotic pathway is conserved in worms, flies and mammals.

Programmed cell death is activated by many stimuli including steroid hormones, cell-lineage information, growth factors, membrane-bound death receptors, and DNA damage induced by radiation. CED-9 (Bcl-2) inhibits activation of CED-3 (Caspases) by binding to CED-4 (Apaf-1). Death signals release CED-4 and cause activation of CED-3, a caspase that regulates apoptosis. In flies, Reaper, Hid and Grim (RHG) proteins interact with IAPs and prevent IAPs from inhibiting caspases so that they can activate apoptotic cell death.

Drosophila contains apoptosis factors that are conserved in organisms that are as different as worms and humans (Abrams, 1999; Aravind et al., 2001) (Table 1). Seven caspases are present in *Drosophila*. Dredd, Dronc and Dream/Strica are apical caspases and Drice, Daydream, Decay and Dcp-1 are effector caspases (Chen et al., 1998; Dorstyn et al., 1999a; Fraser and Evan, 1997; Song et al., 1997; Vernooy et al., 2000). In *Drosophila*, the only Ced-4/Apaf-1 homologue Ark, is required for the activation of Caspase-9 –like homologue Dronc (Dorstyn et al., 1999b; Kanuka et al., 1999; Rodriguez et al., 1999; Zhou et al., 1999). The inhibitors of apoptosis (IAP) Diap1 and Diap2 are the known caspase inhibitors in *Drosophila* (Hay et al., 1995). The cell death inducer genes *head involution defective (hid)*, *reaper (rpr)*, *grim* and *sickle* have also been identified and molecularly characterized (Chen et al., 1996; Grether et al., 1995; White et al., 1994). Ectopic expression of each of these genes is sufficient to induce caspase-dependent programmed cell death (Chen et al., 1996; Grether et al., 1995; Hay et al., 1995; White et al., 1996). Whereas, removal of these three genes by using ~300 kb deletion *Df(3L)H99* in *Drosophila* blocks programmed cell death (White et al., 1994). Genetic studies have indicated that *rpr*, *hid*, *grim* and *sickle* activate caspases by inhibiting DIAP1 and this is similar to the interaction between mammalian Omi/Htra2 and Smac/Diablo with XIAP (Hay et al., 1995; Liu et al., 2000; Srinivasula et al., 2002; Wu et al., 2000; Yoo et al., 2002). *Rpr*, *Hid*, *Grim* and *sickle* contain limited but critical sequence homology with mammalian Smac/Diablo and Omi/Htra2 (Liu et al., 2000; Wu et al., 2000). While the mechanisms that mediate apoptotic cell death are relatively well known, little is known about the regulation of autophagic programmed cell death.

Table 1. Cell death genes are conserved in diverse organisms

Gene Family	Worm 	Fly 	Mammals 
Caspases	Ced-3	Dredd, Dronc, Dream/Strica, Dcp-1, Drice, Decay Daydream/Damm	Caspases 1-14
Bcl-2	Ced-9	Debcl-1/Drob-1/Dborg-1/Dbok, Buffy/Dborg-2	Bcl-2, Bcl-x, Bcl-w, Mcl-1, Al, Diva, Bax, Bak, Bok, Bik, Bid, Bad, Hrk, Bim, Bnip, Bix
Apaf-1	Ced-4	Ark/Dark/Hac-1/dApaf-1	Apaf-1
Iap	Bir-1, Bir-2	Diap-1, Diap-2, Bruce, Deterin	Xiap, C-iap-2, C-ap-2, hIip-2, Mliap, Naip, Survivin, Bruce
RHG	?	Rpr, Hid, Grim, Sickie, Jafrac	Smac/Diablo, Omi/HtrA2

(Adapted from Baehrecke, 2002)

1.4 Autophagy

Autophagy is a catabolic process that delivers substrates to the lysosome for degradation. While the ubiquitin-proteasome system is involved in the destruction of short-lived proteins, autophagy is used for sequestration of long-lived proteins and cytoplasmic components in the lysosome (Klionsky and Emr, 2000). Although three forms of autophagy have been described, only macroautophagy (hereafter referred to as autophagy) has been associated with autophagic programmed cell death (Baehrecke, 2002; Reggiori and Klionsky, 2002). Macroautophagy involves the formation of isolation membranes that enclose cytoplasmic cargo to form autophagosomes, that fuse with lysosomes where hydrolases degrade their cargo (Klionsky, 2007).

Screens for genes that are required for the formation of autolysosomes and lysosomal degradation of substrates resulted in the discovery of the core genes that are required for autophagy (Scott et al., 1996; Thumm et al., 1994; Tsukada and Ohsumi, 1993). The mechanisms that regulate autophagy have been best characterized in the yeast *Saccharomyces cerevisiae* (Klionsky and Emr, 2000; Ohsumi, 2001). Under nutrient-limiting conditions, autophagy is induced in yeast as a survival mechanism. Autophagy is regulated by the class I and class III phosphatidylinositol 3-kinase (PI3K) signaling pathways in *Drosophila* and other higher organisms (Petiot et al., 2000) (Figure 2). TOR (Target of Rapamycin), a member of the class I PI3K pathway inhibits autophagy under nutrient rich conditions by influencing Atg1 kinase (Kamada et al., 2000; Matsuura et al., 1997). The class III PI3K/Vps34 signaling complex that contains Vps15 and Atg6 (known as Beclin1 in mammals) positively regulates the formation of isolation

membranes from the pre-autophagosomal structure by regulating two ubiquitin-like conjugation pathways (Kihara et al., 2001; Kim et al., 1999; Liang et al., 1999). Atg 8 (LC3 in mammals) and Atg12 ubiquitin-like conjugation pathways are required for autophagosome formation (Kabeya et al., 2000; Reggiori and Klionsky, 2002). Atg 4 encodes a cysteine protease that cleaves Atg8. This proteolysis is essential to expose a conserved carboxy-terminal glycine of Atg8 and its lipidation (Kirisako et al., 2000). Atg8 and Atg12 are conjugated with the E1-like protein Atg7, and then get transferred to the E2-like proteins Atg3 and Atg10 respectively (Mizushima et al., 1998; Shintani et al., 1999). Atg12 associates with the Atg5 and Atg16 protein on forming isolation membranes (Mizushima et al., 2003; Suzuki et al., 2001). Although it is not completely clear what the Atg12/Atg5/Atg16 complex does, it has been speculated that it facilitates membrane bending and assembly during autophagosome formation since this complex disassociates once autophagosomes form. By contrast, Atg8 is conjugated to the lipid phosphatidylethanolamine, and is associated with both isolation membranes and autophagosomes until fusion with lysosomes (Ichimura et al., 2000).

Autophagy functions in multiple processes in higher animals, including *Drosophila*, such as nutrient recycling during starvation (Rusten et al., 2004; Scott et al., 2004), host defense during bacterial infection (Yano et al., 2008), and programmed cell death during development (Berry and Baehrecke, 2007). Previous studies have demonstrated that flies with mutations in either *atg8* or *atg18* and flies expressing a dominant negative form of Atg1, fail to induce autophagy (Scott et al., 2007; Scott et al., 2004). In addition, recent studies in *Drosophila* have shown that the autophagy genes

atg2, *atg3*, *atg6*, *atg7*, *atg8*, *atg12* and *atg18* are required for proper degradation of salivary gland cells (Berry and Baehrecke, 2007). The basic mechanism of autophagy is similar in yeast and other higher organisms (Mizushima, 2007). One difference in multicellular organisms is that autophagy is regulated by components of insulin/class I phosphoinositide 3-kinase (PI3K) pathway (Arico et al., 2001; Petiot et al., 2000). In *Drosophila*, for example, starvation induces autophagy in larval fat body that is mediated by components of the class I PI3K pathway including Akt, PTEN, TSC1, TSC2, TOR and also conserved components of Atg machinery (Scott et al., 2004). It is not clear if this pathway always influences autophagy in all tissues, and under all cellular contexts in higher animals, but in *Drosophila* the class I PI3K pathway regulates autophagy in both fat and salivary glands (Neufeld and Baehrecke, 2008).

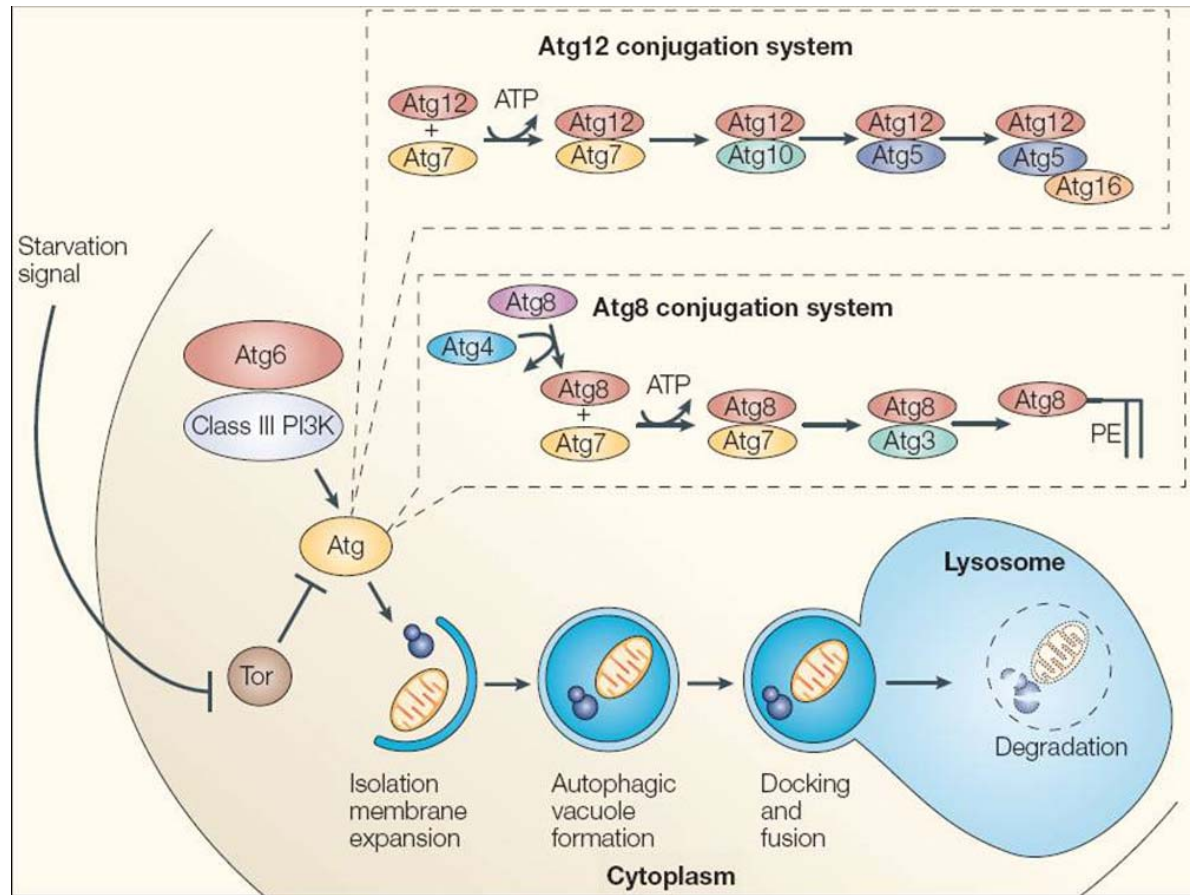


Figure 2. Genetic regulation of autophagy. Autophagy degrades components of the cytoplasm by the formation of an isolation membrane around cytoplasmic cargo, forming the autophagic vacuole that docks and fuses with the lysosome, followed by degradation of the cargo by lysosomal hydrolases. Starvation triggers autophagy by modulating TOR signaling. TOR inhibits autophagy by modulating *atg* genes that are required for autophagic vacuole formation. Class III PI3K, Atg6 (Beclin 1) and Atg8 and Atg12 ubiquitin-like conjugation systems are critical regulators of autophagic vacuole formation. This figure is adapted from Baehrecke, 2005.

1.5 Regulation of cell growth

The insulin/class I PI3K/TOR signaling pathway is well established as a regulator of cell growth, and also contains potent oncogenic activators (Kozma and Thomas, 2002).

Nutrient availability triggers the production of insulin-like growth factors by neurosecretory cells in the brain, and then these secreted growth factors are transported by the circulatory system to their target cells where they are bound by the insulin receptor (InR) (Fernandez et al., 1995). Binding of insulin to the insulin receptor leads to its autophosphorylation and subsequent phosphorylation of the insulin receptor substrate proteins (IRS) (Chico in flies) (Bohni et al., 1999) (Figure 3). This leads to the activation of the catalytic subunit of class I PI3K pathway Dp110 (Leevers et al., 1996). Activated Dp110 converts phosphatidylinositol-4, 5-P (2) (PIP2) to the second messenger phosphatidylinositol-3, 4, 5-P (3) (PIP3), and thereby activates AKT/protein kinase B (PKB) (Rameh and Cantley, 1999). The lipid phosphatase PTEN is a negative regulator of the PI3K pathway that converts PIP3 to PIP2 (Gao et al., 2000; Goberdhan et al., 1999; Huang et al., 1999). In the PI3K signaling cascade, the cytoplasmic protein kinases Akt/PKB contains a phosphoinositide-interacting domain known as the pleckstrin homology (PH) domain. When the PI3K pathway gets activated, PH domains bind to PIP3 on the plasma membrane and activates downstream kinase signaling cascade (Lietzke et al., 2000; Oatey et al., 1999). Active phosphorylated Akt modulates growth by regulating the Target Of Rapamycin (TOR) pathway via the tuberous sclerosis complex (TSC). The TSC1 and TSC2 complex functions to activate the GTPase Rheb (*Ras homolog enriched in brain*) that is a positive regulator of growth (Gao X, 2001; Saucedo et al., 2003; Stocker et al., 2002). Rheb regulates the conserved TOR kinase that

is a central component of the nutrient sensing mechanism in multicellular organisms. TOR mediates a wide variety of processes including cell growth, protein translation, metabolism, autophagy and others (Arsham and Neufeld, 2006; Scott et al., 2004). In mammalian cells, the translational activity of TOR culminates by regulating ribosomal protein S6K and the translational repressor 4E-BP1 (Raught et al., 2004).

The influence of the class I PI3K signaling pathway is clearly demonstrated by the analyses of mutant phenotypes. In *Drosophila*, mutations in components of the insulin signaling cascade, including *InR*, *chico*, *Akt/PKB*, and *PDK1(3-phosphoinositide-dependent protein kinase-1)*, give rise to developmentally delayed and smaller flies due to decrease in cell number and cell size (Bohni et al., 1999; Brogiolo et al., 2001; Rintelen et al., 2001). S6K mutant flies also have reduced body size like other members of *Inr* pathway, but these flies have decreased cell size, without reduction in cell number (Montagne et al., 1999). In humans, loss of the tumor-suppressor gene PTEN is observed in endometrial cancers and glioblastomas (Sulis and Parsons, 2003). Tuberous sclerosis complex (TSC) is an autosomal–dominant disorder in human characterized by the formation of benign tumors in various tissues (Pan et al., 2004). Significantly, mutations in Akt and p110 are among the most common genetic alterations in breast and colon cancer (Wood et al., 2007).

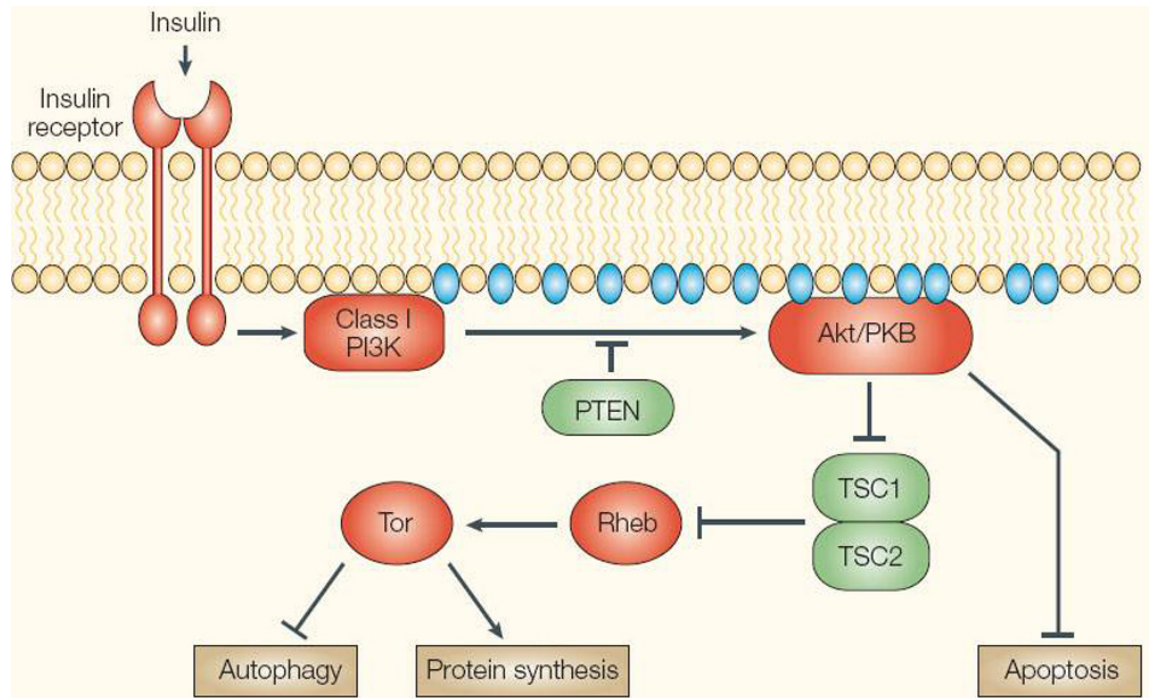


Figure 3. Simplified model of the Insulin/PI3K pathway. The insulin induced class I PI3K signaling pathway regulates growth by influencing autophagy, protein synthesis and apoptosis. Positive regulators of autophagy (green) in this pathway include PTEN, TSC1 and TSC2. Whereas, negative regulators of autophagy (red) include insulin receptor, PI3K/DP110, Akt/PKB, Rheb, Tor. Blue color indicates modified PIP3 lipids. This figure is adapted from Baehrecke, 2005.

1.6 Warts/Hippo signaling pathway

Recent genetic studies in *Drosophila* have unveiled the Warts (Wts) / Hippo (Hpo) tumor-suppressor pathway as an important regulator of tissue growth in animals (Fig 4: *Drosophila* Wts signaling Pathway). The core components of this pathway are conserved in mammals and their deregulation has been linked to cancer (Edgar, 2006). Wts, also known as the Large tumor suppressor (Lats), encodes a kinase of the nuclear Dbf-2 related (NDR) family, and was the first component to be identified in this tumor suppressor pathway (Justice et al., 1995; Xu et al., 1995). *wts* homozygous mutant animals exhibit a dramatic tissue over-growth phenotype in a variety of fly epithelial tissues (Justice et al., 1995; Xu et al., 1995). Subsequent screens for genes that regulate tissue growth resulted in the isolation of additional members of the Wts signaling pathway. Fat, Merlin (Mer), Expanded (Ex), Hpo, Salvador (Sav) and Mats are members of this kinase cascade that have a strikingly similar overgrown phenotype when they are clonally deleted in developing eye and wing tissues in developing *Drosophila* (Bennett and Harvey, 2006; Cho et al., 2006; Hamaratoglu et al., 2006; Harvey et al., 2003; Kango-Singh et al., 2002; Lai et al., 2005; Pantalacci et al., 2003; Silva et al., 2006; Tapon et al., 2002; Udan et al., 2003; Willecke et al., 2006; Wu et al., 2003). The Ste-20/MST2 family protein kinase Hpo along with the WW-repeat protein Sav phosphorylates and activates Wts (Harvey et al., 2003; Pantalacci et al., 2003; Tapon et al., 2002; Udan et al., 2003; Wu et al., 2003). The Mob superfamily protein Mats (Mob as tumor suppressor) physically interact with Wts to stimulate its kinase activity (Lai et al., 2005).

These genes negatively influence the cell cycle regulator Cyclin E to restrict cell proliferation, and negatively regulate the *Drosophila* inhibitor of apoptosis protein DIAP1 to promote apoptosis, to facilitate the appropriate final size of tissues. Therefore, recessive mutations in this pathway result in excess cell division and decreased cell death, resulting in over-grown tissues.

Yorkie (Yki) is a downstream effector of the Wts/Hpo signaling cascade that is a positive regulator of tissue growth (Huang et al., 2005). Yki is the *Drosophila* ortholog of YAP (Yes-associated protein) in mammals and has been characterized as a non-DNA binding transcriptional coactivator (Yagi et al., 1999). In *Drosophila*, Wts phosphorylates and inactivates Yki by exclusion from the nucleus in a Hpo/Sav-dependent manner (Dong et al., 2007; Huang et al., 2005; Oh and Irvine, 2008). Over-expression of Yki recapitulates the tissue over-growth phenotype of loss-of-function mutations in members of the Wts/Hpo signaling pathway (Dong et al., 2007; Huang et al., 2005). Yki interacts with the TEAD/TEF family DNA-binding transcription factor Scalloped (Sd) to regulate transcription of *diap1* (Wu et al., 2008; Zhang et al., 2008), and presumably other downstream targets of the Wts signaling pathway, including cell cycle regulator *cyclin E* and cell growth regulator microRNA *bantam* (Harvey et al., 2003; Nolo et al., 2006; Pantalacci et al., 2003; Thompson and Cohen, 2006; Udan et al., 2003; Wu et al., 2003). Sd directly binds to Yki and forms a transcriptional complex to regulate Wts-pathway responsive genes. Sd overexpression enhances whereas inactivation decreases the overgrowth phenotype that is induced by Yki (Wu et al., 2008; Zhang et al., 2008). The inactivation effect of Sd indicates that requirement of Sd may

vary according to cell type (Zhang et al., 2008). Sd was initially identified as a DNA-binding partner of Vestigial (Vg), a gene required for wing formation (Halder et al., 1998). Sd and Vg together regulate the transcription of target genes involved in wing pattern formation (Halder et al., 1998). It is not clear how Sd select different binding sites and target genes.

The microRNA (miRNA) *bantam* has also been identified as a key downstream target of Wts/Hpo/Yki signaling pathway (Nolo et al., 2006; Thompson and Cohen, 2006). miRNAs are small RNAs of usually 21-23 nucleotides long that direct posttranscriptional regulation of its target genes expression (Ambros, 2001). *bantam* was identified in a gain-of-function genetic screen in *Drosophila* to identify tissue growth regulators (Hipfner et al., 2002). Tissues that overexpress *bantam* are larger than wild-type tissues. Conversely, a loss-of-function mutation of *bantam* gives rise to smaller than normal animals (Brennecke et al., 2003; Hipfner et al., 2002). *bantam* also influences apoptosis during development by inhibiting translation of the pro-apoptotic gene *hid* (Brennecke et al., 2003). Although *bantam*, and other components of the Wts/Hpo pathway, influence tissue and animal size, it is not completely clear how they influence cell growth that is a key requirement of increased cell division and, therefore, tissue growth control.

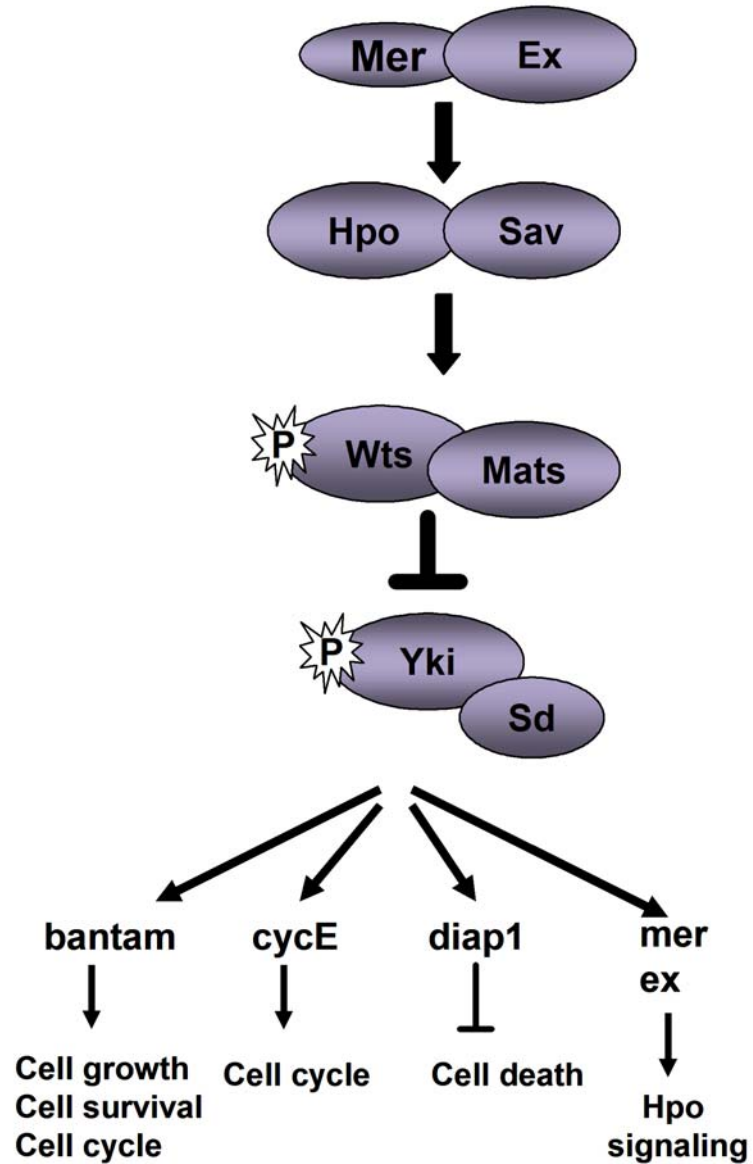


Figure 4. Existing model of Wts/Hpo signaling pathway. In response to some unknown signal, plasma membrane proteins Mer and Ex interact with each other and activate downstream Wts/Hpo signaling pathway. Hpo with the help of Sav phosphorylates and activates Wts. Wts physically interacts with Mats and phosphorylates and inhibits Yki. Yki transcriptionally regulates downstream target genes *cycE*, *bantam*, *mer* and *ex*. Yki also interacts with Sd to regulate transcription of *diap1*.

1.7 Salivary gland model of autophagic cell death

Drosophila larval salivary glands provide an ideal in vivo model system to study steroid regulated developmental autophagic cell death. *Drosophila* is one of the most extensively studied higher eukaryotic model organisms. The highly conserved and molecularly well characterized genome of *Drosophila*, along with its relatively short generation time, provides an excellent opportunity to do molecular and genetic analysis (Rubin and Lewis, 2000).

Steroid hormones regulate various biological processes, such as growth, development, metabolism, and reproduction, in higher eukaryotes. Components of the steroid signaling pathway are conserved between *Drosophila* and vertebrates (Thummel, 1995). 20-hydroxyecdysone (ecdysone) is the only biologically active steroid hormone present at physiologically active titers in *Drosophila*. A pulse of ecdysone at the end of larval development triggers growth arrest and the onset of metamorphosis that is marked by puparium formation. This pulse of ecdysone initiates the morphogenesis of adult structures and also causes destruction of the larval midgut and larval muscles (Jiang et al., 1997). The subsequent pulse of ecdysone 10-12 hours after puparium formation causes the prepupal-pupal transition that is marked by eversion of the future adult head (Sliter and Gilbert, 1992), and triggers larval salivary gland programmed cell death (Jiang et al., 1997).

The degradation of *Drosophila* salivary glands is very rapid and is completed by 16 hours after puparium formation (Jiang et al., 1997). Morphological studies of dying

salivary glands show that they die with an autophagic cell death morphology, and have increased numbers of autophagosomes associated with their destruction (Berry and Baehrecke, 2007; Lee and Baehrecke, 2001). Although caspases are traditionally associated with the apoptotic cell death, several markers of apoptosis including activation of caspases, fragmentation of DNA, presence of processed caspase-3 and cleavage of the caspase substrate nuclear lamin are observed during autophagic cell death of salivary glands (Lee and Baehrecke, 2001; Martin and Baehrecke, 2004). The partial inhibition of salivary gland cell death by expression of the baculovirus inhibitor of caspases p35 (Lee and Baehrecke, 2001; Martin and Baehrecke, 2004), as well as in *dronc*, *drice*, and *ark* loss-of-function mutants (Berry and Baehrecke, 2007; Muro et al., 2006), suggests that caspases are involved in the destruction of salivary glands and that other factors must contribute to the death of these cells. Consistent with these conclusions, both caspases and autophagy (*atg*) genes are induced by ecdysone during autophagic cell death of salivary glands (Lee et al., 2003). Significantly, the combined inhibition of caspases and autophagy leads to an almost complete inhibition of salivary gland degradation than inhibition of either caspases or autophagy alone (Berry and Baehrecke, 2007).

The mechanisms of ecdysone signaling have been well studied in *Drosophila* salivary glands (Thummel, 1996). Ecdysone exerts its effect on the developmental processes through a heterodimer of Ecdysone Receptor (EcR) and Ultraspiracle (Usp) nuclear receptors (Thomas et al., 1993; Yao et al., 1992) (Figure 3). The ecdysone receptor complex then activates the transcription of a small set of early regulatory genes, including *Broad-Complex (BR-C)*, *E74A*, and *E75* (Burtis et al., 1990; DiBello et al.,

1991). These early genes regulate the transcription of a larger set of late genes that are thought to play a more direct roles in development (Urness and Thummel, 1995), including salivary gland cell death. *βFTZ-F1*, an orphan nuclear receptor is transcribed just prior to the increase of ecdysone titer that triggers larval salivary gland cell death (Broadus et al., 1999; Woodard et al., 1994). *βFTZ-F1* acts as a competence factor for the prepupal response to ecdysone and enables this steroid to induce *BR-C*, *E74A* and the stage specific cell death gene *E93* (Broadus et al., 1999; Lee et al., 2002; Woodard et al., 1994). These primary response genes then regulate the transcription of genes that play a more direct role in cell death, including the apoptosis factors *rpr*, *hid*, *croquemort (crq)*, *ark*, *drice* and *dronc*, and autophagy genes, during larval salivary gland destruction (Lee et al., 2003; Lee et al., 2000). Mutations in *BR-C*, *E74* and *E93* prevent salivary gland cell death, and also alter transcription of these cell death and *atg* genes (Jiang et al., 2000; Lee et al., 2003; Lee et al., 2000).

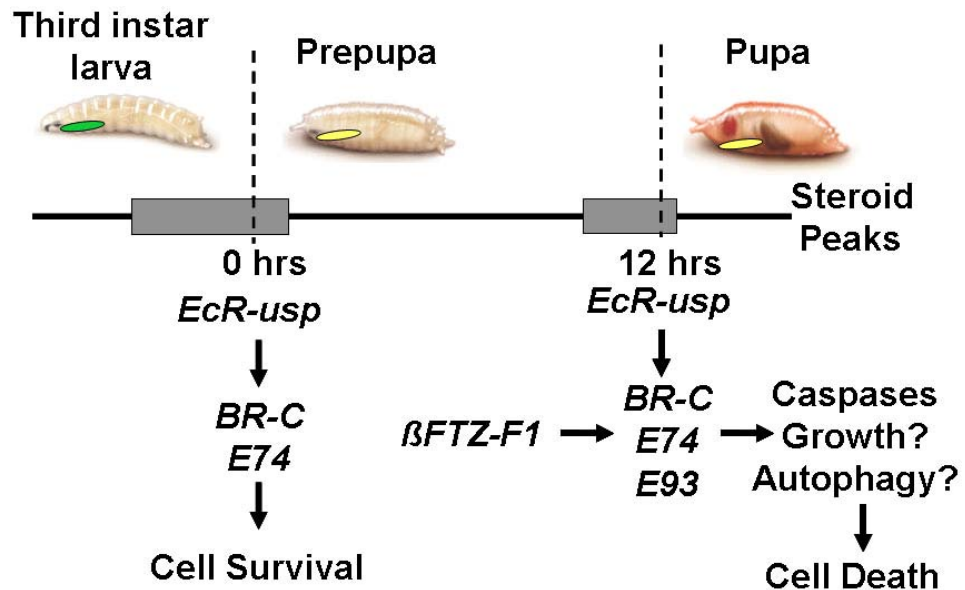


Figure 5. Model for ecdysone regulated salivary gland responses during metamorphosis. The ecdysone level rises at the end of the third larval instar, larvae stop feeding and form prepupae, and the EcR-Usp receptor complex activates the *BR-C* and *E74* genes that regulate the late genes involved in the synthesis and secretion of glue. Ten hours later the subsequent rise in ecdysone titer triggers pupation and ecdysone receptor complex with the help of competence factor β FTZ-F1 activate the *BR-C*, *E74*, and *E93* early genes. *BR-C*, *E74*, and *E93* regulate the caspases, growth and autophagy genes and leads to the death of the salivary glands. This figure is adapted from Baehrecke, unpublished.

E93 is a critical ecdysone-triggered early response gene, and it is the only gene that is both necessary and sufficient for salivary gland cell death (Lee et al., 2000). In addition, recent studies have shown that salivary gland cell growth arrest is a critical determinant of autophagic cell death in this tissue, as maintenance of growth by expression of either activated Ras, Dp110 or Akt is sufficient to suppress autophagy and inhibit salivary gland cell death (Berry and Baehrecke, 2007). Here I continue investigation of the function of *E93* in the regulation of autophagic cell death, and identify putative transcriptional targets of this helix-turn-helix transcription regulator, including *hpo*. Significantly, the Wts/Hpo pathway is required for cell growth arrest, and proper levels of caspase activity and autophagy in dying salivary glands. In addition, I show that Wts-dependent cell growth arrest is mediated by the class I PI3K pathway, and that this appears to occur in a manner that is independent of Yki and the linear Wts/Hpo signaling pathway that has been described in developing adult tissues.

Chapter 2

Characterization of the relationship between *E93* and *Vno*

2.1 Abstract

The steroid hormone ecdysone regulates multiple cellular processes during metamorphosis in *Drosophila*, including cell differentiation, morphogenesis and death. *E93* is necessary and sufficient for larval tissue cell death during metamorphosis, and *E93* is induced by ecdysone in a stage- and tissue- specific manner in dying larval cells. By contrast, the dominant wing vein mutation *Vein-off* (*Vno*) causes patterning defects in adult structures, such as the eye, leg, wing and antenna. Here we characterize new *Vno* mutant alleles, and provide evidence that *E93* and *Vno* are related. *E93* and *Vno* mutations map to the same region of the genome in 93F, and are both pupal lethal. Although *Vno* and *E93* mutant alleles complement each other, such that trans-heterozygous individuals survive to adulthood, they both contain molecular lesions in the *E93* open reading frame. Hetero-allelic combinations of *Vno* cause defects in steroid regulated salivary gland degradation in *Drosophila*. These data indicate that *E93* functions in steroid regulation of both cell development and death during metamorphosis.

Introduction

Programmed cell death is an essential process that is used to maintain cellular and tissue homeostasis by removing unneeded cells during development (Jacobson et al., 1997). Programmed cell death is conserved in organisms that are as different as worms and humans (Aravind et al., 2001). While the mechanism that integrate cell death and cell

division are relatively well studied, less is known about the relationship between cell death and cell differentiation.

Steroid hormones are important regulators of animal development and programmed cell death (Baehrecke, 2000; Evans-Storm and Cidlowski, 1995). Various human disorders including breast, ovarian and prostate cancers have been linked with the dysfunction of steroid-triggered programmed cell death (Thompson, 1995). Little is known about how steroids regulate cell-specific responses, such as differentiation and death, and the fruit fly *Drosophila melanogaster* provide an excellent system to study this relationship.

At the end of third larval instar stage, an increase in the steroid hormone 20-hydroxyecdysone (ecdysone) induces puparium formation and the onset of metamorphosis. During this early stage in metamorphosis, ecdysone triggers adult structures, such as wings and legs, to undergo differentiation and morphogenesis, while larval tissues such as the midgut are destroyed by programmed cell death (Bodenstein, 1965; Robertson, 1936). A rise in steroid hormone 12 hours after puparium formation triggers future adult head eversion and synchronized degradation of larval salivary glands (Jiang et al., 1997). Previous studies have shown that caspases and autophagy both function during *Drosophila* salivary gland autophagic cell death (Berry and Baehrecke, 2007; Lee and Baehrecke, 2001; Martin and Baehrecke, 2004).

Ecdysone is bound by the EcR and USP heterodimeric receptor complex (Thomas et al., 1993; Yao et al., 1992) and acts with the competence factor *βFTZ-F1* to regulate transcription of the primary response genes *BR-C*, *E-74A*, *E93* (Broadus et al., 1999; Lee et al., 2002; Woodard et al., 1994). The ecdysone-regulated genes *EcR*, *usp*, *βFTZ-F1*, *BR-C*, *E74* and *E93* are required for larval salivary gland programmed cell death (Broadus et al., 1999; Hall and Thummel, 1998; Jiang et al., 2000; Restifo and White, 1992). *βFTZ-F1*, *BR-C*, *E74* and *E93* influence transcription of the secondary response cell death genes *rpr*, *hid*, *dark*, *dronc* and *drice* during salivary gland autophagic cell death (Jiang et al., 2000; Lee et al., 2000; Restifo and White, 1992). While *βFTZ-F1*, *BR-C*, and *E74* appear to influence both the destruction of larval structures and formation of adult structures during metamorphosis (Broadus et al., 1999; Fletcher and Thummel, 1995; Fortier et al., 2006; Lee and Baehrecke, 2001; Restifo and White, 1992), *E93* appears to function more specifically in the destruction of larval tissues (Lee et al., 2000).

The ecdysone regulated *E93* gene is induced in a stage- and tissue-specific manner preceding developmental programmed cell death of larval tissues (Baehrecke and Thummel, 1995; Lee et al., 2000). *E93* encodes a novel nuclear protein that binds to specific sites in the polytene chromosome, and is required for autophagic cell death (Lee and Baehrecke, 2001; Lee et al., 2000). Although mutations in *E93* are known to influence the RNA levels of genes that function in apoptosis and autophagy, it is not clear how *E93* differs from other ecdysone responsive genes, such as *BR-C* and *E74*, so that it specifically regulates the death of larval cells.

The *Drosophila* wing is a classic model system for studying genetic control of pattern formation in a cellularized and proliferating epithelial tissue. Adult *Drosophila* wings have a simple pattern of five longitudinal and two transverse veins. Many wing mutants have been identified that affect normal shape and size of the wing, or the normal pattern of veins. Wing vein mutant defects may result from a failure in the developmental process of either wing or vein differentiation, or both (Díaz-Benjumea and García-Bellido, 1990). *Vno* mutants, also known as *Tp (3;3) 89E;93F;96F*, have a gap in longitudinal veins, and enhance the phenotypes of other wing vein mutants, such as *rhomboid*, without significantly affecting the size of the wing (Díaz-Benjumea and García-Bellido, 1990). *Vno* mutants also influence the patterning of several additional adult structures, including the eye, antenna, abdomen and leg (Muskavitch, Duncan and Baehrecke unpublished). These *Vno* adult patterning mutant defects were mapped to the 93F5 breakpoint of the *Tp (3;3) 89E;93F;96F* strain (Baehrecke, unpublished), and recessive pupal lethal mutations were isolated that fail to complement *Tp (3;3) 89E;93F;96F* (Lee et al., 2000); Baehrecke, unpublished), but complement the lethal phenotype of *E93* mutants.

Here we have characterized three new alleles of *Vno*. Animals that are trans-heterozygous for different recessive *vno* mutant alleles fail to undergo salivary gland cell death, but *Vno* mutants complement *E93* mutant alleles when evaluated for a salivary gland destruction phenotype. These new *Vno* alleles possess molecular lesions in *E93*, and the *Tp (3;3) 89E;93F;96F* break point maps near the 5' end of a recently reported alternative form of *E93* (*E93B*) (Mou, Duncan, and Duncan, unpublished). Expression of

either *E93A* or *E93B* is sufficient to induce premature salivary gland cell death. *Vno* mutants also possess adult wing vein defects, and have cell death defects in eye imaginal discs. Together these data suggest that *Vno* and *E93* is the same gene with complex regulation that influences both larval salivary gland autophagic cell death, and adult pattern formation.

2.3 Results

Identification of new *Vno* alleles

Vno alleles were isolated along with *E93* mutants from an ethane methyl sulfonate (EMS)–induced screen for lethal mutations that fail to complement a deficiency for the *E93* region, *Df(3R)93FX2* (Lee et al., 2000). A total of 11,134 F2-mutagenized lines were screened for lethality, and 29 lines which define 11 lethal complementation groups were isolated. Only two of these complementation groups were pupal lethal. The first complementation group consists of three alleles dies early during pupal development. Detailed phenotypic and molecular characterization has revealed that these are *E93* mutants. *E93¹* causes a C-terminal nonsense change at the position 994 of the *E93* coding sequence, whereas, *E93²* and *E93³* mutants cause a significant reduction of *E93* RNA levels (Lee et al., 2000).

The second complementation group that is comprised of three alleles die late during pupal development, and failed to complement dominant wing-vein mutant *Tp(3;3)Vein-off*. Thus, they are called *vno* (*vno^{e18}*, *vno^{e31}* and *vno^{e47}*). Recently, Dr. Ian Duncan's laboratory has shown that these mutants have molecular lesions in the *E93*

open reading frame. These *vno* mutants contain nonsense changes resulting from C to T transitions in glutamine codons at positions 360, 545 and 783 of the 1165 codon open reading frame (Mou, Dutta, Duncan, Lee, Baehrecke and Duncan, unpublished). A P-element insertion *Vno* allele [*l(3)ry93*] is also available, and excision lines of this P-element result in a wide variety of adult patterning defect phenotypes (Baehrecke, unpublished).

The initial molecular characterization of the *E93* gene revealed that it encodes a 9.5 kb mRNA that spans over 50 kb of genomic DNA (Figure 6) (Baehrecke and Thummel, 1995). Later, the *Drosophila* genome project identified an alternate cDNA that lacks the 5' exon of the 9.5 kb RNA, and has three additional exons with the most distant 5' exon lying 26 kb upstream of 5' end of 9.5 kb RNA. We (and Flybase) are referring to the 9.5kb RNA as "E93A" and the recently discovered transcript as "E93B". This alternate E93B transcript encodes a protein that lacks the N-terminal 9 amino acids of the "E93A" protein and instead its 5' alternate exon encodes a sequence of 32 amino acids. The Duncan laboratory also mapped the *Tp(3;3)Vno* breakpoint and the *l(3)ry93* insertion site. The *Tp(3;3)Vno* breakpoint lies approximately 34 kb upstream of the E93A transcript, and 8 kb 5' to the 5'-most exon of *E93B* transcript. The P-element *l(3)ry93* allele is inserted into a Doc element which in turn inserted into another Doc element that is approximately 2-3 kb upstream of the presumed transcription start site of the "E93A" transcript and it lies within one of the introns of the E93B transcript (Figure 6). These data indicate that *vno* and *E93* are related.

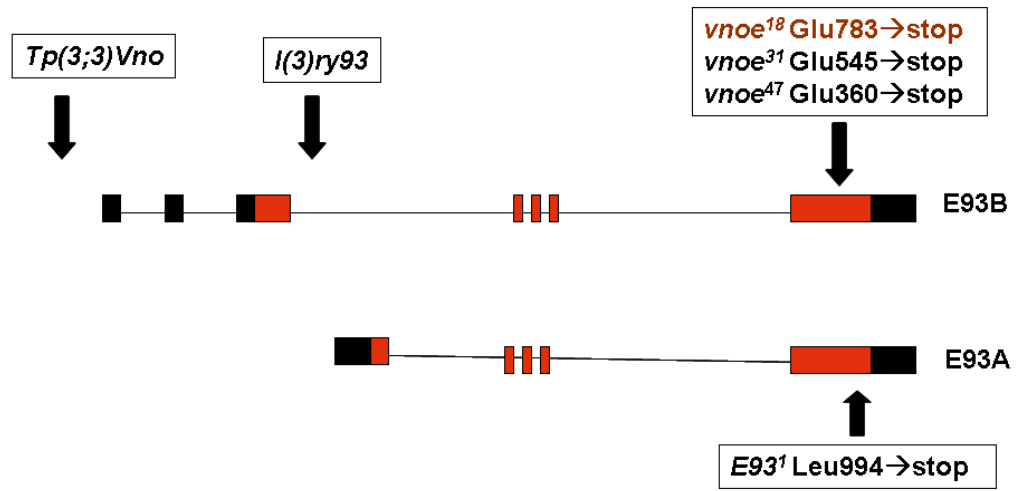


Figure 6. Molecular characterization of *vno* mutants. *E93* and *vno* mutant lesions occur in a common region of protein coding sequence of two alternative protein forms E93B (Top) and E93A transcript (Bottom). Approximate position of the *Tp(3;3)Vno* and *l(3)ry93* and *vno* and *E93* mutations are shown.

Phenotypic characterization of *vno* mutants revealed adult patterning defects, including loss of bracts on the legs, abdominal bristle polarity and cuticle pigmentation patterning defects, wing vein loss and rough eyes (Mou, Dutta, Duncan, Lee, Baehrecke and Duncan, unpublished). The dominant *Tp(3;3)Vno* mutant allele was originally recovered and named because when it is heterozygous with wild type and over balancer, the second and fourth wing veins possess gaps (Díaz-Benjumea and García-Bellido, 1990) (Figure 7A and 7B). Homozygous *Tp(3;3)Vno* mutant escapers lack all wing veins except for the third (Sturtevant and Bier, 1995). Loss of one copy of this gene by combining the newly isolated *vno^{e31}* allele with a balancer chromosome does not influence wing vein formation (Figure 7C). Combination of *Tp(3;3)Vno* and the recessive *vno* mutant allele *vno^{e31}* lack all veins except the third (Figure 7D). These data indicate that *E93* functions in the development of adult structures. In addition, these data suggest that the *Vno* and *E93* mutant classes may affect alternate transcript and protein forms.

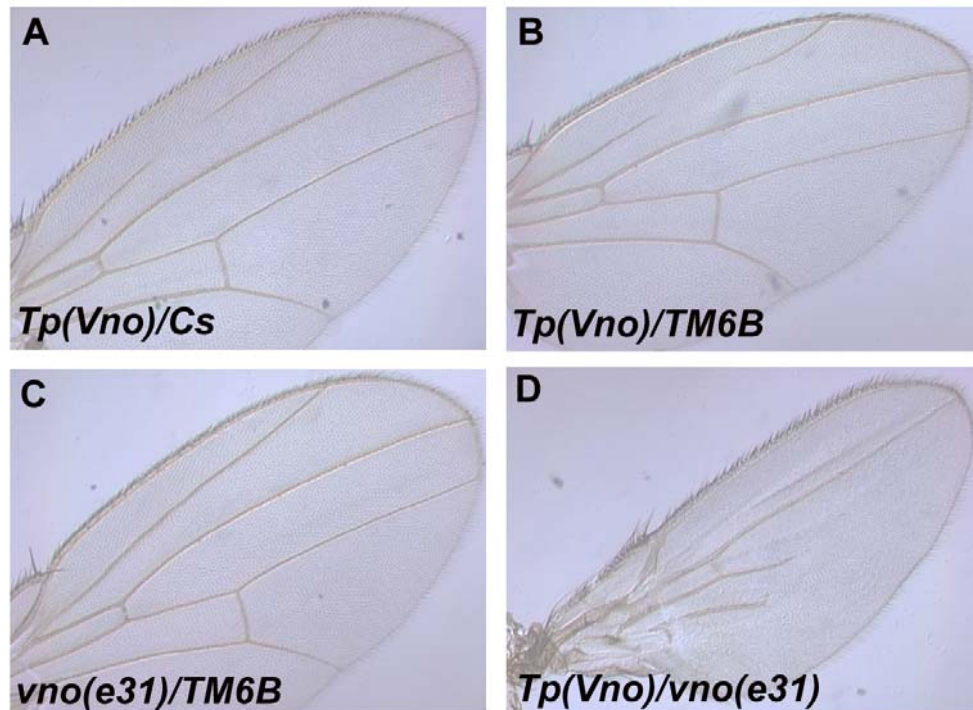


Figure 7. Vein-off wing vein phenotypes (A and B). Heterozygous *Tp(Vno)* with either wild-type Canton S (*Cs*) (A) or a balancer chromosome *TM6B* (B) possess wing vein gaps. (C) The recessive *vno^{e31}* mutant combined with a balancer chromosome *TM6B* has no wing vein defects. (D) The recessive *vno^{e31}* mutant combined with *Tp(Vno)* lacks several veins.

***Vno* mutants influence salivary gland degradation**

Our data indicate that *E93* and *Vno* are related. Since *E93* mutants exhibit defects in cell death during metamorphosis, we tested if these *vno* mutants also exhibit defects in salivary gland degradation. In control animals, salivary glands are completely degraded 24 hours after puparium formation (Figure 8A and Table 2). By contrast, *E93^l* in combination with the deficiency *Df(3R)93F^{X2}* completely inhibits salivary gland degradation as reported earlier (Figure 8B and Table 2) (Lee et al., 2000). Salivary glands are almost completely degraded in either *vno* alleles in combination with a deficiency *Df(3R)93F^{X2}* (Figure 8C and Table 2), or homozygous *vno* mutants (Figure 8D and Table 2). However, animals that are trans-heterozygous for *vno* mutations and *E93^l* do not have any salivary gland persistence (Figure 8E and Table 2). Surprisingly, hetero-allelic combinations of any of the three recessive *vno* alleles results in inhibition of salivary glands degradation 24 hours after puparium formation (Figure 8F and Table 2). These data suggest that a complicated relationship exists between the *vno* and *E93* alleles that are required for salivary gland degradation.

Caspases are critical regulators of apoptosis, and are induced prior to and function during salivary gland cell death (Berry and Baehrecke, 2007; Jiang et al., 1997; Lee and Baehrecke, 2001; Martin and Baehrecke, 2004). Therefore, we tested if DNA fragmentation is altered in *vno* mutants, as this process is regulated by caspases in salivary glands (Lee and Baehrecke, 2001). Although *E93* mutant salivary glands fail to degrade, they do initiate DNA fragmentation following the rise in ecdysone that triggers cell death. As expected, TUNEL-positive nuclei were detected in control

animals during salivary gland autophagic cell death at 13.5 hours after puparium formation (Figure 8G). Caspase-dependent DNA fragmentation was also detected in *vno* mutant salivary glands at 13.5 hours after puparium formation even though these cells fail to be degraded (Figure 8H). These data indicate that caspases are active in *vno* mutant salivary glands.

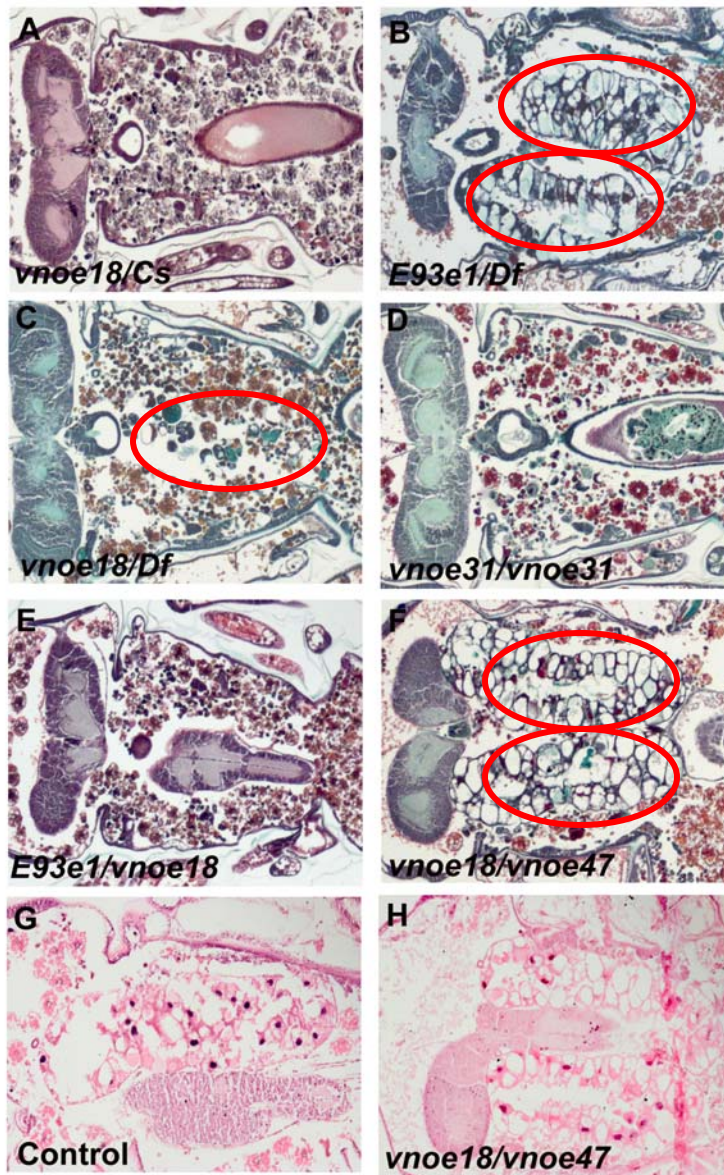


Figure 8. Trans-heterozygous *vno* mutants have salivary gland autophagic cell death defects. (A-F) Paraffin sections of animals 24 hours after puparium formation. (A) Salivary glands are completely degraded in control animals. (B) *E93* mutants have persistent salivary glands. (C and D) Salivary glands are almost completely degraded in *vno/Df* animals and in *vno* homozygous mutants. (E) Hetero-allelic combination of *E93*

and *vno* also did not have any presence of salivary gland remnants. (F) Hetero-allelic combination of *vno*^{e18}/*vno*^{e47} has persistent salivary gland tissue.

(G-H) Visualization of DNA fragmentation by TUNEL assay during salivary gland cell death. TUNEL-positive nuclei were detected in salivary glands at 13.5 hours after puparium formation in control (G) and hetero-allelic combination of *vno* mutant salivary glands (H). Red circles outline the persistent salivary gland tissue in the pupae.

**Table 2: The percent of pupae with salivary gland phenotype
(n > 20 pupae/genotype)**

Genotype	Intact/condensed salivary glands	Fragmented salivary glands	No glands
<i>vno^{e18}/Cs</i>	0	20	80
<i>E93^{e1}/Df</i>	100	0	0
<i>vno^{e18}/Df</i>	10	40	50
<i>vno^{e31}/Df</i>	0	35	65
<i>E93^{e1}/Vno^{e18}</i>	13	20	67
<i>vno^{e18}/vno^{e31}</i>	71	29	0
<i>vno^{e31}/vno^{e47}</i>	54	46	0
<i>vno^{e47}/vno^{e18}</i>	34	66	0
<i>vno^{e31}/vno^{e31}</i>	36	64	0

Ectopic expression of Vno is sufficient to induce premature salivary gland cell death

Previous studies have shown that expression of E93A is sufficient to induce programmed cell death (Lee et al., 2000). Therefore, we investigated if ectopic expression of E93B is sufficient to cause premature destruction of salivary glands. In UAS-E93B/Canton S control animals, salivary glands are present 6 hours after puparium formation (Figure 9A). By contrast, expression of E93B in a salivary gland-specific manner induces premature degradation of salivary gland by 6 hours after puparium formation (Figure 9B). This result prompted us to investigate whether expression of E93B is sufficient to rescue salivary gland cell death defects caused by mutations in *E93* (Figure 9C). Indeed, expression of E93B in salivary glands in a $E93^1 / Df(3R)93F^{X2}$ genetic background suppressed the *E93* mutant degradation defect in this tissue 24 hours after puparium formation (Figure 9D). Animals that are trans-heterozygous for different *vno* alleles possess defects in salivary gland degradation (Figure 9E). Therefore, we tested if ectopic-expression of E93A is sufficient to rescue this *vno* salivary gland degradation phenotype. Significantly, expression of E93A in salivary glands attenuated the salivary gland persistence phenotype of *vno* mutants (Figure 9F). These data indicate both E93A and E93B are sufficient to induce cell degradation of salivary glands.

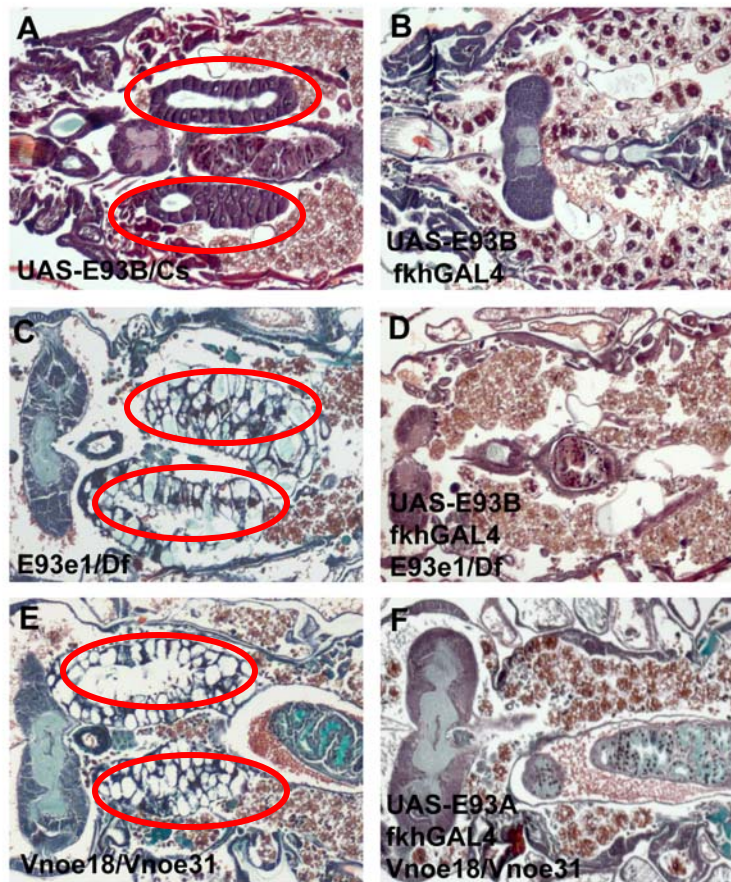


Figure 9. Ectopic-expression of *vno* is sufficient to cause premature degradation of salivary glands. Histological sections of animals at 6 hours (A and B) and 24 hours (C-F) after puparium formation. (A). In control animals, salivary glands are present at 6 hours after puparium formation. (B) Ectopic expression of E93B in a salivary gland-specific manner leads to premature degradation of salivary glands. (C) *E93^{e1}/Df* mutants have salivary gland cell death defects, but expression of E93B in a salivary gland-specific manner rescues normal degradation of salivary glands (D). (E) *vno* mutants exhibit cell death defects that are rescued by expression of E93A in a salivary gland-specific manner (F). Red circles outline the persistent salivary gland tissue in the pupae.

***vno* functions in eye cell death**

The *Drosophila* pupal retina has served as a model system to analyze cell death during development (Wolff and Ready, 1991). The rough eye phenotype that is observed in *vno* mutants prompted us to investigate whether trans-heterozygous *vno* mutant animals exhibit cell death defects in the developing pupa. While the retinal lattice structure is normal in wild-type eye disc at 60 hours after puparium formation (Figure 10B), eye discs from *vno* mutants have cell death defects (Figure 10C). In *vno* mutant eye disc, cone cells that are usually specified during the larval stage appeared to be normal, but a failure in the programmed cell death of secondary and tertiary pigment cells results in an irregular eye pattern.

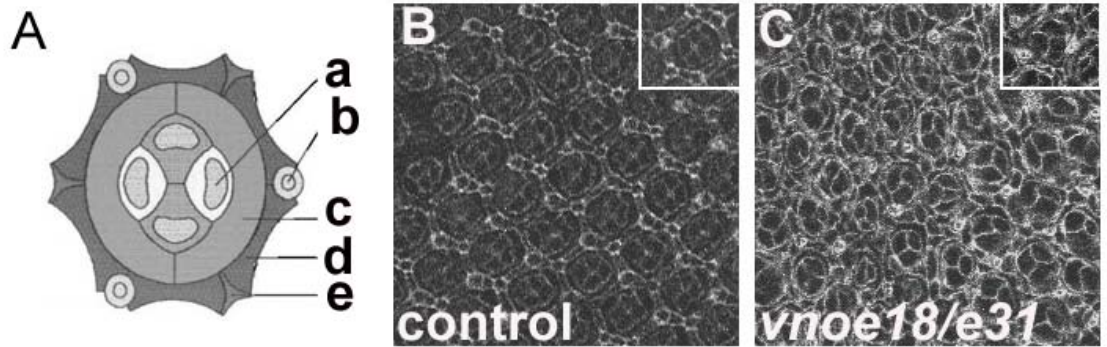


Figure 10. *vno* causes cell death defects in developing eyes. (A) Schematic representation of ommatidium (60 hours after puparium formation) adapted from Wolf and Ready, 1991. Cone cell (a), bristle (b), primary pigment cell (c), secondary pigment cell (d) and tertiary pigment cell (e) are indicated in the figure. (B and C) Mid-pupal retina stained with anti-Disc-large antibody to visualize cell outlines. (B) Control retina exhibits perfect hexagonal structure of retinal lattice. (C) trans-heterozygous *vno* mutants exhibit cell death defects in the retina and have excess secondary and tertiary cells.

2.4 Discussion

As expected, our studies indicate that *vno* mutants affect adult wing vein formation. To our surprise, *vno* is also required for autophagic cell death of *Drosophila* salivary glands. In addition, these mutants also influence proper formation of several adult structures, and in the eye the defect appears to be at least partly caused by a defect in cell death. The early ecdysone responsive gene *E93* is a critical regulator of programmed cell death during *Drosophila* metamorphosis, and given the cell death phenotypes it seems logical that *vno* mutants have lesions in this gene. *E93* is expressed in a stage and tissue specific manner in response to the steroid hormone ecdysone, and it regulates the transcription of several genes that are known to function in cell death, including apoptosis and autophagy genes (Baehrecke and Thummel, 1995; Lee et al., 2003). It is not clear, however, whether *E93* is required for the regulation of target genes that specify the development of various imaginal tissues.

The newly characterized *vno* mutants are lethal at the pharate adult stage, and they cause multiple defects in legs, eyes, wings, abdomens and antennae. Although our studies in eyes suggest that these adult tissue defects could be caused by altered cell death, the fact that *vno* mutant adult abdomens have altered bristle polarity and pigmentation patterning (Baehrecke, unpublished) suggests the possibility that *vno* could function in the development of adult cells.

Surprisingly, *vno* mutations were found in the common coding region of *E93* even though these alleles complemented *E93* mutant alleles in the context of survival to

adulthood and salivary gland cell death. There are at least two possible explanations for these complicated genetic results. One possibility is that *vno* and *E93* mutant classes affect two different alternate products. The *E93B* transcript could be responsible for adult patterning, whereas the original *E93A* transcript may be a critical regulator of the steroid triggered programmed cell death during *Drosophila* metamorphosis. It is possible that combinations of different mutations in a common region may act as a dominant negative form. Although, no evidence is available to support this model other than that *E93* is a transcription factor, some logical reason must explain these complicated genetic results. Alternatively, it is possible that translational re-initiation could occur in the common coding region of *E93*. The coding sequence of *E93A* and *E93B* transcripts are nearly identical apart from their different N-terminal ends. One piece of evidence supporting this re-initiation model is that all of the *vno* allele mutations are closer to the N-terminus than the *E93^l* allele, and the *vno* alleles that are closer to the C-terminus have stronger phenotypes (Mou, Duncan and Duncan, unpublished).

It will be difficult to determine the exact reason for the differences that are observed in *E93* and *vno* mutants without a better understanding of the two *E93* protein forms, and how these forms are regulated. An additional and important approach that can be used to distinguish the difference between *E93* and *vno* mutants is to identify downstream targets of the *E93A* and *E93B* proteins that regulate imaginal patterning and cell death. Previous studies have shown that steroid regulation of *E93* is quite specific and has emphasized the expression in dying larval mid-guts and salivary glands (Baehrecke and Thummel, 1995; Lee et al., 2000). It is worth noting that *E93* RNA was

also detected in imaginal discs (Baehrecke and Thummel, 1995), and E93 protein was localized in specific eye imaginal disc and brain cells (Baehrecke, unpublished).

Therefore, it is possible that *E93* might be regulating different target genes depending on the tissue and stage during development. Future studies should resolve how *E93* regulates both adult cell formation and larval cell death, and this should provide important insight into how steroids regulate specific cell responses.

2.5 Materials and Methods

***Drosophila* Strains**

For loss-of-function studies, *E93^{e1}*, *vno^{e18}*, *vno^{e31}*, *vno^{e47}*, *Df(3R)93F^{X2}*, *Tp(3;3)Vno* strains were analyzed. For ectopic expression studies, UAS-E93A and UAS-E93B (kindly provided by Ian Duncan) were analyzed. Canton-S wild-type was used as a control.

Salivary Gland Histology

Animals of the indicated genotypes were aged to 6 and 24 hours after puparium formation at 25⁰C, fixed in FAAG, dehydrated, embedded in paraffin, sectioned and stained with Weigert's Hematoxylin and Pollack Trichrome and analyzed using Zeiss Axio Imager.Z1 (Muro et al., 2006). TUNEL assay was performed using the Apoptag kit (Chemicon) with semi-thin paraffin sections of the embedded tissue as previously described (Wang et al., 1999), and examined using Zeiss Axio Imager.Z1. For TUNEL assays, a minimum of 10 pupae were examined for each genotype. For all other experiments, a minimum of 20 pupae were analyzed for each genotype.

Immunohistochemistry

For immunohistochemistry, *vno^{e18}*/Canton-S control and *vnoe¹⁸/vnoe⁴⁷* experimental animals were aged to 60 hours after puparium formation at 25⁰C and eye imaginal discs were dissected. Eye discs were fixed with 4% paraformaldehyde/heptane for 20 minutes at room temperature and rinsed three times each with methanol and phosphate buffered saline containing 0.1% Tween-20 (PBST). The eye discs were then blocked in phosphate buffered saline containing 1% BSA and 0.1% Tween-20 (PBSBT) for 2 hours at room temperature and incubated with mouse anti-Disc large (1:200) (Developmental Studies Hybridoma Bank) (Parnas et al., 2001) primary antibody for overnight at 4⁰C. The following day, eye discs were washed for 2 hours in PBSBT and incubated with appropriate fluorescent secondary antibody for 2 hours at room temperature at dark. The following procedures were performed at room temperature in absence of light. After secondary antibody staining, the eye discs were washed for another 30 minutes then mounted with Vectashield (Vector Laboratories) and imaged using Zeiss Axiovert confocal microscope.

Chapter 3

Identification of targets of E93

3.1 Abstract

E93 is required for steroid-triggered autophagic cell death of salivary glands. *E93* encodes a putative helix-turn-helix DNA binding motif, and this motif is conserved in organisms that are as different as worms and humans. Mutations in *E93* cause alterations in RNA transcript levels, including regulators of caspases and autophagy genes. Here we have used genetic and genomic approaches to identify downstream targets of *E93*. We have identified numerous candidate *E93* target genes using DNA microarrays. We have also generated transgenic animals to identify downstream target genes of *E93* by chromatin immune precipitation. We show that one of these putative *E93* target genes, *hippo* (*hpo*), is required for salivary gland cell death.

3.2 Introduction

The two most prominent forms of programmed cell death that occur during development are apoptosis and autophagic cell death (Clarke, 1990; Schweichel and Merker, 1973). Apoptosis, the most thoroughly studied form of programmed cell death, is characterized by activation of caspases, nuclear condensation, cytoplasmic blebbing and finally phagocytic engulfment of the dying cell where degradation is completed by the lysosome (Clarke, 1990; Kerr et al., 1972). By contrast, cells dying by autophagic cell death are usually not phagocytosed, contain large numbers of autophagosomes, and appear to use their own lysosome for degradation. While the molecular and biochemical mechanisms

that regulate apoptosis have been well characterized, far less is known about the autophagic cell death.

Drosophila larval salivary glands provide an excellent in-vivo model system to study steroid triggered autophagic cell death during development. A rise in the steroid hormone 20-hydroxyecdysone (ecdysone) 10-12 hours after puparium formation induces synchronized cell death of this tissue. Salivary glands are then rapidly degraded by 16 hours after puparium formation (Jiang et al., 1997). The ecdysone receptor complex acts with the competence factor β FTZ-F1 to regulate transcription of the primary response genes *E93*, *Broad-Complex (BR-C)*, and *E74* (Broadus et al., 1999; Woodard et al., 1994). Mutations in either β FTZ-F1, *E93*, *BR-C*, or *E74* prevent degradation of salivary glands, and impact the transcription of the secondary response cell death genes, including *rpr*, *hid*, *crq*, *ark*, *drice*, *dronc* during autophagic cell death (Broadus et al., 1999; Jiang et al., 2000; Lee et al., 2003; Lee et al., 2002; Lee et al., 2000; Restifo and White, 1992). Significantly, genome-wide studies of dying salivary glands indicate that over 932 genes that are induced 5-fold or greater following the rise in ecdysone that triggers salivary cell death. However, we do not know how most of these genes are regulated, how they are influenced by the primary ecdysone response genes, and if they function in dying salivary glands.

rpr, *hid*, and *grim* reside in a single genetic interval *Df(3L)H99* that is required for apoptosis in *Drosophila* (Chen et al., 1996; Grether et al., 1995; White et al., 1994), and expression of either *rpr*, *hid*, or *grim* is sufficient to induce caspase-dependent

programmed cell death (White et al., 1996; Chen et al., 1996; Grether et al., 1995). Rpr, Hid and Grim activate caspases by inhibiting the *Drosophila* inhibitor of apoptosis 1 (DIAP1) (Goyal et al., 2000; Wang et al., 1999). Although caspase proteases are traditionally associated with apoptotic cell death, they also participate in autophagic cell death of salivary glands (Jiang et al., 2000; Lee and Baehrecke, 2001; Martin and Baehrecke, 2004). Expression of the baculovirus inhibitor of caspases, p35, blocks DNA fragmentation and cleavage of the caspase substrate nuclear lamin, but it fails to completely inhibit salivary gland degradation (Lee and Baehrecke, 2001; Martin and Baehrecke, 2004). Recent studies have shown caspases and autophagy genes function in an additive manner in the regulation of autophagic cell death during development (Berry and Baehrecke, 2007). However, it is not clear how caspases and autophagy genes are regulated during salivary gland cell death.

Coordination between cell proliferation and cell death is crucial to maintain homeostasis and avoid tumor growth in multicellular organisms (Conlon and Raff, 1999; Green and Evan, 2002). Significantly, studies in salivary glands suggest that growth arrest is required for salivary gland degradation. Recent genetic studies in *Drosophila* have identified members of the conserved Warts (Wts)/ Hippo (Hpo) tumor-suppressor pathway as an important regulator of cell proliferation, cell death and tissue growth in higher animals (Edgar, 2006; Harvey et al., 2003; Udan et al., 2003; Wu et al., 2003). *hippo* (*hpo*), the *Drosophila* homologue of the mammalian Ste20-like kinases MST1/2, mutations result in severe tissue over-growth phenotype in fly epithelial tissues (Harvey et al., 2003; Udan et al., 2003; Wu et al., 2003). *hpo* is required for proper termination of

cell proliferation and induction of apoptosis by negatively regulating expression of the cell cycle regulator Cyclin E and the *Drosophila* inhibitor of apoptosis protein (DIAP1).

E93 is necessary and sufficient for autophagic cell death of salivary glands (Lee et al., 2000). Here we have developed approaches to identify *E93* target genes in *Drosophila*. Transgenic strains were developed that will enable the use of the adult eye as a system to screen for genetic modifiers of *E93*-induced cell death. Expression of *E93* is sufficient to induce cell death in the adult eye that is caspase-dependent and suppressed by expression of DIAP1 and p35. We have also identified candidate *E93* target genes by analyzing DNA microarray data that was previously generated from purified wild-type and *E93* mutant salivary glands. Myc-tagged *E93* transgenic flies were produced so that targets can be identified that are directly bound by *E93* using in-vivo chromatin immunoprecipitation (ChIP). *hpo* was identified as a candidate target gene of *E93* that is required for autophagic cell death of salivary glands.

3.3 Results

***E93* encodes a conserved DNA-binding protein**

E93 contain a helix-turn-helix motif in the pipsqueak super-family of DNA binding proteins (Siegmond and Lehmann, 2002). This domain of the pipsqueak protein binds to the GAGA sequence (Lehmann et al., 1998). The putative DNA binding motif of *E93* is conserved in honey bees (*Apis mellifera*), nematodes (*Caenorhabditis elegans*), mice (*Mus musculus*), human (*Homo sapiens*), and other species (Figure 11).

D.melanogester	KGTRPKRGKYRNYDRDSLVEAVKAVQRGEMSVHRAGSYYGVPHSTLEYKVKER
A.mellifera	KGTRPKRGKYRNYDRDSLVEAVRAVQRGEMSVHRAGSYYGVPHSTLEYKVKER
C.briggsae	KRSRPKRGQYRKYDKNALDEAVRSVRRGEMTVHRAGSFFGVPHSTLEYKVKER
C.elegans	KRSRPKRGQYRKYDKNALDEAVRSVRRGEMTVHRAGSFFGVPHSTLEYKVKER
M.musculus	KQPRKKRGRYRQYDHEIMEEAIAMVMSGKMSVSKAQGIYGVPHSTLEYKVKER
H.sapiens	KQPRKKRGRYRQYNSEILEEAI SVVMSGKMSVSKAQSIYGI PHSTLEYKVKER

Figure 11. Alignment of the putative DNA binding helix-turn-helix motif of E93.

The E93 helix-turn-helix motif is conserved in fly (*D. melanogester*), honey bee (*A. mellifera*), worms (*C. elegans* and *C. briggsae*), mouse (*M.musculus*) and human (*H.sapiens*). Red color indicates the conserved region.

In order to identify candidate *E93* downstream target genes during ecdysone-induced programmed cell death, total RNA was isolated from wild-type Canton S and homozygous *E93* mutant salivary glands dissected from stages before (8 hours after puparium formation), during (12 hours after puparium formation), and after (14 hours after puparium formation) ecdysone-triggered autophagic cell death. It is important to note that 14-hour wild-type samples were compared to 16-hour *E93* mutant samples to compensate for a developmental delay in *E93* mutants. Three independent samples of salivary gland RNAs were collected for each stage and genotype, and were used to hybridize Affymetrix *Drosophila* oligonucleotide GeneChips (Clough et al., unpublished). By comparing these microarray data, we have identified 100 genes that increase 3-fold or greater in wild-type, but lack 80% of this increase in magnitude in *E93* mutant salivary glands (Table 3). For example, if a gene has increased 50-fold in wild-type salivary glands following the rise of ecdysone, but it has increased only 10-fold or less in *E93* mutant salivary glands, it qualifies as a candidate target gene.

The bioinformatics resource DAVID (<http://david.abcc.ncifcrf.gov/>) was used to identify the genes on this list that are involved in cell death (Table 4).

Table 3: Candidate E93 target genes

FlyBase Number	CG number	Symbol	Name	Function	Fold change in 8-12 hour wild-type	Fold lower in E93 mutant
FBgn0031780	CG31641	stai	stathmin	Microtubule binding	89.80828	-101.5936673
FBgn0039160	CG5510	CG5510	CG5510	unknown	41.88506	-51.18956274
FBgn0039861	CG1800	Pasha	partner of drosha	Double stranded RNA-binding protein	25.51393	-36.19648694
FBgn0003997	CG5123	w/hid	Wrinkled	Apoptotic cell death	20.27389	-35.36975803
FBgn0030749	CG9968	Anxb11	Annexin B11	calcium-dependent phospholipid binding	20.38541	-35.09839935
FBgn0000277	CG1367	CecA2	Cecropin A2	antibacterial humoral response, defense response to bacterium and fungi	28.55832	-33.51341193
FBgn0027053	CG14884	CSN5	COP9 complex homolog subunit 5	NEDD8 activating enzyme activity, glial cell migration	25.79928	-33.51341193
FBgn0035925	CG5797	Fhos	Fhos	actin binding	39.4313	-32.4967204
FBgn0033569	CG12942	CG12942	CG12942	zinc ion binding	41.79952	-30.08789165
FBgn0031165	CG1726	CG1726	CG1726	unknown	33.39228	-27.43180745

FBgn0005278	CG2674	M(2)21AB	Minute (2) 21AB	methionine adenosyltransferase activity, ATP binding	28.64328	-27.43180745
FBgn0028932	CG16890	CG16890		unknown	35.20285	-26.8052641
FBgn0030396	CG2556	CG2556		unknown	18.6407	-26.19303102
FBgn0029681	CG15239	CG15239		unknown	21.21859	-22.627417
FBgn0037290	CG1124	CG1124		unknown	21.49505	-21.77264
FBgn0034584	CG9364	Treh	Trehalase	alpha, alpha-trehalase activity	37.49159	-21.43983982
FBgn0038279	CG3837	CG3837		insulin-like growth factor receptor activity	22.52979	-20.62992494
FBgn0000276	CG1365	CecA1	Cecropin A1	defense response to bacterium, fungi; autophagic cell death	20.78107	-19.39721707
FBgn0037925	CG17309	Csk	C-terminal Src kinase	protein tyrosine kinase activity, protein binding	16.43628	-18.8087665
FBgn0028563	CG8714	sut1	sugar transporter 1	glucose transmembrane transporter activity	17.38712	-15.87724714
FBgn0035945	CG5026	CG5026		protein tyrosine/serine/threonine phosphatase activity	18.32045	-15.04394583
FBgn0039139	CG5933	CG5933		RNA methylation	20.18139	-14.92852786
FBgn0029598	CG3981	Unc-76	Unc-76	axon cargo transport; phagocytosis, engulfment	12.92712	-14.36458536
FBgn0040916	CG11465	CG32758	CG32758	protein binding	10.28611	-12.99603834
FBgn0013272	CG5820	Gp150	Gp150	Catalytic activity ; protein binding	14.91459	-12.79739068

FBgn0040594	CG11957	CG33111	CG33111	oxidoreductase activity; transition metal ion binding	11.73839	-12.21948105
FBgn0033125	CG12846	Tsp42Ed	Tetraspanin 42Ed	unknown	9.061594	-12.12573253
FBgn0033495	CG12214	CG12214		Protein binding	11.82955	-12.03270326
FBgn0039767	CG2218	CG2218		ubiquitin-protein ligase activity, protein binding	9.55297	-12.03270326
FBgn0039775	CG12088	PH4 α EFB	prolyl-4- hydroxylase-alpha EFB	iron ion binding	8.846552	-11.66766888
FBgn0038826	CG17838	CG17838		mRNA binding	10.72322	-11.3137085
FBgn0039506	CG5938	CG5938		unknown	10.32306	-11.22690912
FBgn0035350	CG16757	Spn	Spinophilin	Protein binding	8.830099	-11.22690912
FBgn0036980	CG5701	RhoBTB	RhoBTB	GTPase activity; GTP binding	14.46451	-11.05530304
FBgn0032497	CG6043	CG6043		unknown	15.85181	-10.97048616
FBgn0040551	CG11686	CG11686		unknown	9.530369	-10.23582552
FBgn0032482	CG5547	Pect	Phosphoethanolamin e cytidyltransferase	ethanolamine and derivative metabolic process	10.16727	-10.15729572
FBgn0031915	CG12789	santa- maria	scavenger receptor acting in neural tissue and majority of rhodopsin is absent	defense response; autophagic cell death	11.5246	-9.550362907
FBgn0034453	CG11228	Hpo	hippo	Cell proliferation; programmed cell death	8.783213	-9.477092009
FBgn0037728	CG16817	CG16817		unknown	12.80588	-9.119083836
FBgn0031011	CG8034	CG8034		unknown	10.72574	-8.774599838
FBgn0040595	CG11945	CG33111		oxidoreductase activity	7.862507	-8.707280636

FBgn0011712	CG6625	Snap	Soluble NSF attachment protein	phagocytosis, engulfment	8.097467	-8.707280636
FBgn0033923	CG8603	CG8603		cell morphogenesis;	12.92094	-8.5741877
FBgn0036518	CG7396	RhoGAP71E	RhoGAP71E	signal transduction	12.63751	-8.314073808
FBgn0037929	CG14714	CG14714		protein tyrosine phosphatase activity	6.553712	-8.1241801
FBgn0030038	CG1440	CG1440		cysteine-type endopeptidase activity	6.277776	-8
FBgn0035773	CG8580	Akirin	akirin	muscle development; positive regulation of innate immune response	9.664861	-7.697790695
FBgn0031814	CG9528	Retm	real-time	phosphatidylinositol transporter activity	7.249794	-7.237821637
FBgn0028539	CG7559	CG31731		ATPase activity	6.381196	-7.237821637
FBgn0027569	CG7207	CG7207		protein serine/threonine kinase activity	8.176829	-7.018248889
FBgn0031972	CG7221	Wwox	Wwox	oxidoreductase activity	6.631816	-6.857951863
FBgn0014010	CG3664	Rab5	Rab-protein 5	GTP binding; GTPase activity	9.874033	-6.857951863
FBgn0038065	CG6359	CG6359		phosphoinositide binding;	9.255649	-6.701316026
FBgn0001229	CG4190	Hsp67Bc	Heat shock gene 67Bc	unknown	6.028816	-6.701316026
FBgn0004237	CG12749	Hrb87F	Heterogeneous nuclear ribonucleoprotein at 87F	alternative nuclear mRNA splicing	5.159589	-6.701316026
FBgn0030890	CG7536	CG7536		unknown	6.47413	-6.598884755

FBgn0032405	CG14946	CG14946		oxidoreductase activity	5.325153	-6.498019171
FBgn0020647	CG5405	KrT95D	Krueppel target at 95D	protein targeting to Golgi	7.138432	-6.252548939
FBgn0039061	CG6747	Ir	Inwardly rectifying potassium channel	potassium ion transport	8.018547	-6.252548939
FBgn0036185	CG7346	CG7346		ATPase activity	6.343171	-6.204579047
FBgn0039607	CG11754	CG11754		GTPase binding	6.41744	-6.204579047
FBgn0028523	CG5888	CG5888		transmembrane receptor activity	7.600425	-6.109740524
FBgn0035595	CG10668	shep	alan shepard	RNA binding	6.283281	-6.062866266
FBgn0030838	CG5445	CG5445		unknown	9.072999	-6.01635163
FBgn0039751	CG1983	CG1983		unknown	8.820586	-5.74466284
FBgn0026084	CG4944	Cib	ciboulot	cytoskeleton organization and biogenesis	7.803261	-5.656854249
FBgn0015776	CG9258	nrv1	nervana 1	cation transmembrane transporter activity	4.516945	-5.61345456
FBgn0036685	CG6664	CG6664		unknown	4.090698	-5.61345456
FBgn0032123	CG3811	Oatp30B	Organic anion transporting polypeptide 30B	organic anion transport	4.25453	-5.570387835
FBgn0035107	CG1216	mri	mrityu	autophagic cell death; potassium ion transport	4.251947	-5.48524308
FBgn0039808	CG12071	CG12071		phagocytosis, engulfment	4.64741	-5.443160001
FBgn0037231	CG9779	CG9779		phagocytosis, engulfment; protein transport	8.20215	-5.443160001
FBgn0004108	CG9704	Nrt	Neurotactin	central nervous system development	5.802057	-5.318838054

FBgn0036770	CG5485	Prestin	Prestin	sulfate transport	6.276281	-5.197355625
FBgn0004865	CG18023	Eip78C	Ecdysone-induced protein 78C	instar larval or pupal development; regulation of transcription	7.85306	-5.117912761
FBgn0038634	CG7696	CG7696		nucleic acid binding	4.795585	-5.0396842
FBgn0029914	CG4558	CG4558		unknown	5.979403	-5.0396842
FBgn0035651	CG10977	CG10977		structural molecule activity	4.994462	-4.886796029
FBgn0037468	CG1943	CG1943		unknown	5.238079	-4.630317464
FBgn0039276	CG11938	CG11938		unknown	4.169655	-4.630317464
FBgn0035975	CG4384	PGRP-LA	Peptidoglycan recognition protein LA	innate immune response	3.627978	-4.630317464
FBgn0031458	CG2855	aph-1	anterior pharynx defective 1	Notch signaling pathway	4.082617	-4.489848193
FBgn0015218	CG4035	eIF-4E	Eukaryotic initiation factor 4E	cell cycle process; programmed cell death	4.679505	-4.489848193
FBgn0035285	CG12025	CG12025		unknown	6.923085	-4.387299919
FBgn0033438	CG1794	Mmp2	Matrix metalloproteinase 2	Oogenesis; proteolysis	4.499345	-4.353640318
FBgn0034669	CG13487	Fili	Fish-lips	protein binding	4.278448	-4.353640318
FBgn0035346	CG1146	CG1146		unknown	4.851819	-4.28709385
FBgn0003048	CG3443	pcx	pecanex	unknown	4.308572	-4.254203036
FBgn0027572	CG5009	CG5009		fatty acid beta-oxidation	4.122932	-4.157036904
FBgn0030996	CG14194	CG14194		unknown	6.241548	-4.125143894
FBgn0035119	CG7020	DIP2	DISCO Interacting Protein 2	transcription factor binding	6.987394	-4.125143894
FBgn0033688	CG8877	prp8	prp8	nuclear mRNA splicing	4.290658	-4.125143894
FBgn0039623	CG1951	CG1951		protein kinase activity	5.246137	-4.093495568
FBgn0014020	CG8416	Rho1	Rho1	GTPase activity	6.650376	-4.06209005

FBgn0003731	CG10079	Egfr	Epidermal growth factor receptor	organ morphogenesis; epidermal growth factor receptor activity	3.311506	-4.030925477
FBgn0029529	CG13365	CG13365		unknown	3.683852	-4.030925477
FBgn0036092	CG6491	CG6491		unknown	3.210079	-4.030925477
FBgn0036556	CG5830	CG5830		phosphoric monoester hydrolase activity	5.282832	-4.030925477
FBgn0032342	CG4713	l(2)gd1	lethal (2) giant discs 1	sensory organ development; wing disc morphogenesis	3.563145	-3.969311785

Table 4. Candidate genes to be verified by Chromatin immunoprecipitation

Flybase number	CG number	Gene	Function
FBgn0000276	CG1365	cecropin a1	Salivary gland autophagic cell death, programmed cell death, salivary gland development, cellular developmental processes, cell differentiation
FBgn0035107	CG1216	cg1216-pc, isoform c	Salivary gland autophagic cell death, programmed cell death, salivary gland development, cellular developmental processes, cell differentiation
FBgn0025697	CG12789	cg12789-pa, isoform a	Salivary gland autophagic cell death, programmed cell death, salivary gland development, cellular developmental processes, cell differentiation
FBgn0027053	CG14884	cop9 complex homolog subunit 5	Metamorphosis, larval development, organ morphogenesis, cell development and differentiation
FBgn0003731	CG10079	epidermal growth factor receptor	EGFR signaling, Metamorphosis, larval development, organ morphogenesis, cell development and differentiation
FBgn0015218	CG4035	eukaryotic initiation factor 4e	Salivary gland autophagic cell death, programmed cell death, salivary gland development, cellular developmental processes, cell differentiation, cellular developmental processes, cell differentiation
FBgn0034453	CG11228	Hippo	Salivary gland autophagic cell death, programmed cell death, salivary gland development, cellular developmental processes, cell differentiation
FBgn0039767	CG2218	ld28173p	Protein ubiquitination, ubiquitine cycle, protein modification by small protein conjugation,

FBgn0003731	CG10079	lp05058p	EGFR signaling, Metamorphosis, larval development, organ morphogenesis, cell development and differentiation
FBgn0033438	CG1794	matrix metalloprotease 2	Salivary gland autophagic cell death, programmed cell death, salivary gland development, cellular developmental processes, cell differentiation
FBgn0004108	CG9704	Neurotactin	cellular developmental processes, cell differentiation
FBgn0014010	CG3664	rab-protein 5	cellular developmental processes, cell differentiation
FBgn0014020	CG8416	ras-like GTP-binding protein rho1	EGFR signaling, Metamorphosis, larval development, organ morphogenesis, cell development and differentiation
FBgn0003997	CG5123	wrinkled/hid	Salivary gland autophagic cell death, programmed cell death, salivary gland development, cellular developmental processes, cell differentiation, protein ubiquitination, ubiquitine cycle, protein modification by small protein conjugation,
FBgn0039767	CG2218	at27758p	Protein ubiquitination, ubiquitine cycle, protein modification by small protein conjugation,

Identification of Hpo as a E93 target that functions in salivary gland cell death

We have identified *hippo* (*hpo*) as a putative E93 target gene based on analyses of our microarray data. To validate the presence of *hpo* RNA in salivary glands, I examined if *hpo* RNA is present in purified dying salivary glands by northern blot hybridization (Figure 12A). *hpo* transcript is expressed at stages preceding and following the rise in ecdysone that triggers autophagic cell death of *Drosophila* salivary gland. Therefore, I tested if expression of a *hippo*RNAi construct (*hpo-IR*) (Pantalacci et al., 2003) in salivary glands prevented degradation of this tissue. In *UAS-hpoIR*/wild-type control animals, salivary glands are completely degraded at 24 hours after puparium formation (Figure 12 B). By contrast, knockdown of *hpo* (*hpo-IR*) in a salivary gland specific manner lead to incomplete degradation of salivary glands in 40% of the specimens at 24 hours after puparium formation (Figure 12C). These results indicate that *hpo* functions in autophagic cell death of salivary glands.

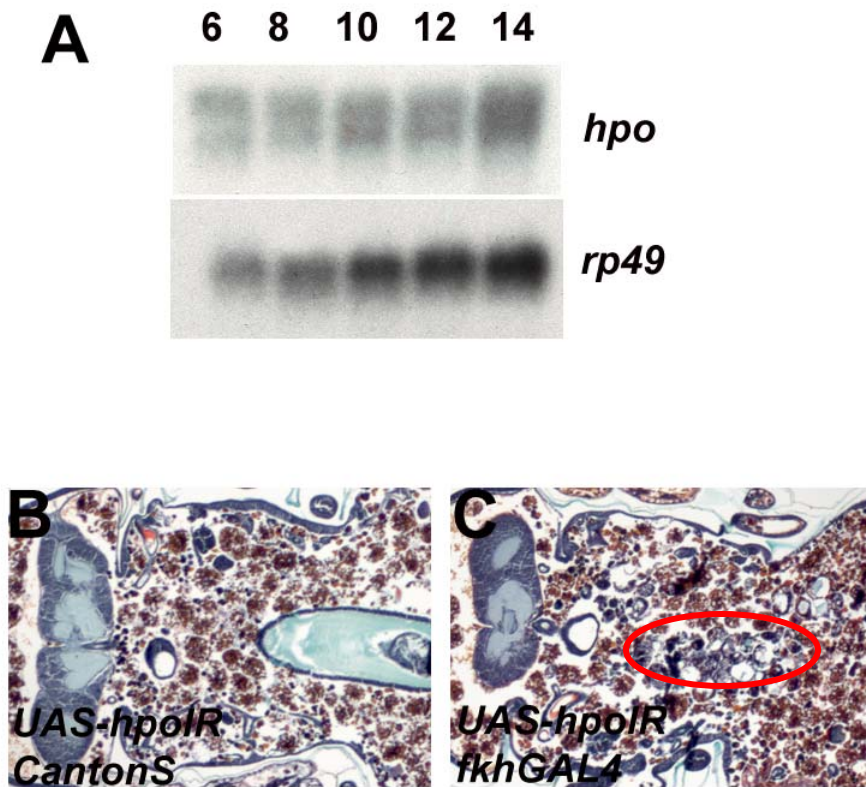


Figure 12. *hpo* is required for salivary gland cell death. (A) Northern blot showing that *Hpo* is present in salivary glands at 6, 8, 10, 12 and 14 hours after puparium formation. Hybridization of *rp49* as a control for loading. (B and C) Paraffin sections of pupae 24 hours after puparium formation. (B) Salivary glands are completely degraded in control (*UAS-hpoIR/Canton S*) animals. (C) Expression of *hpo-IR* in a salivary gland specific manner causes incomplete degradation of salivary glands. Red circles outline the persistent salivary gland tissue in the pupae.

Development of approaches to identify E93 targets

E93 is required for ecdysone-triggered autophagic cell death of salivary glands, and expression of *E93* is sufficient to induce cell death in both salivary glands (Lee et al., 2000) and embryos (Lee and Baehrecke, 2001). Unfortunately, progeny of crosses between UAS-*E93* and eye GAL4 drivers, including GMR-GAL4 and Eyeless-GAL4, die during metamorphosis (Lee and Baehrecke, unpublished). We assume that this pupal lethality is caused by “leaky” GAL4 expression, and wanted to test whether expression of *E93* is sufficient to induce cell death in the eye as this could be used to screen for suppressors of *E93*-induced cell death.

The *E93* open reading frame was inserted into the pGMR (*glass* multimer reporter) vector for specific expression in the *Drosophila* eye (Hay et al., 1994). Expression of *E93* in the developing eye gave a smaller rough eye with blister like phenotype (Figure 13A). Expression of either DIAP1 or p35 in the eye has no impact on normal adult eye structure (Figure 13B and 13C) (Hay et al., 1995; Hay et al., 1994). Caspases function in salivary gland cell death (Jiang et al., 1997; Lee and Baehrecke, 2001; Martin and Baehrecke, 2004). Therefore, we tested if co-expression of DIAP1 in the eye (GMR-DIAP1) with *E93* is sufficient to suppress the eye phenotype that is induced by GMR-*E93*. Indeed, *Drosophila* eyes expressing both *E93* and DIAP1 have a normal eye (Figure 13D). Similarly, co-expression of *E93* and p35 in an eye specific manner also suppressed the rough eye phenotype induced by *E93* (Figure 13E). Together these results indicate that expression of *E93* is sufficient to induce caspase-dependent cell

death in the adult eye. Furthermore, these results suggest that the GMR-E93 strains produced in this study could be used to screen for suppressors of E93 that could be targets of this novel regulator of cell death. Unfortunately, such an approach may not distinguish direct targets of E93, but the identification of mutations in genes that are required for E93-induced cell death would be extremely useful.

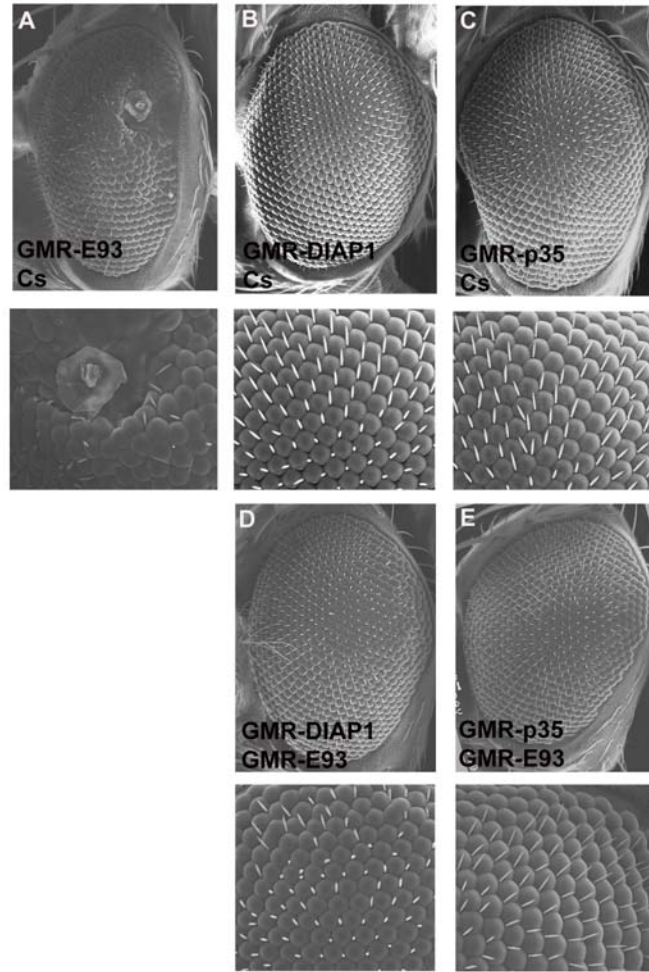


Figure 13. Expression of E93 induces caspase-dependent eye cell death. Scanning electron microscopy (SEM) images of control and experimental fly eyes, with lower panels showing magnification of ommatidia. (A) Expression of E93 causes a rough eye phenotype. (B) Eyes expressing DIAP1 are normal. (C) Eyes expressing p35 have minor abnormalities in bristle orientation. (D) Eye degeneration that was induced by *E93* was suppressed by co-expression of DIAP1. (E) Expression of p35 suppresses the rough eye phenotype induced by E93.

E93 contains a putative helix-turn-helix DNA binding motif (Siegmund and Lehmann, 2002), and this suggests that this protein directly regulates genes that function in cell death. We have taken multiple approaches to identify E93 binding sites in putative target genes. We have obtained nucleotide sequences 1000 and 2000 bp upstream of the transcription start site of the candidate E93 target genes (Table 3), and entered those sequences into Improbizer (<http://www.soe.ucsc.edu/~kent/improbizer/improbizer.html>) and MEME (<http://meme.sdsc.edu/meme/intro.html>) to identify common motifs that may be putative E93 binding site. As a control, we also examined nucleotide sequences 1000 and 2000 bp upstream of the transcription start site of the genes that are transcribed in dying salivary glands but their levels are not so much altered during cell death in wild-type and *E93* mutant salivary glands. This helped us to eliminate common elements (such as TATA box) in many genes from true candidate E93 binding sites. Although we managed to identify sequences that may be candidate E93 binding sites, the lack of consistency across the E93 target genes decreased our confidence in this computational approach (Alva and Dutta, unpublished). We have also tried to identify E93 binding site by reverse mobility shift assay (Urness and Thummel, 1990), but we were unable to identify direct targets of E93 by this approach due to technical difficulties. Therefore, we decided to consider an alternative in-vivo chromatin immuno-precipitation assay (ChIP) approach to identify E93 target genes.

We generated transgenic animals that express full length of E93 protein fused to Myc-tag on both N- and C- termini that can be used for ChIP. Previous studies have shown that expression of E93 is sufficient to induce premature degradation of salivary glands (Lee et al., 2000). Therefore, we tested if expressions of Myc-tagged versions of E93 are sufficient to induce a similar phenotype. Control animals that contain UAS-E93-Myc combined with wild-type Canton S have intact salivary glands 6 hours after puparium formation (Figure 14A). By contrast, experimental animals that express E93-Myc in a salivary gland-specific manner lack this tissue 6 hours after puparium formation (Figure 14B). Importantly, we were able to express full-length 213-kDa E93 protein using Myc-tagged E93 transgenic animals during embryogenesis (*da-GAL4/UAS-E93-Myc*), while controls (*UAS-E93-Myc/Canton-S*; *da-GAL4/Canton-S*) lacked this protein expression (Figure 14C). Together these data indicate that expression of E93 is sufficient to induce cell death, and our data suggests that we can use ChIP to identify E93 targets in vivo.

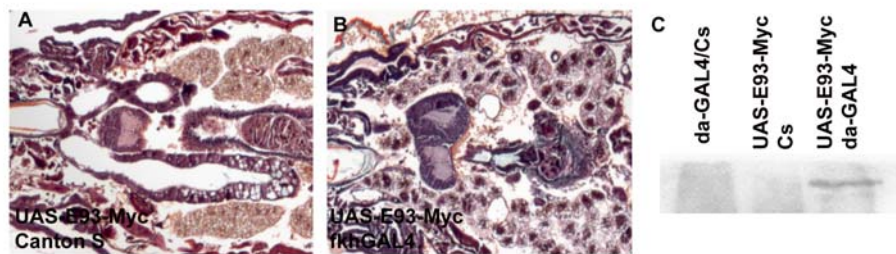


Figure 14. Ectopic expression of Myc-tagged E93 is sufficient to induce salivary gland cell death. (A-B) Paraffin sections of animals staged 6 hours after puparium formation. (A) In control animals (*UAS-E93Myc/Canton S*), salivary glands are present. (B) Expression of E93-Myc in a salivary gland-specific manner induces early cell death. (C) Immunoblot showing that full length E93 protein is expressed in experimental (*daughterless-GAL4/ UAS-E93Myc*) embryos, but not in control animals containing either the GAL4 driver (*daGAL4/Cs*) or the UAS transgene (*UAS-E93-Myc/Canton S*).

3.4 Discussion

Although much is known about the mechanisms that control apoptotic cell death, less is known about the regulation of autophagic cell death. Genetic analyses have revealed that *E93* is required for steroid triggered autophagic programmed cell death in *Drosophila* salivary glands. Here we show that expression of *E93* in the *Drosophila* eye is sufficient to induce caspase-dependent cell death. We have identified putative *E93* target genes using DNA microarrays, and preliminary results suggest that it will be possible to identify direct *E93* targets using ChIP.

In order to identify genes that function in the *E93*-induced autophagic cell death of salivary glands, we have taken a genomic approach by analyzing whole genome DNA microarrays. We have identified 100 gene transcripts that increase 3-fold or more in mRNA levels in wild-type salivary glands following the rise in ecdysone, but lack >80% or more of this change in RNA transcript level in *E93* mutant salivary glands. The identification of a large number of genes with reduced RNA levels in *E93* mutants suggests that *E93*-induced transcription may play an important role in cell death. It is promising to see that a large number of the genes that were identified using this approach have been previously associated with programmed cell death and salivary gland development (Table 4). We are using these putative target genes to identify in vivo *E93* targets by ChIP.

ChIP is a well-established procedure to investigate the *in vivo* interaction between DNA binding proteins and their target DNA (Orlando and Paro, 1993). ChIP involves chemical cross-linking of DNA-protein in living cells. Transcriptional regulation is complex in *Drosophila* and other organisms. While our DNA microarray approach has identified possible targets of E93, ChIP will enable us to determine if these are target gene promoters that are directly bound by E93 (Orlando et al., 1997). We hope to take advantage of whole-genome DNA microarrays along with ChIP (ChIP-chip) to create a high-resolution whole genome map of *in vivo* interactions between E93 and its target genes.

We identified *hpo* as a putative target of E93 that is required for autophagic cell death. Members of the Wts/Hpo tumor-suppressor signaling pathway regulate cell division, cell death and tissue growth (Harvey et al., 2003; Udan et al., 2003; Wu et al., 2003). Previous studies suggested that cell growth arrest is required for autophagy and degradation of salivary glands, as maintenance of growth by expression of either activated Ras, Dp110 or Akt was sufficient to inhibit these processes (Berry and Baehrecke, 2007). These were artificial experiments based on over-expression of growth regulators, however, and the identification of *hpo* as a candidate regulator of salivary gland cell death may provide insight into how growth arrest is regulated in salivary glands. Until now, studies of salivary glands have suggested that their death is regulated by a steroid-triggered transcriptional mechanism. The identification of *hpo* (a kinase) suggests that it is possible that both transcriptional and post-translational mechanisms

need to be integrated to regulate autophagic cell death. Additional studies are required to determine the relationship between cell growth and cell death, and how these processes are integrated.

3.5 Materials and Methods

Generation of *GMR-E93* and Myc-tagged E93 constructs

For the generation of GMR-E93, we isolated the *E93* open reading frame (ORF) by restriction digestion with KpnI and NdeI from an existing E93-pBluescript construct. We used one restriction enzyme at a time to isolate the E93 ORF, made that end blunt by T4 DNA polymerase treatment. Agarose gel-purified E93 ORF was then ligated into linearized pGMR vector (Hay et al., 1994). For generating N- and C-termini Myc-tagged E93 constructs, the 4 kb E93 ORF was PCR amplified from wild-type genomic DNA, and introduced into the recombination based *Drosophila* Gateway Vector system to obtain the final construct. All constructs were sequenced to determine the integrity of the E93 ORF and Myc fusion proteins. P-element-mediated transformation of these constructs into wild-type *w¹¹¹⁸ Drosophila melanogaster* was performed using standard procedures by BestGene Inc (Rubin and Spradling, 1982).

Salivary Gland Histology

For all studies, animals were reared and maintained at 25⁰C. For controls, wild-type Canton-S was crossed to either the experimental UAS-transgenic line, or the fkhGAL4/fkhGAL4 line. Animals of the indicated genotypes were aged to 6 and 24 hours after puparium formation at 25⁰C, fixed in FAAG, dehydrated, embedded in

paraffin, sectioned and stained with Weigert's Hematoxylin and Pollack Trichrome as previously described (Muro et al., 2006) and examined using Zeiss Axio Imager.Z1 microscope.

Protein Extracts and Western Blotting

Protein extracts were collected from embryos in control (wild-type Canton-S crossed to either *daughterless-GAL4* (*da-GAL4*) or *UAS-E93Myc*) and experimental (*da-GAL4; UAS-E93*) animals. Adults were allowed to lay eggs for 8 hours when embryos were harvested with phosphate buffer, washed several times, homogenized in Laemmli buffer (0.1% glycerol, 2%SDS, 0.125 M Tris (pH6.8), 0.05% β -mercaptoethanol, and 0.05% Bromo-phenol blue) and boiled for 5 minutes at 100⁰C. Equal amounts of proteins were separated on 10% SDS polyacrylamide gels. Proteins were transferred to 0.45 μ m Immobilon-P membranes (Millipore) following standard procedures. Duplicate gels of identical extracts were also assessed for equal loading and integrity by Coomassie blue staining solution (Bio-Rad). Membranes were blocked in 10% non-fat milk in PBS with 1% Tween 20 for 1 hour at 37⁰C, washed in PBS containing 1% Tween 20 at room temperature and incubated with mouse anti C-Myc (1:200) (Santa Cruz Biotechnology) primary antibody for overnight at 4⁰C. Next day the membrane was washed again in PBS containing 1% Tween 20 at room temperature and incubated with HRP-goat-anti mouse (1:2000) secondary antibody for 1 hour at room temperature. The membrane was then washed and developed using ECL detection reagents 1 and 2 (Amersham) and exposed to film.

Northern Blot Analysis

To determine *hpo* RNA transcript levels in larval salivary glands during prepupal and pupal developmental stages, total RNA was collected from wild-type Canton-S salivary glands staged 6, 8, 10, 12, and 14 hours following puparium formation at 25⁰C and analyzed by Northern Blot hybridization as previously described (Baehrecke and Thummel, 1995). Northern Blots were hybridized to detect *hpo* and *rp49* as a loading and transfer control. All probes were prepared using random labeling gel-purified DNA fragments (Stratagene Prime-It).

SEM

Fly heads were collected and fixed in 2.5% gluteraldehyde (Electron Microscopy Sciences) in PBS, and post-fixed in 1.5% osmium tetroxide (Stevens Metallurgical) in PBS. Samples were then dehydrated in serial dilutions of ethanol, immersed in hexamethyldisilazane (Polysciences Inc.) and dried in a dessicator for at least three days. Specimens were then mounted onto stubs, coated with gold: palladium using a Denton DV-503 vacuum evaporator and analyzed using an AMRAY 1820D scanning electron microscope.

Chapter 4

Warts is required for PI3K-regulated growth arrest, autophagy and autophagic cell death in *Drosophila*

4.1 Abstract

Cell growth arrest and autophagy are required for autophagic cell death in *Drosophila*. Maintenance of growth by expression of either activated Ras, Dp110, or Akt is sufficient to inhibit autophagy and cell death in *Drosophila* salivary glands, but the mechanism that controls growth arrest is unknown. While the Warts (Wts) tumor-suppressor is a critical regulator of tissue growth in animals, it is not clear how this signaling pathway controls cell growth. Here we show that genes in the Wts pathway are required for salivary gland degradation, and that *wts* mutants have defects in cell growth arrest, caspase activity, and autophagy. Expression of Atg1, a regulator of autophagy, in salivary glands is sufficient to rescue *wts* mutant salivary gland destruction. Surprisingly, expression of Yorkie (Yki) and Scalloped (Sd) in salivary glands fails to phenocopy *wts* mutants. By contrast, mis-expression of the Yki target *bantam* was able to inhibit salivary gland cell death, even though mutations in *bantam* fail to suppress the *wts* mutant salivary gland persistence phenotype. Significantly, *wts* mutant salivary glands possess altered phosphoinositide signaling, and decreased function of the class I PI3K pathway genes *chico* and *TOR* suppressed *wts* defects in cell death. Although we have previously shown that salivary gland degradation requires genes in the Wts pathway, this study provides the first evidence that Wts influences autophagy. Our data indicates that

the Wts pathway components Yki, Sd, and *bantam* fail to function in salivary glands, and that Wts regulates salivary gland cell death in a PI3K-dependent manner.

4.2 Introduction

Cell growth, division, and death are important determinants of tissue and animal size (Conlon and Raff, 1999), and disruption in their balance can lead to physiological disorders including cancer (Thompson, 1995). While the mechanisms that integrate cell division checkpoints with cell death are relatively well studied (Lowe et al., 2004), less is known about the relationship between cell growth and death.

Apoptosis and autophagic cell death are the two most prominent morphological forms of cell death that occur during animal development (Clarke, 1990; Schweichel and Merker, 1973). The mechanisms that regulate apoptosis have been extensively studied, but far less is known about autophagic cell death. *Drosophila* larval salivary glands are an excellent system for investigating autophagic cell death during development. A rise in the steroid hormone 20-hydroxyecdysone (ecdysone) 12 hours after puparium formation triggers future adult head eversion, salivary gland cell death, and the synchronized degradation of salivary gland cells is completed by 16 hours after puparium formation (Jiang et al., 1997). Both caspases and autophagy are induced following the rise in ecdysone that triggers cell death (Lee and Baehrecke, 2001; Martin and Baehrecke, 2004). Caspases and autophagy function in an additive manner in dying salivary glands, as evidenced by the finding that the combined inhibition of both caspases and autophagy

results in a stronger salivary gland persistence phenotype than inhibition of either caspases or autophagy alone (Berry and Baehrecke, 2007). Cell growth stops prior to salivary gland cell death, and maintenance of growth is sufficient to suppress both autophagy and degradation of this tissue (Berry and Baehrecke, 2007), but the mechanism that regulates this growth arrest is not clear.

The insulin-triggered class I phosphoinositide 3-kinase (PI3K) pathway is highly conserved and regulates cell and tissue growth (Kozma and Thomas, 2002). Binding of insulin to the insulin receptor leads to the phosphorylation of the receptor and the insulin receptor substrate protein Chico (Bohni et al., 1999). This phosphorylation cascade activates the catalytic subunit Dp110 of the class I PI3K pathway (Kozma and Thomas, 2002; Leever et al., 1996). Activated Dp110 converts phosphatidylinositol-4, 5-P (2) to the second messenger phosphatidylinositol-3, 4, 5-P (3) (PIP3). The pleckstrin homology (PH) domain of Akt interacts with PIP3 on the cell membrane and activates the downstream effector target-of-rapamycin (TOR), an evolutionarily conserved kinase (Wullschleger et al., 2006). TOR influences a wide range of cellular processes such as protein translation, cell cycle progression, growth and autophagy. Although activation of the class I PI3K pathway by expression of either activated Ras, Dp110, or Akt is sufficient to inhibit autophagy and degradation of salivary glands (Berry and Baehrecke, 2007), the mechanism that is responsible for the regulation of PI3K-dependent growth arrest in this tissue is not fully understood.

Recent studies in *Drosophila* have identified the evolutionarily conserved Warts (Wts) signaling pathway as an important regulator of tissue growth. Wts, Fat, Merlin (Mer), Expanded (Ex), Hippo (Hpo), Salvador (Sav), and Mats are members of a kinase cascade that negatively regulates tissue growth (Bennett and Harvey, 2006; Cho et al., 2006; Hamaratoglu et al., 2006; Harvey et al., 2003; Justice et al., 1995; Kango-Singh et al., 2002; Lai et al., 2005; Pantalacci et al., 2003; Silva et al., 2006; Tapon et al., 2002; Udan et al., 2003; Willecke et al., 2006; Wu et al., 2003; Xu et al., 1995). Mutations in any of these recessive genes causes increased cell division, and several of these mutants exhibit decreased cell death. These Wts pathway defects in cell division and cell death are caused by altered levels of the cell cycle regulator Cyclin E and the inhibitor of apoptosis DIAP1 (Tapon et al., 2002). Wts, also known as the large tumor suppressor Lats, encodes a NDR family kinase that phosphorylates the transcriptional coactivator Yorkie (Yki) (Huang et al., 2005), and inactivates Yki by exclusion from the nucleus (Dong et al., 2007). Yki, the orthologue of mammalian Yes associated protein Yap, is a positive regulator of growth, and over-expression of Yki results in overgrowth phenotypes in tissues that resemble loss-of-function mutations in members of the Wts pathway (Huang et al., 2005). Yki functions with the TEAD/TEF DNA binding family member protein Scalloped (Sd) to regulate transcription of the inhibitor of apoptosis *diap1* (Wu et al., 2008; Zhang et al., 2008), and presumably other Wts signaling targets, including the microRNA *bantam* and the cell cycle regulator *cyclin E* (Harvey et al., 2003; Nolo et al., 2006; Pantalacci et al., 2003; Thompson and Cohen, 2006; Wu et al., 2003). While mutations in Wts pathway genes, and over-expression of Yki, cause tissue

overgrowth, it is not clear how this pathway influences cell growth, and if the PI3K pathway is influenced by this tumor suppressor pathway.

Here we show that *wts* mutant salivary glands fail to arrest growth, exhibit decreased caspase activity, have attenuated autophagy, and are not degraded. Although previous studies indicate that expression of Yki phenocopies *wts* mutants, this was not the case in salivary glands. By contrast, expression of the Yki target *bantam* was sufficient to induce cell growth and inhibit salivary gland cell death. However, *bantam* loss-of-function mutations failed to suppress the *wts* mutant salivary gland persistence phenotype. These data suggest that Wts is capable of regulating growth and autophagy independent of Yki. *wts* mutants had altered PI3K markers and required the function of *TOR* and *chico* to inhibit salivary gland degradation. These data suggest that Wts influences the PI3K signaling pathway, growth, and autophagy in a manner that is distinct from its regulation of Yki.

4.3 Results

Wts, Sav and Mats are required for salivary gland degradation

Wts was identified as a protein that is expressed during autophagic cell death of *Drosophila* larval salivary glands using a high throughput proteomics approach (Martin et al., 2007). This was surprising, as we failed to detect *wts* RNA using DNA microarrays (Lee et al., 2003). Therefore, we investigated whether Wts is present in salivary glands, and determined that it is constitutively expressed at stages preceding and

following the rise in ecdysone that triggers autophagic cell death (Figure 15A).

Significantly, 2 forms of Hpo are expressed during stages preceding salivary gland cell death, suggesting that phosphorylated Hpo is present in these cells and that this signaling pathway is activated (Figure 15 A).

We had previously shown that animals that are homozygous for the hypomorphic *wts^{P2}* allele, that is caused by a P element insertion (Justice et al., 1995), are defective in salivary gland cell death (Martin et al., 2007). Since strong loss-of-function *wts* mutants are homozygous lethal prior to the stage of salivary gland cell death, we tested if the *wts^{P2}* allele in combination with the stronger X-ray-induced *lats^{X1}* allele (Xu et al., 1995) caused a defect in salivary gland degradation. In control animals, ecdysone-triggered head eversion occurs 12 hours after puparium formation and salivary glands are absent 24 hours after puparium formation (12 hours after head eversion) (Figures 15B). By contrast, *wts^{P2}/lats^{X1}* mutants fail to degrade salivary glands by 12 hours after head eversion (Figure 15C). Previous studies indicated that *hpo* is required to complete degradation of salivary glands (Martin et al., 2007). Therefore, we tested if other Wts pathway components are required for salivary gland degradation. While control animals had no salivary gland remnants 24 hours after puparium formation (Figure 15D), knock-down of *sav* by tissue-specific expression of RNAi (*sav*-IR) inhibited the degradation with 58% of the animals having incompletely degraded vacuolated cell fragments (Figure 15E). Similarly, knock-down of *mats* by tissue-specific expression of RNAi (*mats*-IR) inhibited the degradation with 62% of the animals possessing incompletely degraded

salivary gland cell fragments (Figure 15F). These data indicate that *wts*, *sav* and *mats* are required for degradation of salivary glands in *Drosophila*.

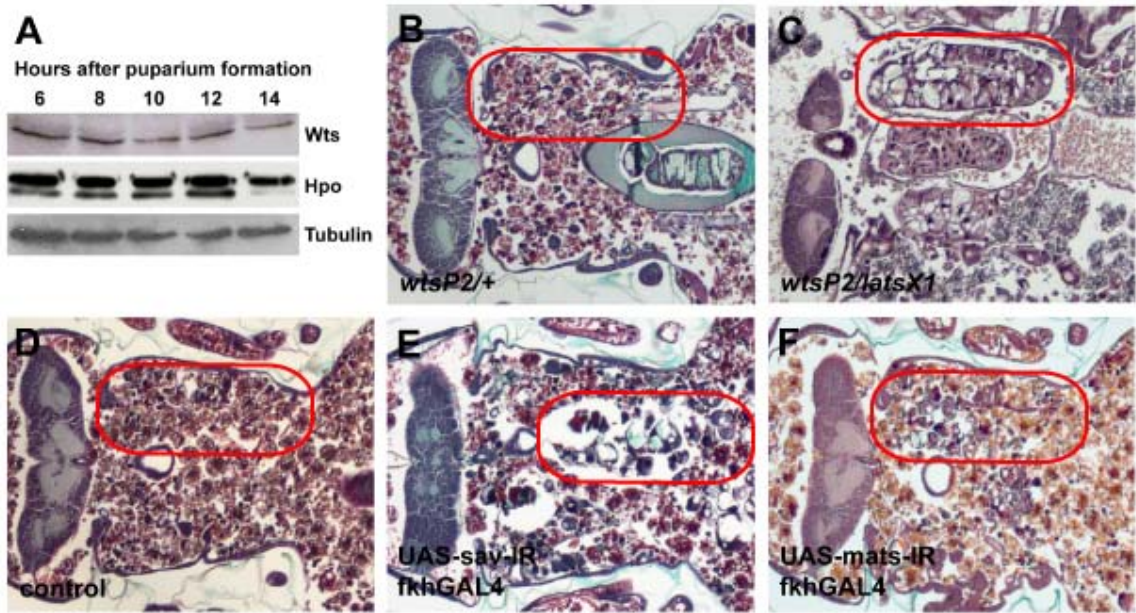


Figure 15. Wts signaling pathway is active and required for salivary gland degradation. (A) Immunoblot showing that Wts and Hpo are present in salivary glands at 6, 8, 10, 12 and 14 hours after puparium formation. (B-F) Paraffin sections of pupae 12 hours after head eversion. (B and D) Salivary glands are completely degraded in control animals. (C) Loss of *wts* in *wts^{P2}/lats^{X1}* inhibits salivary gland degradation. Expression of *sav-IR* (E) and *mats-IR* (F) in a tissue-specific manner causes incomplete degradation of salivary glands. Red circles outline the persistent or degraded salivary gland tissue in the pupae.

***wts* influences caspase activity, autophagy and cell growth**

Previous studies have shown that both caspases and autophagy are induced prior to and function in salivary gland autophagic cell death (Berry and Baehrecke, 2007; Lee and Baehrecke, 2001; Martin and Baehrecke, 2004). Therefore, we investigated whether caspases are altered in *wts* mutant salivary glands. Caspase-dependent DNA fragmentation was detected by TUNEL assay in both control *wts^{P2}/wild-type* and *wts^{P2}/wts^{P2}* mutant salivary glands 1.5 hours after head eversion even though *wts* mutant salivary glands fail to degrade (Figures 16A and 16B). Although *wts* mutant salivary glands appeared to possess approximately half as many TUNEL-positive nuclei compared to controls, the qualitative nature of this assay limits our ability to make strong conclusions about caspase activity based on this approach. Loss of nuclear lamins and increased levels of cleaved caspase-3 were also observed in both control and mutant salivary glands (data not shown). In addition, we detected caspase-3-like activity by cleavage of the caspase substrate DEVD-AMC in both *wts^{P2}/wild-type* control and *wts^{P2}/wts^{P2}* mutant animals 4 hours after puparium formation, although caspase-3-like activity was reduced in homozygous mutant animals (Figure 16C). Together, these data indicate that caspases are present but reduced in homozygous *wts^{P2}* mutant animals compared to controls.

The inhibitor of apoptosis DIAP1 suppresses caspases, functions downstream of *wts*, and DIAP1 was previously shown to be elevated in *wts* mutant cells (Harvey et al., 2003; Huang et al., 2005; Pantalacci et al., 2003; Tapon et al., 2002). Therefore, we

tested if expression of DIAP1 is sufficient to inhibit salivary gland autophagic cell death. In control animals, salivary glands are completely degraded 24 hours after puparium formation (Figure 16D). By contrast, salivary glands are partly degraded in DIAP1-expressing salivary glands (Figure 16E), which is consistent with previous studies indicating that salivary glands are partially degraded when caspases are blocked by either expression of p35, or caspase loss-of-function mutants (Berry and Baehrecke, 2007; Lee and Baehrecke, 2001; Martin and Baehrecke, 2004). Significantly, combined inhibition of caspases and autophagy by co-expression of DIAP1 and a dominant negative form of Atg1, Atg1^{KQ}, resulted in an almost complete inhibition of salivary gland cell death (Figure 16F). These results support the conclusion that both caspases and autophagy function in an additive manner during cell death of salivary glands.

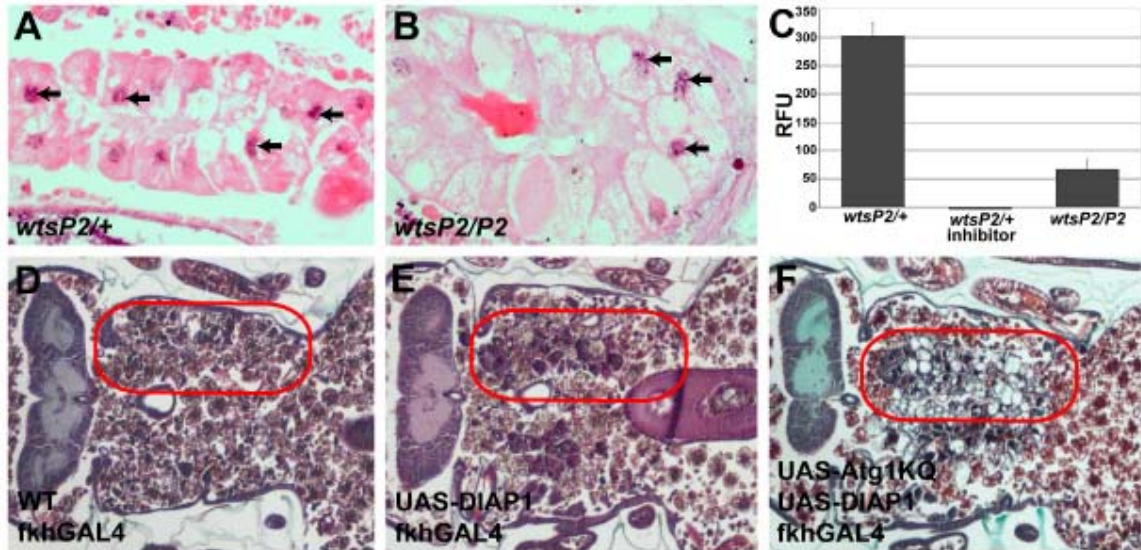


Figure 16. Caspases are reduced in *wts* mutants, and DIAP1-induced inhibition of salivary gland degradation is enhanced by reduced Atg1 function. (A-B)

Visualization of DNA fragmentation by TUNEL assay. TUNEL-positive nuclei are indicated by black arrowheads in both control *wts^{P2/+}* (A) and *wts* homozygous mutant *wts^{P2/P2}* (B) salivary glands. (C) Cleavage of the caspase-3-like substrate Z-DEVD-AMC was measured in whole pupae staged 4 hours after puparium formation in control (*wts^{P2/+}*), control plus Ac-DEVD-CHO inhibitor, and experimental *wts^{P2/P2}* mutant pupae. Data are presented as the mean ± SE, n = 3/treatment. (D-F) Paraffin sections 24 hours after puparium formation. (D) Salivary glands are completely degraded in control animals. (E) Partial degradation occurs in salivary glands expressing DIAP1. (F) Coexpression of dominant negative Atg1^{KQ} and DIAP1 increases the persistence of salivary glands. Red circles outline the persistent salivary gland tissue in the pupae.

The number of autophagosomes increases following the rise in steroid that triggers autophagic cell death of salivary glands, and autophagy is required for degradation of this tissue (Berry and Baehrecke, 2007; Lee and Baehrecke, 2001). Therefore, we analyzed the number of autophagosomes in dying salivary glands of control and *wts* mutants using the autophagy reporter GFP-LC3. Interestingly, the number of GFP-LC3 puncta were reduced in homozygous *wts^{P2}* mutant salivary glands compared to control *wts^{P2}/wild-type* salivary glands (Figure 17A - 17C). Previous studies have shown that expression of Atg1 is sufficient to induce autophagy (Berry and Baehrecke, 2007; Scott et al., 2007), so we tested if expression of Atg1 in *wts* mutant salivary glands is sufficient to suppress the *wts* mutant salivary gland degradation phenotype. While control *wts^{P2}/wts^{P2}* mutant animals all possess salivary glands 24 hours after puparium formation (Figures 17D and 17F), expression of Atg1 in salivary glands leads to almost complete degradation of this tissue in *wts^{P2}/wts^{P2}* animals (Figures 17E and 17F) even though they had salivary glands during early pupal stages (data not shown). Together these results indicate that decreased autophagy contributes to the cell death defect in *wts* mutant animals.

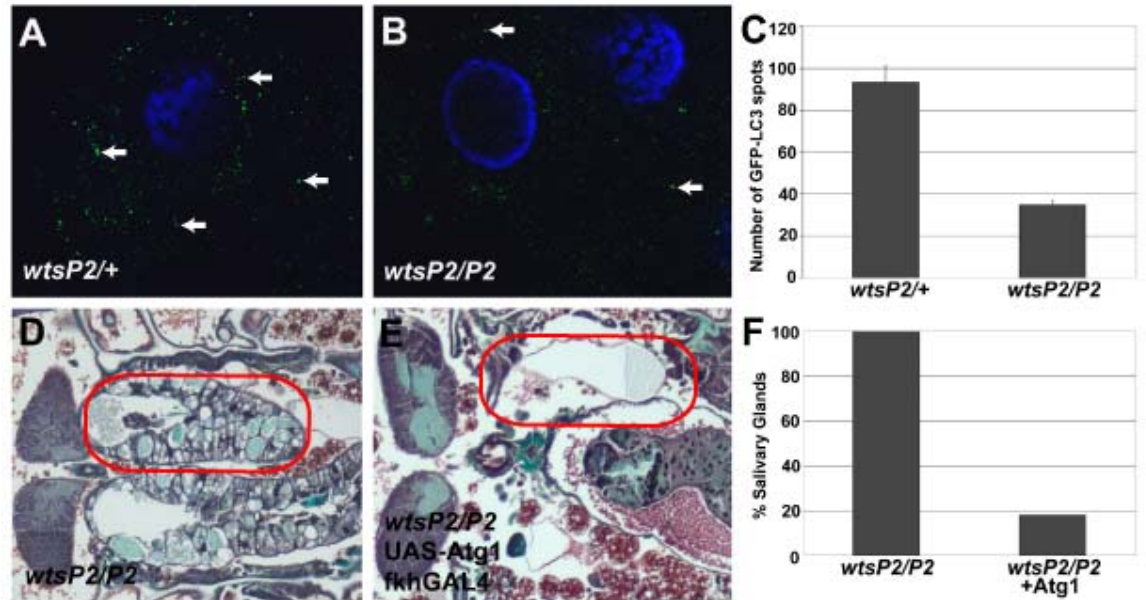


Figure 17. Autophagy is decreased in *wts* mutants, and expression of *Atg1* rescues *wts* salivary gland persistence. (A-C) Autophagy is indicated by the presence of GFP-LC3 puncta (autophagosomes) in salivary glands. (A and C) Abundant GFP-LC3 spots are detected in control salivary glands 1.5 hours after head eversion. (B and C) *wts* mutant salivary glands possess attenuated autophagy based on the detection of fewer GFP-LC3 spots than in control salivary glands. (D and E) Histological sections 12 hours after head eversion. (D and F) Loss of *wts* in *wts^{P2/P2}* animals prevent salivary gland degradation. (E and F) Expression of *Atg1* in *wts* mutant salivary glands suppresses the persistence phenotype. (F) Quantification of the percent of pupae with persistent salivary glands ($n > 20$ pupae/genotype). Red circles outline the persistent salivary gland tissue in the pupae.

Growth arrest is required for induction of autophagy and salivary gland degradation (Berry and Baehrecke, 2007). Therefore, we investigated whether decreased autophagy in *wts* mutants is associated with altered salivary gland cell growth by measuring the cell area in control *wts^{P2}/wild-type* and experimental *wts^{P2}/wts^{P2}* salivary glands. While the cell area of control and homozygous *wts^{P2}* mutant salivary gland cells were similar at the onset of puparium formation (Figures 18A and 18B), *wts^{P2}* mutant salivary gland cells were 2.5-fold larger than control salivary glands 6 hours after puparium formation (Figures 18C, 18D and 18E). We observed similar numbers of salivary gland nuclei in control *wts^{P2}/wild-type* (mean = 117.7, n = 15) and homozygous *wts^{P2}* mutants (mean = 118.9, n = 15), and the larval developmental period was similar in control and homozygous *wts^{P2}* mutants (Figure 18F). These data indicate that a failure in cell growth arrest at the onset of puparium formation is responsible for the larger size of *wts^{P2}* mutant salivary gland cells.

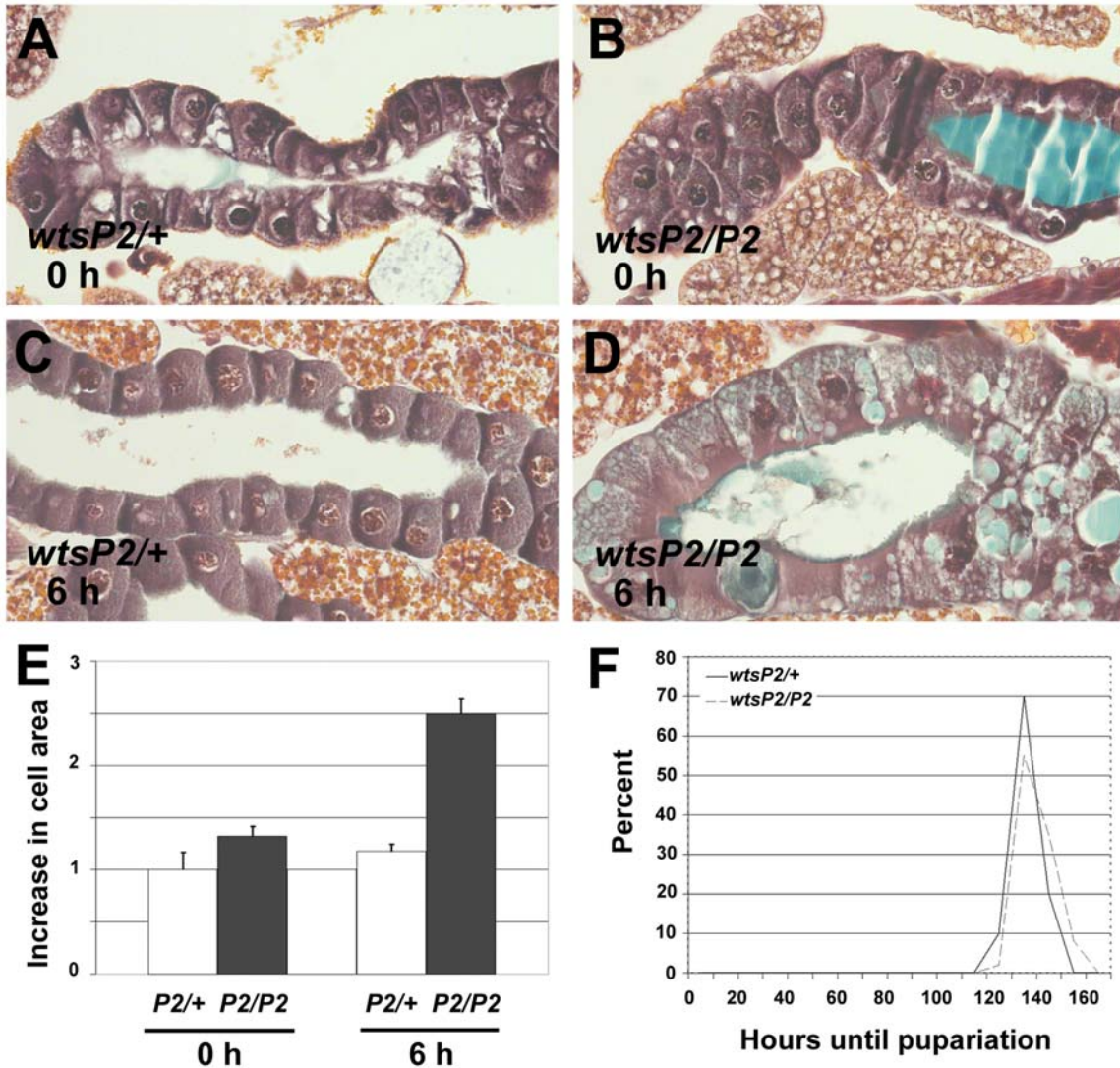


Figure 18. *wts* mutant salivary gland cells fail to arrest growth at pupariation. (A-D) Paraffin sections of salivary glands. (A, B and E) Cells of control *wts^{P2/+}* and mutant *wts^{P2/P2}* salivary glands are similar in size at puparium formation. (C, D and E) While control *wts^{P2/+}* salivary gland cells have not significantly increased in size by 6 hours after puparium formation, mutant *wts^{P2/P2}* salivary gland cells doubled in size during this period. (E) Cell area measurements of control and *wts* mutant salivary glands are presented as fold increase in cell area compared to control salivary gland cells at

puparium formation, and are presented as mean \pm SE. (F) Timing of pupariation in control (solid line) and *wts* mutant (dotted line) animals show that they have comparable developmental period.

Expression of Bantam, but not Yki and Sd, phenocopies *wts* in salivary glands

The transcriptional coactivator Yorkie (Yki) is phosphorylated by Wts inactivating its influence on cell cycle and cell death effectors (Huang et al., 2005). Yki, the DNA binding protein Sd, and their target the microRNA *bantam* are positive regulators of tissue growth (Huang et al., 2005; Nolo et al., 2006; Thompson and Cohen, 2006; Wu et al., 2008; Zhang et al., 2008). Over-expression of either Yki or *bantam* in developing adult eyes phenocopies *wts* loss-of-function mutants in this tissue (Huang et al., 2005; Nolo et al., 2006; Thompson and Cohen, 2006), and expression of Sd enhances Yki-induced growth and target gene activities (Zhang et al., 2008). Therefore, we tested if expression of Yki in salivary glands prevents the death of this tissue. Surprisingly, expression of Yki fails to inhibit salivary gland degradation (Figure 19B) even though expression of this transgene causes overgrowth in developing adult eyes (data not shown). In addition, expression of either Sd alone, or co-expression of Sd and Yki, induces premature degradation of salivary glands by 6 hours after puparium (Figures 19C and 20A). Expression of Yki alone failed to induce premature salivary gland cell death in animals 6 hours after puparium formation (Figure 19A). These data indicate that expression of neither Yki, Sd, nor Yki and Sd together phenocopies the loss-of-function phenotype of *wts* in salivary glands. Significantly, our data also indicate that the Wts pathway that has been described in developing adult *Drosophila* tissues is different in salivary glands. To test this possibility, we determined if DIAP1 levels are altered in *wts* mutant salivary glands. Indeed, DIAP1 protein levels are not altered in homozygous

wts^{P2} mutants (Figure 19D), further supporting our data that Wts alters salivary gland growth and cell death in a Yki- and Sd-independent manner.

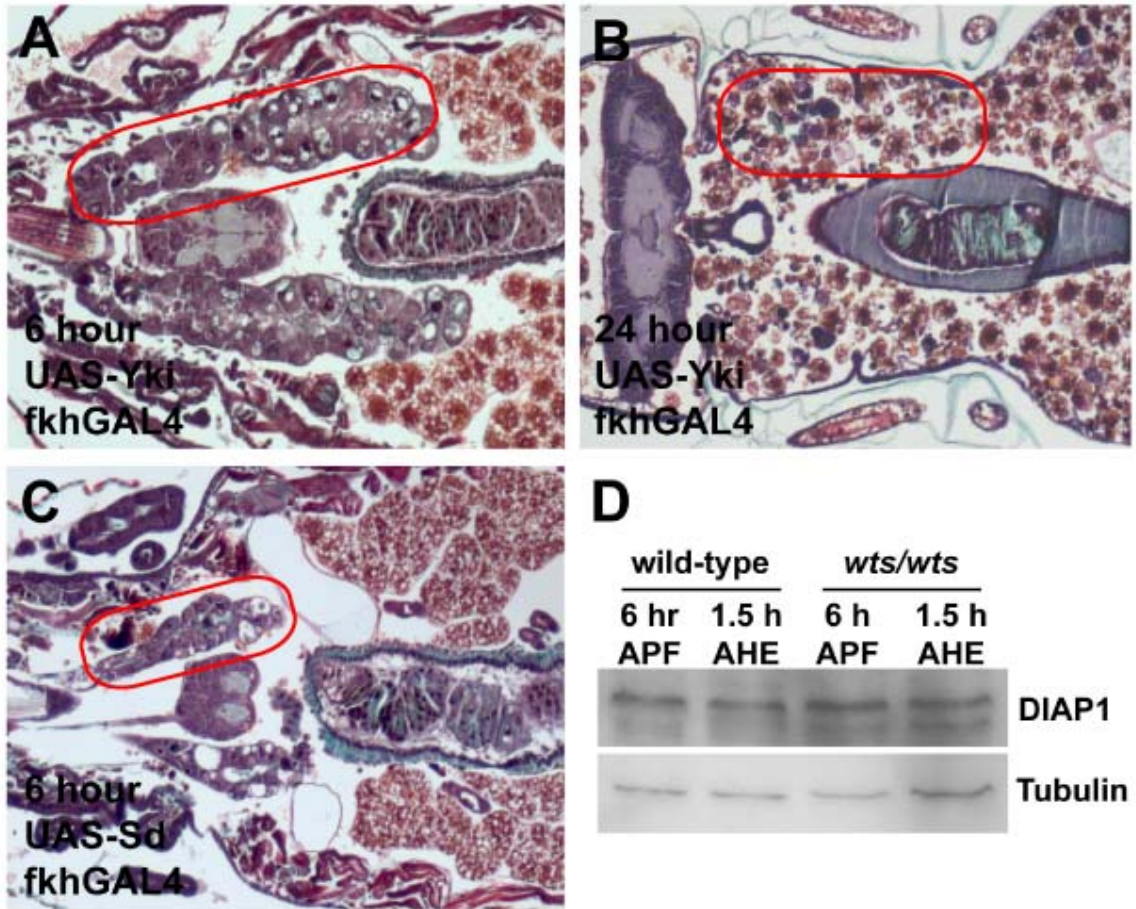


Figure 19. Expression of Yki and Sd fail to phenocopy the *wts* salivary gland phenotype, and DIAP1 levels are not altered in *wts* mutants. (A-C) Paraffin sections of animals 6 and 24 hours after puparium formation. (A) Paraffin sections of animals mis-expressing Yki in salivary glands at 6 hours after puparium formation have normal salivary glands. (B) Paraffin sections of animals mis-expressing Yki in salivary glands completely lack this tissue 24 hours after puparium formation. (C) Mis-expression of Sd in salivary glands causes premature degradation such that almost no tissue is present 6 hours after puparium formation. (D) Immunoblot showing the DIAP-1 levels are similar

in control ($wts^{P2/+}$) and wts mutant ($wts^{P2/P2}$) salivary glands. The lanes contain salivary gland extracts isolated from control and mutant animals staged at 6 hours after puparium formation (APF) and 1.5 hours after head eversion (AHE). Red circles outline the persistent and degraded salivary gland tissue in the pupae.

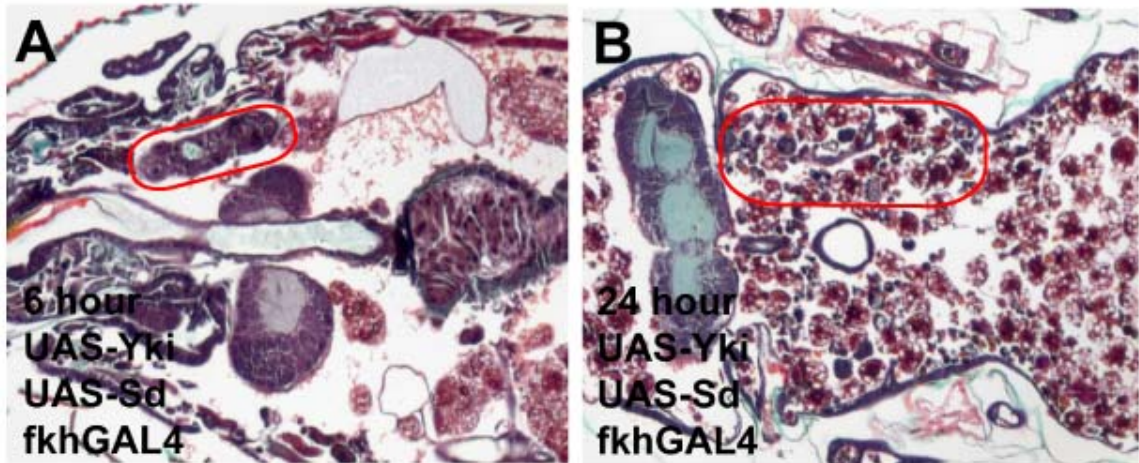


Figure 20. Co-Expression of Yki and Sd induces premature degradation of salivary glands. (A-B) Paraffin sections of animals co-expressing Yki and Sd. Expression of Yki and Sd in salivary glands leads to premature degradation of salivary glands at 6 hours after puparium formation (A) and salivary glands are completely degraded by 24 hours after puparium formation (B).

Our data suggests that salivary gland cells are not sensitive to Yki- and Sd-induced growth, but it is not clear if this is because of differences in the response of Yki and Sd target genes, or if Yki and Sd targets are not sufficient to induce the growth and inhibit degradation of these cells. Expression of DIAP1 is sufficient to inhibit complete salivary gland degradation (Figure 16E), but DIAP1 does not influence salivary gland cell growth (data not shown). By contrast, mis-expression of *bantam* in salivary glands was sufficient to inhibit salivary gland degradation and induce significant cell growth (Figure 21A and data not shown). Co-expression of dominant negative TOR (TOR^{ted}) with *bantam* failed to suppress the *bantam*-induced salivary gland persistence phenotype compared to control animals 24 hours after puparium formation (Figures 21B and 21C). In addition, loss-of-function mutations in the insulin receptor substrate orthologue *chico* also failed to suppress the *bantam*-induced defect in salivary gland degradation 24 hours after puparium formation (Figure 21D). Consistent with these genetic findings, mis-expression of *bantam* is not sufficient to maintain cortical localization of the reporter of Class I PI3K activity sensor tGPH sensor (data not shown). These data indicate that expression of *bantam*, but not Yki, phenocopies the loss-of-function phenotype of *wts*, but does so in a manner that is independent of two conserved genes in the PI3K pathway. These data support the conclusion that Yki and Sd target gene promoters, such as *bantam*, may not be active in salivary glands. Consistent with this conclusion, we failed to detect evidence of *bantam* RNA in late larval and prepupal salivary glands using a *bantam* sensor (data not shown). In addition, *bantam* loss-of-function mutants failed to suppress

the homozygous *wts* mutant salivary gland cell death phenotype (Figures 21E and 21F), even though *bantam* mutants animals are smaller as previously described (Hipfner et al., 2002). These data support the conclusion that Wts regulates growth and death of salivary glands using a mechanism that is different from the pathway that has been described in developing adult tissues of *Drosophila*.

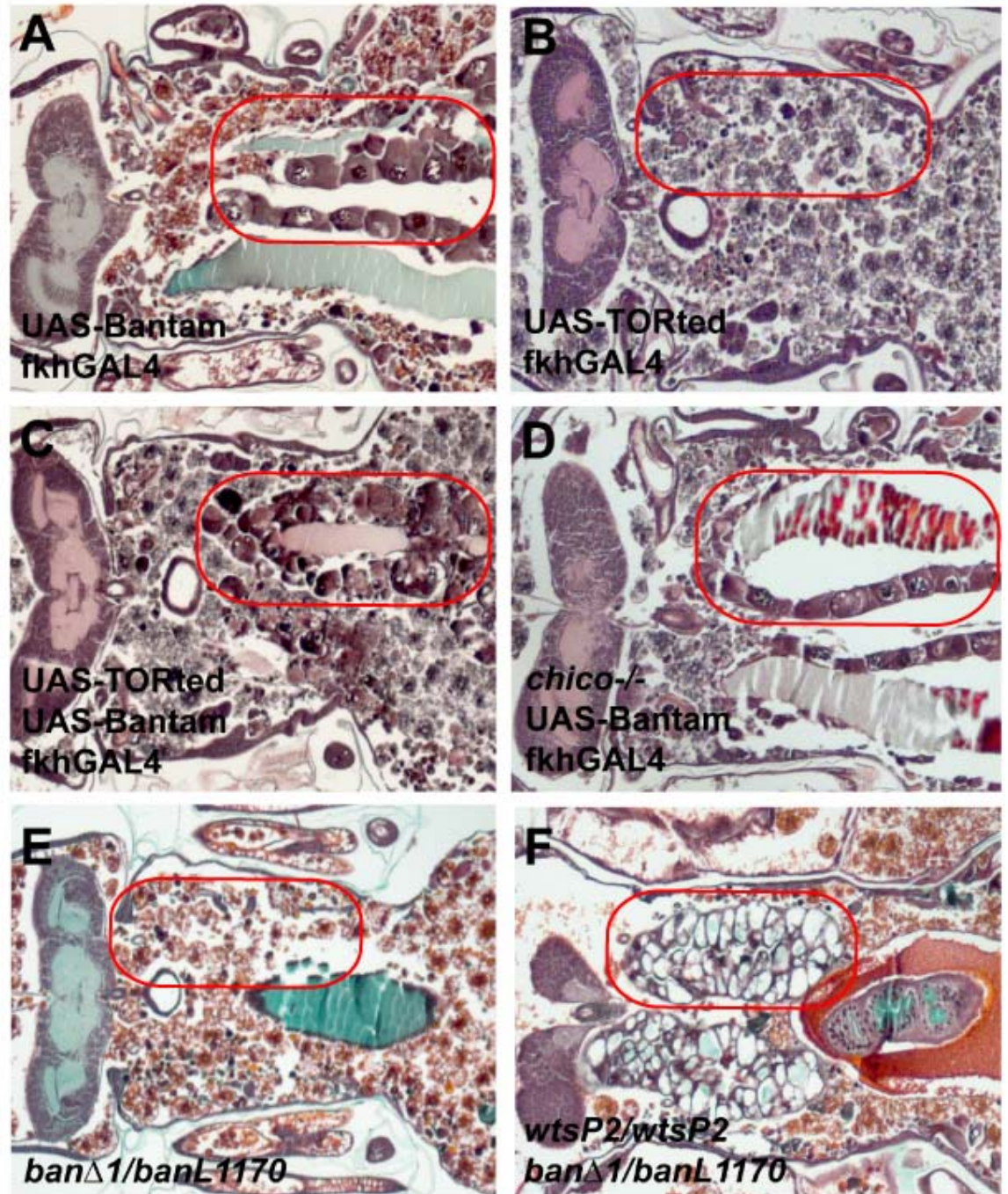


Figure 21. *bantam* mis-expression inhibits salivary gland degradation in a PI3K-independent manner. (A-F) Paraffin sections of animals 24 hours after puparium

formation. (A) Animals that mis-express *bantam* in salivary glands fail to degrade this tissue 24 hours after puparium formation. (B) Salivary glands expressing TOR^{ted} are degraded by 24 hours after puparium formation. (C) Coexpression of TOR^{ted} does not overcome inhibition of salivary gland removal caused by mis-expression of *bantam*. (D) *chico* mutants fail to suppress salivary gland persistence that is induced by mis-expression of *bantam*. (E) Salivary glands are degraded in *bantam* mutants (*ban^{A1}/ban^{L1170}*). (F) Salivary glands fail to degrade in *wts^{P2}* and *bantam* double-mutant animals. Red circles outline the persistent salivary gland tissue in the pupae.

PI3K signaling is required for *wts* to inhibit cell death

Maintenance of growth by expression of positive regulators of the class I PI3K pathway inhibits autophagy and salivary gland degradation (Berry and Baehrecke, 2007). Since Yki and Sd expression failed to phenocopy the *wts* mutant salivary gland phenotype, and *bantam* appears to regulate growth in a PI3K-independent manner, we investigated if *wts* may influence PI3K signaling. We monitored PI3K activity in salivary glands using the tGPH (tubulin-GFP-Pleckstrin Homology) reporter (Britton and Edgar, 1998; Britton et al., 2002). During the larval feeding stage when animals are growing, tGPH is cortically localized in salivary gland cells of both control and homozygous *wts* mutant animals (data not shown). The cortical localization of tGPH is lost in salivary glands of control *wts^{P2}/wild-type* animals when they stop feeding and growth arrest occurs (Figure 22A). By contrast, cortical localization of tGPH was maintained in *wts^{P2}/wts^{P2}* and *wts^{P2}/lats^{XI}* mutant animals even after the onset of puparium formation (data not shown) and continued during prepupal development (Figure 22B). Consistent with the larger salivary gland cell size of *wts^{P2}* mutants (Figures 18C, 18D, and 18E), these data indicate that *wts* mutant salivary gland cells fail to arrest growth at puparium formation.

The maintenance of growth and presence of tGPH at the cell cortex in *wts* mutant salivary glands suggests that the class I PI3K pathway remains activated following puparium formation in this tissue. Activation of Class I PI3K pathway causes recruitment of Akt to the plasma membrane where phosphorylated Akt initiates downstream signaling via TOR to regulate growth (Wullschleger et al., 2006). To our

surprise, the levels Akt and phosphorylated Akt were very similar in wild-type and *wts* mutant animals following growth arrest of salivary glands at the onset of puparium formation (Figures 22C and S2). However, immuno-localization of phosphorylated Akt changed from cortical (Figure 22D) to cytoplasmic in control salivary glands following puparium formation (Figure 22E), while much of the phosphorylated Akt remained associated with the cell cortex in homozygous *wts* mutant salivary glands (Figure 22F).

tGPH and phosphorylated Akt localization indicated that the class I PI3K pathway is altered in *wts* mutant salivary glands. Therefore, we investigated whether *wts* mutant salivary gland degradation is dependent on the PI3K pathway and TOR. Salivary glands are present in control *wts^{P2}/wts^{P2}* animals that possess a dominant negative TOR (UAS-TOR^{ted}) transgene that is not expressed because they lack the *fkhGAL4* activator (Figures 22G). By contrast, expression of TOR^{ted} in salivary glands suppressed the *wts* mutant degradation defect in this tissue (Figure 22H). Similarly, decreased function of the insulin receptor substrate encoding gene *chico* by expression of *chico*-RNAi in salivary glands attenuated the *wts* mutant salivary gland persistence phenotype (Figure 22I). Together these data indicate that Wts is regulating salivary gland degradation in a PI3K-dependent manner.

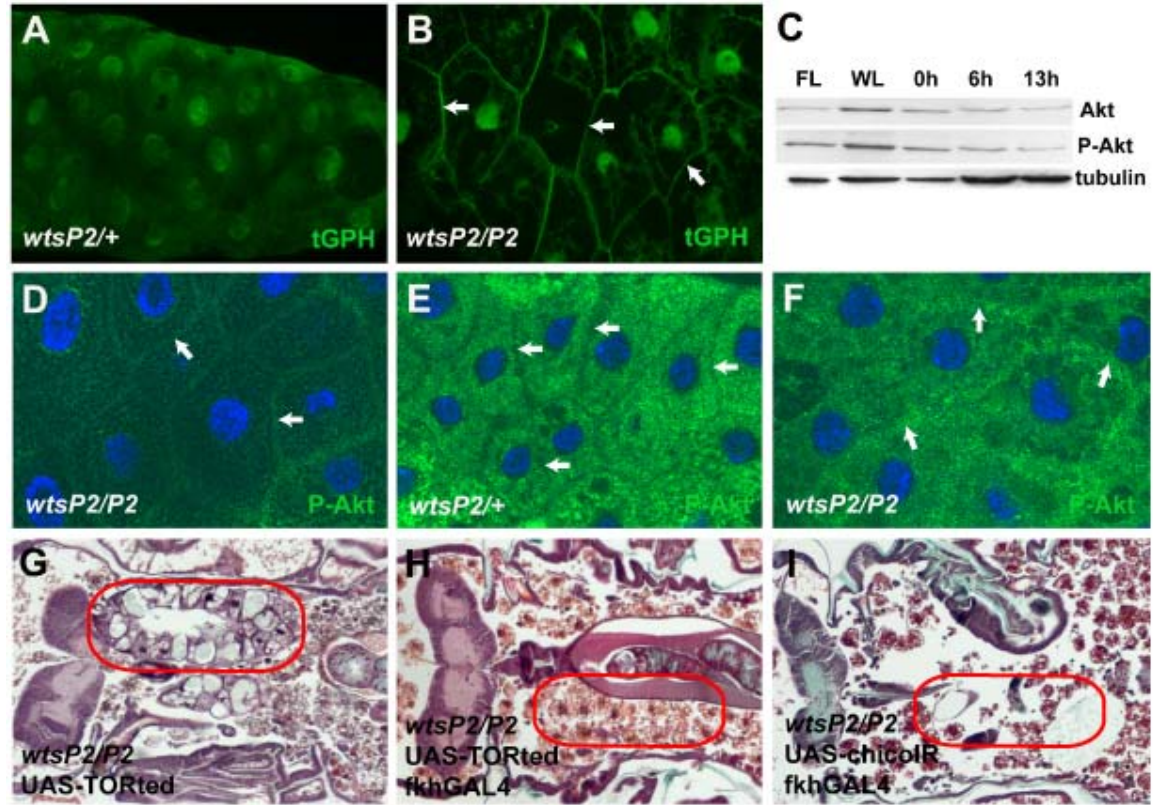


Figure 22. Wts regulates growth in a PI3K pathway-dependent manner. (A) Salivary glands of control *wts^{P2/+}* animals 6 hours after puparium formation lack cortical tGPH indicating that growth has arrested. (B) *wts* mutant (*wts^{P2/P2}*) salivary glands isolated 6 hours after puparium formation possess cortically localized tGPH indicating that they have not arrested growth. (C) Immunoblot showing the levels of Akt and its activated form phosphorylated Akt (P-Akt) in wild-type salivary glands during larval and pupal stages. The lanes contain salivary gland extracts isolated from feeding larvae (FL), wandering larvae (WL), and stages 0, 6, and 13 hours after puparium formation. (D-F) Salivary glands stained with anti-phospho-Akt (P-Akt). (D) Salivary glands from both control (not shown) and *wts* mutant feeding larvae contain P-Akt that is associated with the cell cortex (white arrows). (E) P-Akt changes localization to the cytosol and is

excluded from the cell cortex (white arrows) in control *wts*^{P2/+} 6 hours after puparium formation. (F) Although some P-Akt is relocalized in the cytosol, it remains associated with the cell cortex (white arrows) in *wts* mutant salivary gland cells 6 hours after puparium formation. (G-I) Paraffin sections of pupae 24 hours after puparium formation. (G) The presence of dominant negative TOR^{ted} without any GAL4 driver in *wts* mutant animals does not prevent salivary gland degradation. (H) Expression of TOR^{ted} in salivary glands of *wts* mutant animals results in complete degradation of salivary glands. (I) Decreased function of *chico* by expression of RNAi (*chico-IR*) in salivary glands suppresses the *wts* mutant persistent salivary gland phenotype. Red circles outline the persistent salivary gland tissue in the pupae.

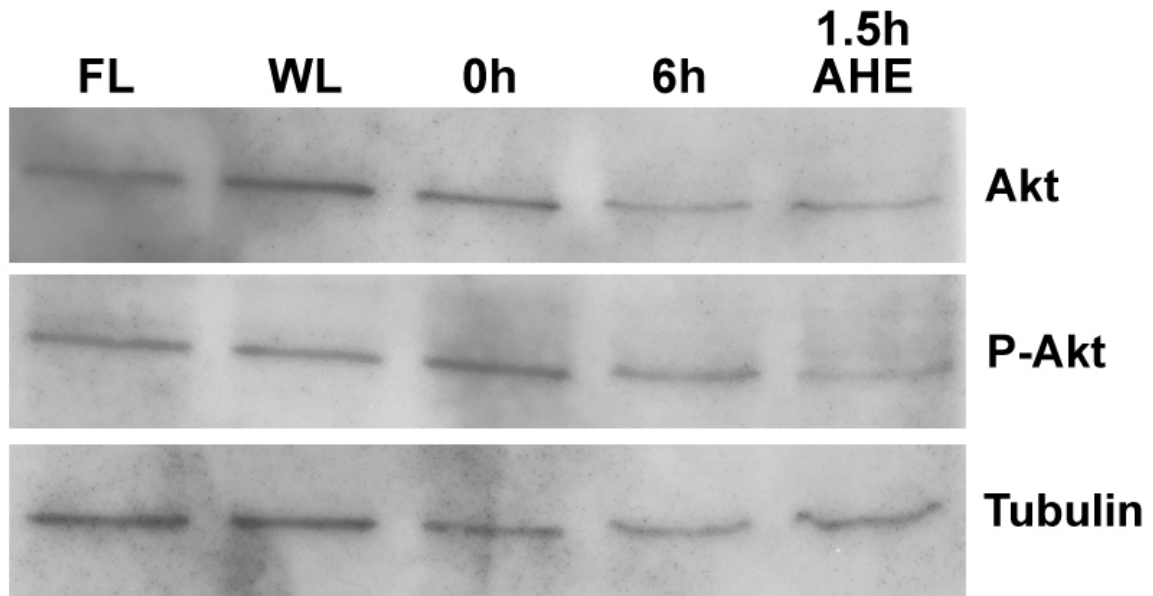


Figure 23. *wts* mutants do not have altered Akt and P-Akt protein levels in salivary glands. Immunoblot showing level of Akt and its activated form phosphorylated Akt (P-Akt) in salivary glands during larval and pupal stages in *wts^{P2}* homozygous mutant animals. The lanes contain salivary gland extracts isolated from feeding larvae (FL), wandering larvae (WL), 0 and 6 hours after puparium formation, and 1.5 hours after head eversion in *wts^{P2}* mutant animals.

4.4 Discussion

Our studies indicate that Wts and other core components of this tumor suppressor pathway are required for autophagic cell death of *Drosophila* salivary glands. *wts* is required for cell growth arrest, and proper regulation of caspases and autophagy that contribute to the destruction of salivary glands. Although it is well known that cell division, cell growth and cell death are important regulators of tissue and tumor size (Conlon and Raff, 1999), it has been unclear if a mechanistic relationship exists between cell growth and control of cell death.

It is possible that *wts*, and associated downstream growth regulatory mechanisms, could suppress cell death in other animals and cell types. Autophagic cell death morphology has been reported in diverse taxa (Baehrecke, 2002; Clarke, 1990), but we know little about the mechanisms that control this form of cell death, and this is likely related to the limited investigation of physiologically relevant models of this process. Here we have used steroid-activated autophagic cell death of salivary glands as a system to study the relationship between cell growth and cell death. It is logical that cell growth influences death in salivary glands, as autophagy is known to be regulated by class I PI3K signaling that contributes to the death of these cells (Berry and Baehrecke, 2007). It is unclear if growth arrest is a determinant of autophagic cell death in other cell types and animals, and this is important to resolve because of the importance of growth and autophagy in multiple disorders including cancer (Mizushima et al., 2008). *wts* mutant salivary gland cells fail to arrest growth at the onset of puparium formation, and this

suppresses the induction of autophagy. As previously reported, the inhibitor of apoptosis DIAP1 influences salivary gland cell death (Yin et al., 2007) and is one of the best characterized target genes of the Wts signaling pathway (Harvey et al., 2003; Pantalacci et al., 2003; Udan et al., 2003; Wu et al., 2003), but DIAP1 levels are not altered in *wts* mutant salivary glands. Significantly, our data provide the first evidence that Wts regulates autophagy, and support previous studies indicating that caspases and autophagy function in an additive manner during autophagic cell death (Berry and Baehrecke, 2007; Lee and Ambros, 2001). Given the importance of both the Wts pathway and autophagy in human health (Dong et al., 2007; Mizushima et al., 2008; Zeng and Hong, 2008), it is critical to determine if this relationship exists in other cells.

Cell growth and division are often considered to be synonymous even though they are controlled by independent mechanisms. The Wts signaling pathway must influence cell growth, but most studies have emphasized the influence of this pathway on cell division and death. *bantam* is the only previously studied gene that is regulated by the Wts pathway that is known to regulate cell growth (Nolo et al., 2006; Thompson and Cohen, 2006). However, the mechanism of *bantam* action remains obscure. Our studies suggest the possibility that Wts may regulate growth via different mechanisms, and that this may depend on cell context. It is premature to conclude that *bantam* regulates a completely novel cell growth program, but the fact that mis-expression of *bantam* stimulates cell growth in the absence of changes in a phosphoinositide marker, and that *chico* and *TOR* fail to suppress the *bantam*-induced salivary gland persistence phenotype,

minimally suggests that this microRNA regulates genes downstream of TOR. Significant progress has been made in the identification of microRNA targets (Burgler and Macdonald, 2005; Ruby et al., 2007; Stark et al., 2003), and future studies should resolve mechanism underlying *bantam* regulation of cell growth.

Recent studies of Wts signaling in *Drosophila* have identified a linear pathway that terminates with Yki and Sd regulation of effector genes that influence cell growth, cell division and cell death (Dong et al., 2007; Huang et al., 2005). Our studies indicate that the Wts pathway may not always regulate downstream effector genes via Yki and Sd, as Yki expression was not able to phenocopy the *wts* mutant salivary gland destruction, and expression of Sd induced premature degradation of salivary glands. Although *bantam* expression was sufficient to induce growth and inhibit cell death in salivary glands, *bantam* function was not required for the *wts* mutant phenotype. *wts* mutant salivary glands possess altered markers of PI3K signaling, and their defect in cell death is suppressed by *chico* and *TOR*. Combined, these results indicate that Wts regulates cell growth and cell death via a PI3K-dependent, and Yki- and Sd-independent, mechanism. Future studies will determine if Wts regulates cell growth in a PI3K-dependent manner in other cells and animals.

4.5 Materials and Methods

Drosophila Strains

For loss of function studies, *wts^{P2}* (Justice et al., 1995), *lats^{XI}* (Xu et al., 1995), *chico^I* (Bohni et al., 1999), and *ban^{A1}* (Hipfner et al., 2002) strains were analyzed. *sav-IR*, *mats-IR* and *chico-IR* stocks were obtained from the VDRC stock center. For ectopic expression studies, UAS-DIAP1 (Hay et al., 1995), UAS-Atg1^{KQ} (Scott et al., 2007), UAS-Atg1 (Scott et al., 2007), UAS-Yki (Huang et al., 2005), UAS-Sd (Simmonds et al., 1998), UAS-Bantam A (Brennecke et al., 2003), UAS-TOR^{ted} (Hennig and Neufeld, 2002) were used. UAS-GFP-LC3 (Rusten et al., 2004) was used as a marker of autophagy and tGPH served as a PI3K activity sensor (Britton et al., 2002). Canton-S wild-type was used as a control.

Protein Extracts and Western Blotting

Salivary glands were dissected from wild-type Canton S and *wts^{P2}* homozygous animals staged as feeding larvae, wandering larvae, and 0, 6, 8, 10, 12, and 14 hours following puparium formation at 25⁰C. Salivary glands were homogenized in Laemmli buffer (0.1% glycerol, 2%SDS, 0.125% 1M Tris (pH6.8), 0.05% β-mercaptoethanol, and 0.05% Bromo-phenol blue) and boiled for 5 minutes at 100⁰C. Equal amounts of proteins were separated on 10-12% SDS polyacrylamide gels. Proteins were transferred to 0.45μm Immobilon-P membranes (Millipore) following standard procedures. Blots were stripped using low pH stripping buffer (25mM glycine-HCl, pH 2, 15(w/v) SDS) between antibodies. Primary antibodies used were rabbit anti-Wts (1:5000)(Cho et al., 2006),

guineapig anti-Hpo (1:2000) (Hamaratoglu et al., 2006), mouse anti-DIAP1 (1:100) (Yoo et al., 2002), rabbit anti-Akt (1:1000) (Cell Signaling), rabbit anti-phospho-*Drosophila* Akt (Ser505)(1:1000)(Cell Signaling) and mouse anti-beta-Tubulin (1:50)(Developmental Studies Hybridoma Bank).

Caspase Substrate Assays

The EnzChek Caspase-3 Assay (Molecular Probes) was used for caspase substrate assays. Whole *wts^{P2}/Canton-S* (control) and *wts^{P2}/wts^{P2}* (experimental) pupae were staged at 4 hours after puparium formation, homogenized in lysis buffer and reaction buffer was added to the lysates. After centrifugation, clear lysates were assayed with Z-DEVD-AMC to detect caspase-3-like activity. To confirm the specificity of this assay to detect caspase-3-like activity, Ac-DEVD-CHO was added to the control (*wts^{P2}/Canton-S*) lysate as a competitive inhibitor. All the genotypes for caspase substrate assays were analyzed in triplicate.

Salivary Gland Histology

Animals of the indicated genotypes were aged to 6, 13.5 and 24 hours after puparium formation at 25⁰C, fixed in FAAG, dehydrated, embedded in paraffin, sectioned and stained with Weigert's Hematoxylin and Pollack Trichrome as previously described (Muro et al., 2006). TUNEL assay was performed using the Apoptag kit (Chemicon) as previously described (Lee and Baehrecke, 2001) and examined using Zeiss Axio Imager.Z1 microscope. For TUNEL assays, a minimum of 10 pupae were examined for

each genotype. For all other experiments, a minimum of 20 pupae were analyzed for each genotype. Cell area measurements were done using ImageJ software (Abraham and Shaham, 2004). Area measurements represent an average of at least 6 cells per salivary gland and a minimum of 7 animals for each genotype.

Fluorescence Microscopy

For autophagy assays, salivary glands of fkhGAL4; UAS-GFP-LC3; *wts^{P2}/wts^{P2}* experimental animals and fkhGAL4; UAS-GFP-LC3; *wts^{P2}/wild-type* controls were isolated 1.5 hr after head eversion, stained with Hoechst 33342, and imaged immediately as unfixed tissue using Zeiss Axio Imager.Z1 with apotome. The numbers of GFP-LC3 punctate spots were counted using Zeiss image counting software. To detect PI3K activity using the tGPH sensor, tGPH; *wts^{P2}/wts^{P2}* and fkhGAL4; tGPH/wild-type; UAS-Bantam A experimental, and tGPH/wild-type salivary glands were dissected from third instar larvae, staged 6 hours after puparium formation, and immediately imaged with a Zeiss Axio Imager.Z1 microscope. To count salivary gland nuclei, salivary glands were dissected from *wts^{P2}/wildtype* control and *wts^{P2}/wts^{P2}* experimental animals staged 6 hours after puparium formation. Dissected glands were then mounted with vectashield with DAPI (Vector Laboratories) and imaged using a Zeiss Axio Imager.Z1 with apotome. The numbers of nuclei per salivary gland was determined using Zeiss image counting software.

Immunohistochemistry

For immunohistochemistry, wts^{P2} /Canton-S control and wts^{P2}/wts^{P2} experimental salivary glands were dissected from feeding larvae and animals staged 6 hours after puparium formation, fixed with 4% paraformaldehyde, and processed according to standard procedures (Martin and Baehrecke, 2004). Rabbit anti-phospho-*Drosophila*-Akt (1:500)(Cell Signaling) and Toto-3 (Molecular Probes) were used to stain salivary glands, and they were imaged using Zeiss Axiovert confocal microscope.

Chapter 5

Conclusions and future directions

Cell growth, division and death are determinants of tissue and organ size; yet these processes are also influenced by environmental factors, availability of nutrients, neighboring cells and genetic factors (Conlon and Raff, 1999). Disruption of the balance between cell proliferation, growth and death can lead to physiological disorders, including cancer (Lowe et al., 2004). Although cell growth is a prerequisite for cell proliferation, it is unclear how cell growth and cell death are coordinated to maintain tissue and organ size. Apoptosis and autophagic cell death are the two most prominent morphological forms of programmed cell death (Clarke, 1990; Schweichel and Merker, 1973). While apoptotic cell death is well characterized, much less is known about autophagic cell death and its regulation of animal development. The recent association of autophagy with cancer and neurodegeneration indicates the importance of understanding how this catabolic process is regulated during cell death (Baehrecke, 2005; Levine and Klionsky, 2004; Yuan et al., 2003).

We are studying steroid activated autophagic programmed cell death in *Drosophila melanogaster*, using the larval salivary gland as a model. Salivary gland cell death is induced by a rise in the steroid hormone ecdysone 10 - 12 hours after puparium formation, and the rapid degradation of this tissue is completed by 16 hours after puparium formation (Jiang et al., 1997). Ecdysone acts through its EcR and Usp heterodimeric receptor complex, and with the help of competence factor $\beta FTZ-F1$,

activates the early cell death genes *BR-C*, *E74A* and *E93* (Broadus et al., 1999; Lee et al., 2002; Thomas et al., 1993; Woodard et al., 1994; Yao et al., 1992). These primary response genes then play a more direct role in cell death by influencing apoptotic cell death regulators *rpr*, *hid*, *croquemort*, *ark*, *drice* and *dronc* and the autophagy genes *atg2*, *atg4*, *atg5*, *atg7*, *atg9* during salivary gland programmed cell death (Lee et al., 2003; Lee et al., 2000).

Previous studies identified the ecdysone-regulated *E93* gene as a critical regulator of the spatial and temporal pattern of programmed cell death during *Drosophila* metamorphosis (Baehrecke and Thummel, 1995; Lee et al., 2000). A genetic screen for lethal mutations in the *E93* region resulted in the isolation of three pupal lethal mutations that fail to complement *Vno*, but complement *E93* mutants.. The distinct nature of the previously described lethal phases, complementation of adult viability, and phenotypes of *E93* and *Vno* mutants suggests that these are distinct genes, but our studies suggest that both *E93* and *Vno* are mutations in the *E93* transcript (Chapter 2). This is an example of intragenic complementation in which two mutations in the same gene complement each other. Therefore, our studies indicate *E93* is part of a complex genetic locus. This is not a novel concept, as other complex loci have been described in *Drosophila* including bithorax complex by E.B .Lewis (Duncan 2002). Similar to *E93*, mutations in Antennapedia have multiple complementation groups even though the molecular lesions are in the same gene (Duncan and Montgomery, 2002; Duncan and Kaufman, 1974). In support of this conclusion, specific allelic combinations of *E93^{vno}* mutants result in

salivary gland phenotypes, but it is not clear why *E93^{vno}* in combination with a deficiency does not result in defects in salivary gland cell death. While it is possible that one protein form of E93 affects larval cell death and the other protein form may influence differentiating cells, both *E93* and *Vno* mutations are in common regions of the protein. E93 is expressed in a stage and tissue specific manner (Baehrecke and Thummel, 1995; Lee et al., 2000), but we do not know if the specific protein forms of E93 are expressed in different cells and tissues at distinct stages. Future studies of E93 forms should help us resolve the complexity of E93. In addition, the identification of targets of these two forms of E93 protein will enable us to better understand the relationship between E93 and Vno.

Genetic studies indicate that *E93* functions in the regulation of steroid-triggered autophagic cell death. E93 encodes a nuclear protein that binds to specific chromosome sites in larval salivary gland polytene chromosomes (Lee et al., 2000), but specific target genes of this conserved helix-turn-helix protein remain unknown. The identification of downstream targets of E93 should enable us to identify novel cell death regulators and signaling pathways. We have developed tools to identify E93 targets (Chapter 3). Our preliminary characterization of GMR-E93 strains suggests that this tool will be useful for future genetic screens to identify suppressors of E93 induced cell death in the eye. In addition, we implemented a genome-wide approach by using DNA microarrays to identify candidate E93 downstream target genes (Clough et al., unpublished). A list of candidate E93 target genes was identified using DNA microarrays; we identified a large

list of genes that increase following the rise in ecdysone that triggers salivary gland cell death, but have reduced induction in *E93* mutants. We also generated transgenic animals that express full length of E93 protein that is fused to Myc with the hope that these animals can be used for chromatin immuno-precipitation assay (ChIP) (Chapter 3). Preliminary results from in-vivo ChIP suggest that E93 binds to genes that function in salivary gland cell death, including the caspase *dronc* (Dutta and Das, unpublished). We have also identified genes that have not been characterized yet. We hope to study the function of these genes in salivary gland cell death by either knocking-down or knocking out function of those genes by analyzing either animals expressing RNAi in salivary glands or loss-of-function mutants. Future analyses should identify in-vivo interactions between E93 and its target genes.

Recent studies have shown that cell growth arrest and autophagy are required for salivary gland degradation in *Drosophila* (Berry and Baehrecke, 2007). Maintenance of growth by expression of either activated Ras, Dp110 or Akt is sufficient to inhibit autophagy and block salivary gland degradation, but the exact mechanism of PI3K-dependent cell growth arrest and its relationship with cell death in this tissue were not well understood. We have shown that *wts*, *hpo*, *mats* and *sav* are required for complete salivary gland degradation (Chapter 4). *wts* influences salivary gland cell growth arrest and autophagy, and it regulates salivary gland degradation in a class I PI3K-dependent manner (Chapter 4). Our studies argue against the existing linear model of Wts signaling pathway in *Drosophila* that terminates with transcriptional regulators Yorkie (Yki) and

Scalloped (Sd) modulating effector genes that influence cell division, growth and death (Dong et al., 2007; Huang et al., 2005; Wu et al., 2008; Zhang et al., 2008). It is critical to identify the factor(s) in the PI3K pathway that are phosphorylated and modulated by Wts

Members of the Wts/Hpo signaling pathway are conserved in mammals and some of them have been implicated in cancer. Wts, a protein kinase, shows significant homology with the human myotonic dystrophy kinase. Although myotonic dystrophy is commonly defined as a neuromuscular disorder, it has been associated with multiple pilomatrixomas, rare epithelial tumors, and other tumors, including neurofibromas and parathyroid adenomas (Kopeloff et al., 1992; Reimund et al., 1992). The human orthologue of *salvador* (hWW45), is also found to be mutated in colon and renal cancer cell lines (Tapon et al., 2002). Mer is the fly homologue of mammalian *Neurofibromatosis type-2 (NF2)* encoded protein. Mutations in the tumor suppressor gene *NF2* cause development of tumor in the central nervous system (McClatchey, 2003; Rouleau et al., 1993; Trofatter and MacCollin, 1993). Similarly an essential autophagy gene Beclin 1, mammalian orthologue of Atg6/Vps30 is a haplosufficient tumor suppressor, and Beclin1 mutations are found with high frequency in human ovarian, breast and prostate cancers (Qu et al., 2003; Yue et al., 2003). Our studies indicate that Wts regulates autophagy, indicating the possible importance of autophagy in cancer. Future studies should enable us to understand the intricate balance between cell growth

and cell death in other cell contexts and in other higher organisms, and such discoveries may help us understand abnormal growth in the context of disorders, including cancer.

5.1 Revised model for genetic regulation of autophagic cell death of *Drosophila* salivary glands

The rise in the steroid hormone ecdysone that triggers the onset of metamorphosis is responsible for termination of larval growth in *Drosophila*. Cell growth arrest precedes and is required for developmental autophagic cell death of salivary glands (Berry and Baehrecke, 2007). Here, we show that the tumor suppressor pathway that includes Hpo, Wts, Mats, and Sav is required for cell growth arrest, autophagy and degradation of salivary glands (Figure 24). One of the most characterized downstream targets of Wts/Hpo tumor-suppressor pathway *Drosophila* inhibitor of apoptosis (DIAP1) is also known to be critical regulator of steroid activated salivary gland cell death (Yin et al., 2007), but DIAP1 levels remain unaltered in *wts* mutant salivary glands (Chapter 4). These data, combined with the fact that expression of neither Yki, Sd, nor Yki and Sd are sufficient to inhibit salivary gland cell death, suggests that the Hpo/Wts pathway influences salivary gland cell death in a manner that is different from previous models.

Our data indicate that Wts regulates class I PI3K signaling, but the precise mechanism of regulation is not clear. Although either decreased *chico* function or dominant negative TOR are capable of suppressing the *wts* phenotype in salivary glands, it is possible that Wts is regulating this pathway at the level of *chico* or the insulin

receptor. Since DIAP1 does regulate salivary gland cell death (Yin et al., 2007), this raises another question about how DIAP1 is regulated if Yki and Sd are not involved. Previous studies indicate that *diap1* and several other regulators of caspases are regulated by ecdysone and other regulators of transcription (Jiang et al., 2000; Lee and Baehrecke, 2001; Yin et al., 2007), and these data indicate that the Wts and ecdysone pathways must integrate information that is regulated at the levels of both RNA transcription and post-translation of proteins. Therefore, much work is needed to integrate the complex biochemical mechanisms that regulate salivary gland autophagic cell death. In addition, other *in vivo* models of autophagic cell death in flies and higher organism should determine if the mechanisms that are discovered in salivary glands occur in other cell types and organisms.

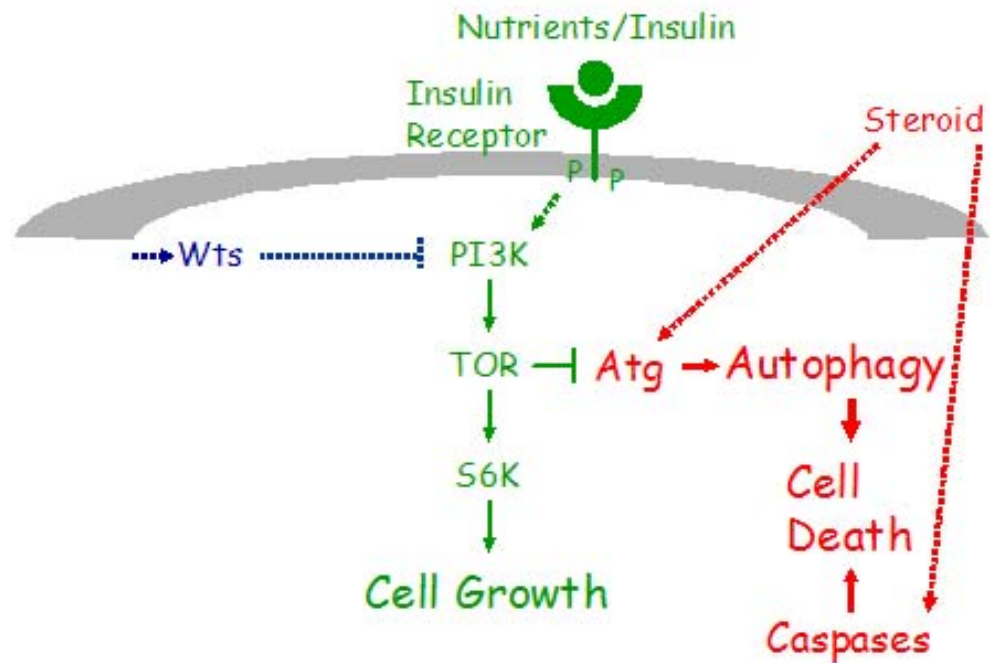


Fig 24 . Model for autophagic cell death in salivary glands. This model provides a relationship between steroid signaling, nutrient availability, cell growth and cell death. Nutrient availability regulates cell growth and autophagy via Target of Rapamycin (TOR). Wts regulates cell growth and autophagy by modulating PI3K pathway. Steroid signaling also modulates cell death by influencing transcription of many genes including regulators of caspases and autophagy.

References

- Abràmoff, M. D., Magelhaes, P. J., and Ram, S. J. (2004). Image processing with ImageJ. *Biophotonics Int 11*, 36-42.
- Abrams, J. M. (1999). An emerging blueprint for apoptosis in *Drosophila*. *Trends Cell Biol 9*, 435-440.
- Adams, J. M., and Cory, S. (1998). The Bcl-2 protein family: arbiters of cell survival. *Science 281*, 1322-1326.
- Alnemri, E. S., Livingston, D. J., Nicholson, D. W., Salvesen, G., Thornberry, N. A., Wong, W. W., and Yuan, J. (1996). Human ICE/CED-3 protease nomenclature. *Cell 87*, 171.
- Ambros, V. (2001). microRNAs: tiny regulators with great potential. *Cell 107(7)*, 823-826.
- Aravind, L., Dixit, V. M., and Koonin, E. V. (2001). Apoptotic molecular machinery: vastly increased complexity in vertebrates revealed by genome comparisons. *Science 291*, 1279-1284.
- Arico, S., Petiot, A., Bauvy, C., Dubbelhuis, P. F., Meijer, A. J., Codogno, P., and Ogier-Denis, E. (2001). The tumor suppressor PTEN positively regulates macroautophagy by inhibiting the phosphatidylinositol 3-kinase/protein kinase B pathway. *J Biol Chem 276*, 35243-35246.
- Arsham, A., and Neufeld, T. (2006). Thinking globally and acting locally with TOR. *Curr Opin Cell Bio 18(6)*, 589-597.
- Baba, M., Osumi, M., Scott, S., Klionsky, D., and Y, O. (1997). Two distinct pathways for targeting proteins from the cytoplasm to the vacuole/lysosome. *J Cell Biol 139*, 1687-1695.
- Baehrecke, E. H. (2000). Steroid regulation of programmed cell death during *Drosophila* development. *Cell Death & Differ 7*, 1057-1062.
- Baehrecke, E. H. (2002). How death shapes life during development. *Nature Reviews Mol Cell Biol 3*, 779-787.
- Baehrecke, E. H. (2005). Autophagy: dual roles in life and death? *Nature Reviews Mol Cell Biol 6*, 505-510.

- Bennett, F. C., and Harvey, K. F. (2006). Fat cadherin modulates organ size in *Drosophila* via the Salvador/Warts/Hippo signaling pathway. *Curr Biol* 16, 2101-2110.
- Berry, D. L., and Baehrecke, E. H. (2007). Growth arrest and autophagy are required for salivary gland cell degradation in *Drosophila*. *Cell* 131, 1137-1148.
- Bohni, R., Riesgo-Escovar, J., Oldham, S., Brogiolo, W., Stocker, H., Andruss, B. F., Beckingham, K., and Hafen, E. (1999). Autonomous control of cell and organ size by CHICO, a *Drosophila* homolog of vertebrate IRS1-4. *Cell* 97, 865-875.
- Brennecke, J., Hipfner, D. R., Stark, A., Russell, R. B., and Cohen, S. M. (2003). *bantam* encodes a developmentally regulated microRNA that controls cell proliferation and regulates the proapoptotic gene *hid* in *Drosophila*. *Cell* 113, 25-36.
- Britton, J. S., Lockwood, W. K., Li, L., Cohen, S. M., and Edgar, B. A. (2002). *Drosophila*'s insulin/PI3-kinase pathway coordinates cellular metabolism with nutritional conditions. *Dev Cell* 2, 239-249.
- Broadus, J., McCabe, J. R., Endrizzi, B., Thummel, C. S., and Woodard, C. T. (1999). The *Drosophila* β FTZ-F1 orphan nuclear receptor provides competence for stage-specific responses to the steroid hormone ecdysone. *Mol Cell* 3, 143-149.
- Brogiolo, W., Stocker, H., Ikeya, T., Rintelen, F., Fernandez, R., and Hafen, E. (2001). An evolutionarily conserved function of the *Drosophila* insulin receptor and insulin-like peptides in growth control. *Curr Biol* 11(4), 213-221.
- Burgler, C., and Macdonald, P. M. (2005). Prediction and verification of microRNA targets by MovingTargets, a highly adaptable prediction method. *BMC Genomics* 6, 88.
- Burtis, K. C., Thummel, C. S., Jones, C. W., Karim, F. D., and Hogness, D. S. (1990). The *Drosophila* 74EF early puff contains *E74*, a complex ecdysone-inducible gene that encodes two *ets*-related proteins. *Cell* 61, 85-99.
- Chen, P., Nordstrom, W., Gish, B., and Abrams, J. M. (1996). *grim*, a novel cell death gene in *Drosophila*. *Genes & Dev* 10, 1773-1782.
- Chen, P., Rodriguez, A., Erskine, R., Thach, T., and Abrams, J. M. (1998). *Dredd*, a novel effector of the apoptosis activators *Reaper*, *Grim*, and *Hid* in *Drosophila*. *Dev Biol* 201, 202-216.
- Cho, E., Feng, Y., Rauskolb, C., Maitra, S., Fehon, R., and Irvine, K. D. (2006). Delineation of a Fat tumor suppressor pathway. *Nat Genet* 38, 1142-1150.

- Clarke, P. G. H. (1990). Developmental cell death: morphological diversity and multiple mechanisms. *Anat Embryol* *181*, 195-213.
- Conlon, I., and Raff, M. (1999). Size control in animal development. *Cell* *96*, 235-244.
- Cryns, V., and Yuan, J. (1998). Proteases to die for. *Genes & Dev* *12*, 1551-1570.
- DiBello, P. R., Withers, D. A., Bayer, C. A., Fristrom, J. W., and Guild, G. M. (1991). The *Drosophila Broad-Complex* encodes a family of related proteins containing zinc fingers. *Genetics* *129*, 385-397.
- Dong, J., Feldmann, G., Huang, J., Wu, S., Zhang, N., Comerford, S. A., Gayyed, M. F., Anders, R. A., Maitra, A., and Pan, D. (2007). Elucidation of a universal size-control mechanism in *Drosophila* and mammals. *Cell* *130*, 1120-1133.
- Dorstyn, L., Colussi, P. A., Quinn, L. M., Richardson, H., and Kumar, S. (1999a). DRONC, an ecdysone-inducible *Drosophila* caspase. *Proc Natl Acad Sci USA* *96*, 4307-4312.
- Dorstyn, L., Read, S. H., Quinn, L. M., Richardson, H., and Kumar, S. (1999b). DECAY, a novel *Drosophila* caspase related to mammalian caspase-3 and caspase-7. *J Biol Chem* *274*, 30778-30783.
- Edgar, B. (2006). From cell structure to transcription: Hippo forges a new path. *Cell* *124*(2), 267-273.
- Ellis, R. E., and Horvitz, R. H. (1986). Genetic control of programmed cell death in the nematode *C. elegans*. *Cell* *44*, 817-829.
- Evans-Storm, R. B., and Cidlowski, J. A. (1995). Regulation of apoptosis by steroid hormones. *J Steroid Biochem Molec Biol* *53*, 1-6.
- Fernandez, R., Tabarini, D., Azpiazu, N., Frasch, M., and Schlessinger, J. (1995). The *Drosophila* insulin receptor homolog: a gene essential for embryonic development encodes two receptor isoforms with different signaling potential. *EMBO J* *14*, 3373-3384.
- Fraser, A. G., and Evan, G. I. (1997). Identification of a *Drosophila melanogaster* ICE/CED-3-related protease, drICE. *EMBO J* *16*, 2805-2813.
- Gao, X., Neufeld, T. P., and Pan, D. (2000). *Drosophila* PTEN regulates cell growth and proliferation through PI3K-dependent and -independent pathways. *Dev Biol* *221*, 404-418.
- Gao X, P. D. (2001). TSC1 and TSC2 tumor suppressors antagonize insulin signaling in cell growth. *Genes Dev* *15*, 1383-1392.

- Goberdhan, D. C., Paricio, N., Goodman, E. C., Mlodzik, M., and Wilson, C. (1999). *Drosophila* tumor suppressor PTEN controls cell size and number by antagonizing the Chico/PI3-kinase signaling pathway. *Genes Dev* 13, 3244-3258.
- Gorski, S. M., Chittaranjan, S., Pleasance, E. D., Freeman, J. D., Anderson, C. L., Varhol, R. J., Coughlin, S. M., Zuyderduyn, S. D., Jones, S. J., and Marra, M. A. (2003). A SAGE Approach to Discovery of Genes Involved in Autophagic Cell Death. *Curr Biol* 13, 358-363.
- Grether, M. E., Abrams, J. M., Agapite, J., White, K., and Steller, H. (1995). The *head involution defective* gene of *Drosophila melanogaster* functions in programmed cell death. *Genes & Dev* 9, 1694-1708.
- Halder, G., Polaczyk, P., Kraus, M., Hudson, A., Kim, J., Laughon, A., and Carroll, S. (1998). The Vestigial and Scalloped proteins act together to directly regulate wing-specific gene expression in *Drosophila*. *Genes Dev* 12(24), 3900-3909.
- Hamaratoglu, F., Willecke, M., Kango-Singh, M., Nolo, R., Hyun, E., Tao, C., Jafar-Nejad, H., and Halder, G. (2006). The tumour-suppressor genes NF2/Merlin and Expanded act through Hippo signalling to regulate cell proliferation and apoptosis. *Nat Cell Biol* 8, 27-36.
- Harvey, K. F., Pflieger, C. M., and Hariharan, I. K. (2003). The *Drosophila* Mst ortholog, hippo, restricts growth and cell proliferation and promotes apoptosis. *Cell* 114, 457-467.
- Hay, B. A., Wassarman, D. A., and Rubin, G. M. (1995). *Drosophila* homologs of baculovirus inhibitor of apoptosis proteins function to block cell death. *Cell* 83, 1253-1262.
- Hengartner, M. O., and Horvitz, H. R. (1994). *C. elegans* cell survival gene *ced-9* encodes a functional homolog of the mammalian proto-oncogene *bcl-2*. *Cell* 76, 665-676.
- Hennig, K. M., and Neufeld, T. P. (2002). Inhibition of cellular growth and proliferation by dTOR overexpression in *Drosophila*. *Genesis* 34, 107-110.
- Hipfner, D. R., Weigmann, K., and Cohen, S. M. (2002). The bantam gene regulates *Drosophila* growth. *Genetics* 161, 1527-1537.
- Huang, H., Potter, C. J., Tao, W., Li, D. M., Brogiolo, W., Hafen, E., Sun, H., and Xu, T. (1999). PTEN affects cell size, cell proliferation and apoptosis during *Drosophila* eye development. *Development* 126, 5365-5372.

- Huang, J., Wu, S., Barrera, J., Matthews, K., and Pan, D. (2005). The Hippo signaling pathway coordinately regulates cell proliferation and apoptosis by inactivating Yorkie, the *Drosophila* Homolog of YAP. *Cell* *122*, 421-434.
- Ichimura, Y., Kirisako, T., Takao, T., Satomi, Y., Shimonishi, Y., Ishihara, N., Mizushima, N., Tanida, I., Kominami, E., Ohsumi, M., *et al.* (2000). A ubiquitin-like system mediates protein lipidation. *Nature* *408*, 488-492.
- Jacobson, M. D., Weil, M., and Raff, M. C. (1997). Programmed Cell Death in Animal Development. *Cell* *88*, 347-354.
- Jiang, C., Baehrecke, E. H., and Thummel, C. S. (1997). Steroid regulated programmed cell death during *Drosophila* metamorphosis. *Development* *124*, 4673-4683.
- Jiang, C., Lamblin, A.-F. J., Steller, H., and Thummel, C. S. (2000). A steroid-triggered transcriptional hierarchy controls salivary gland cell death during *Drosophila* metamorphosis. *Mol Cell* *5*, 445-455.
- Justice, R. W., Zilian, O., Woods, D. F., Noll, M., and Bryant, P. J. (1995). The *Drosophila* tumor suppressor gene warts encodes a homolog of human myotonic dystrophy kinase and is required for the control of cell shape and proliferation. *Genes Dev* *9*, 534-546.
- Kabeya, Y., Mizushima, N., Ueno, T., Ohsumi, Y., and Yoshimori, T. (2000). LC3, a mammalian homologue of yeast Apg8p, is localized in autophagosome membranes after processing. *EMBO J* *19*(21), 5720-5728.
- Kamada, Y., Funakoshi, T., Shintani, T., Nagano, K., Ohsumi, M., and Ohsumi, Y. (2000). Tor-mediated induction of autophagy via an Apg1 protein kinase complex. *J Cell Biol* *150*, 1507-1513.
- Kango-Singh, M., Nolo, R., Tao, C., Verstreken, P., Hiesinger, P. R., Bellen, H. J., and Halder, G. (2002). Shar-pei mediates cell proliferation arrest during imaginal disc growth in *Drosophila*. *Development* *129*, 5719-5730.
- Kanuka, H., Sawamoto, K., Inohara, N., Matsuno, K., Okano, H., and Miura, M. (1999). Control of the cell death pathway by Dapaf-1, a *Drosophila* Apaf-1/CED-4-related caspase activator. *Mol Cell* *4*, 757-769.
- Kerr, J. F., Wyllie, A. H., and Currie, A. R. (1972). Apoptosis: a basic biological phenomenon with wide-ranging implications in tissue kinetics. *Br J Cancer* *26*, 239-257.

- Kihara, A., Kabeya, Y., Ohsumi, Y., and Yoshimori, T. (2001). Beclin-phosphatidylinositol 3-kinase complex functions at the trans-Golgi network. *EMBO Rep* 2(4), 330-335.
- Kim, J., Dalton, V. M., Eggerton, K. P., Scott, S. V., and Klionsky, D. J. (1999). Apg7p/Cvt2p is required for the cytoplasm-to-vacuole targeting, macroautophagy, and peroxisome degradation pathways. *Mol Biol Cell* 10, 1337-1351.
- Kirisako, T., Ichimura, Y., Okada, H., Kabeya, Y., Mizushima, N., Yoshimori, T., Ohsumi, M., Takao, T., Noda, T., and Ohsumi, Y. (2000). The reversible modification regulates the membrane-binding state of Apg8/Aut7 essential for autophagy and the cytoplasm to vacuole targeting pathway. *J Cell Biol* 151, 263-276.
- Klionsky, D. J., and Emr, S. D. (2000). Autophagy as a regulated pathway of cellular degradation. *Science* 290, 1717-1721.
- Kozma, S. C., and Thomas, G. (2002). Regulation of cell size in growth, development and human disease: PI3K, PKB and S6K. *Bioessays* 24, 65-71.
- Lai, Z. C., Wei, X., Shimizu, T., Ramos, E., Rohrbaugh, M., Nikolaidis, N., Ho, L. L., and Li, Y. (2005). Control of cell proliferation and apoptosis by mob as tumor suppressor, mats. *Cell* 120, 675-685.
- Lee, C.-Y., and Baehrecke, E. H. (2001). Steroid regulation of autophagic programmed cell death during development. *Development* 128, 1443-1455.
- Lee, C.-Y., Clough, E. A., Yellon, P., Teslovich, T. M., Stephan, D. A., and Baehrecke, E. H. (2003). Genome-wide analyses of steroid- and radiation-triggered programmed cell death in *Drosophila*. *Curr Biol* 13, 350-357.
- Lee, C.-Y., Simon, C. R., Woodard, C. T., and Baehrecke, E. H. (2002). Genetic mechanism for the stage- and tissue-specific regulation of steroid-triggered programmed cell death in *Drosophila*. *Dev Biol* 252, 138-148.
- Lee, C.-Y., Wendel, D. P., Reid, P., Lam, G., Thummel, C. S., and Baehrecke, E. H. (2000). *E93* directs steroid-triggered programmed cell death in *Drosophila*. *Mol Cell* 6, 433-443.
- LeEVERS, S. J., Weinkove, D., MacDougall, L. K., Hafen, E., and Waterfield, M. D. (1996). The *Drosophila* phosphoinositide 3-kinase Dp110 promotes cell growth. *EMBO J* 15, 6584-6594.
- Levine, B., and Kroemer, G. (2008). Autophagy in the Pathogenesis of Disease. *Cell* 132, 27-42.

- Li, P., Nijhawan, D., Budihardjo, I., Srinivasula, S. M., Ahmad, M., Alnemri, E. S., and Wang, X. (1997). Cytochrome c and dATP-dependent formation of Apaf-1/Caspase-9 complex initiates an apoptotic protease cascade. *Cell* *91*, 479-489.
- Liang, X. H., Jackson, S., Seaman, M., Brown, K., Kempkes, B., Hibshoosh, H., and Levine, B. (1999). Induction of autophagy and inhibition of tumorigenesis by *beclin 1*. *Nature* *402*, 672-676.
- Lietzke, S., Bose, S., Cronin, T., Klarlund, J., Chawla, A., Czech, M., and Lambright, D. (2000). Structural basis of 3-phosphoinositide recognition by pleckstrin homology domains. *Mol Cell* *6*(2), 385-394.
- Liu, Z., Sun, C., Olejniczak, E. T., Meadows, R. P., Betz, S. F., Oost, T., Herrmann, J., Wu, J. C., and Fesik, S. W. (2000). Structural basis for binding of Smac/DIABLO to the XIAP BIR3 domain. *Nature* *408*, 1004-1008.
- Lockshin, R. A., and Williams, C. M. (1965). Programmed cell death-I. Cytology of degeneration in the intersegmental muscles of the pernyi silkworm. *J Insect Physiol* *11*, 123-133.
- Lowe, S. W., Cepero, E., and Evan, G. (2004). Intrinsic tumour suppression. *Nature* *432*, 307-315.
- Martin, D. N., and Baehrecke, E. H. (2004). Caspases function in autophagic cell death in *Drosophila*. *Development* *131*, 275-284.
- Martin, D. N., Balgley, B., Dutta, S., Chen, J., Rudnick, P., Cranford, J., Kantartzis, S., DeVoe, D. L., Lee, C., and Baehrecke, E. H. (2007). Proteomic analysis of steroid-triggered autophagic programmed cell death during *Drosophila* development. *Cell Death Differ* *14*, 916-923.
- Matsuura, A., Tsukada, M., Wada, Y., and Ohsumi, Y. (1997). Apg1p, a novel protein kinase required for the autophagic process in *Saccharomyces cerevisiae*. *Gene* *192*(2), 245-250.
- Mizushima, N., Kuma, A., Ohsumi, Y., and Yoshimori, T. (2003). Mouse Apg16L, a novel WD-repeat protein, targets to the autophagic isolation membrane with the Apg12-Apg5 conjugate. *J Cell Sci* *116*(Pt 9), 1679-1688.
- Mizushima, N., Levine, B., Cuervo, A. M., and Klionsky, D. J. (2008). Autophagy fights disease through cellular self-digestion. *Nature* *451*, 1069-1075.

Mizushima, N., Noda, T., Yoshimori, T., Tanaka, Y., Ishii, T., George, M. D., Klionsky, D. J., Ohsumi, M., and Ohsumi, Y. (1998). A protein conjugation system essential for autophagy. *Nature* 395, 395-398.

Montagne, J., Stewart, M., Stocker, H., Hafen, E., Kozma, S., and Thomas, G. (1999). *Drosophila* S6 kinase: a regulator of cell size. *Science* 285(5436), 2126-2129.

Muro, I., Berry, D. L., Huh, J. R., Chen, C. H., Huang, H., Yoo, S. J., Guo, M., Baehrecke, E. H., and Hay, B. A. (2006). The *Drosophila* caspase Ice is important for many apoptotic cell deaths and for spermatid individualization, a nonapoptotic process. *Development* 133, 3305-3315.

Nolo, R., Morrison, C. M., Tao, C., Zhang, X., and Halder, G. (2006). The bantam microRNA is a target of the hippo tumor-suppressor pathway. *Curr Biol* 16, 1895-1904.

Oatey, P., Venkateswarlu, K., Williams, A., Fletcher, L., Foulstone, E., Cullen, P., and Tavaré, J. (1999). Confocal imaging of the subcellular distribution of phosphatidylinositol 3,4,5-trisphosphate in insulin- and PDGF-stimulated 3T3-L1 adipocytes. *Biochem J* 344 Pt 2, 511-518.

Oh, H., and Irvine, K. (2008). In vivo regulation of Yorkie phosphorylation and localization. *Development* 135(6), 1081-1088.

Ohsumi, Y. (2001). Molecular dissection of autophagy: two ubiquitin-like systems. *Nature Reviews Mol Cell Biol* 2, 211-216.

Pan, D., Dong, J., Zhang, Y., and Gao, X. (2004). Tuberous sclerosis complex: from *Drosophila* to human disease. *Trends Cell Biol* 14(2), 78-85.

Pantalacci, S., Tapon, N., and Leopold, P. (2003). The Salvador partner Hippo promotes apoptosis and cell-cycle exit in *Drosophila*. *Nat Cell Biol* 5, 921-927.

Petiot, A., Ogier-Denis, E., Blommaert, E. F., Meijer, A. J., and Codogno, P. (2000). Distinct classes of phosphatidylinositol 3'-kinases are involved in signaling pathways that control macroautophagy in HT-29 cells. *J Biol Chem* 275, 992-998.

Raff, M. C. (1992). Social controls on cell survival and cell death. *Nature* 356, 397-400.

Rameh, L., and Cantley, L. (1999). The role of phosphoinositide 3-kinase lipid products in cell function. *J Biol Chem* 274(13), 8347-8350.

Raught, B., Peiretti, F., Sonenberg, N., and Hershey, J. (2004). Phosphorylation of eucaryotic translation initiation factor 4B Ser422 is modulated by S6 kinases. *23(8)*, 1761-1769.

- Reggiori, F., and Klionsky, D. J. (2002). Autophagy in the eukaryotic cell. *Eukaryot Cell* 1, 11-21.
- Rintelen, F., Stocker, H., Thomas, G., and Hafen, E. (2001). PDK1 regulates growth through Akt and S6K in *Drosophila*. *Proc Natl Acad Sci U S A* 98(26), 15020-15025.
- Rodriguez, A., Oliver, H., Zou, H., Chen, P., Wang, X., and Abrams, J. M. (1999). Dark is a *Drosophila* homologue of Apaf-1/CED-4 and functions in an evolutionarily conserved death pathway. *Nat Cell Biol* 1, 272-279.
- Rubin, G. M., and Lewis, E. B. (2000). A brief history of *Drosophila's* contributions to genome research. *Science* 287, 2216-2218.
- Ruby, J. G., Stark, A., Johnston, W. K., Kellis, M., Bartel, D. P., and Lai, E. C. (2007). Evolution, biogenesis, expression, and target predictions of a substantially expanded set of *Drosophila* microRNAs. *Genome Res* 17, 1850-1864.
- Rusten, T. E., Lindmo, K., Juhasz, G., Sass, M., Seglen, P. O., Brech, A., and Stenmark, H. (2004). Programmed autophagy in the *Drosophila* fat body is induced by ecdysone through regulation of the PI3K pathway. *Dev Cell* 7, 179-192.
- Saucedo, L., Gao, X., Chiarelli, D., Li, L., Pan, D., and Edgar, B. (2003). Rheb promotes cell growth as a component of the insulin/TOR signalling network. *Nat Cell Biol* 5(6), 566-571.
- Schweichel, J.-U., and Merker, H.-J. (1973). The morphology of various types of cell death in prenatal tissues. *Teratology* 7, 253-266.
- Scott, R. C., Juhász, G., and Neufeld, T. P. (2007). Direct induction of autophagy by Atg1 inhibits cell growth and induces apoptotic cell death. *Curr Biol* 17, 1-11.
- Scott, R. C., Schuldiner, O., and TP., N. (2004). Role and regulation of starvation-induced autophagy in the *Drosophila* fat body. *Dev Cell* 7, 167-178.
- Scott, S., Hefner-Gravink, A., Morano, K., Noda, T., Ohsumi, Y., and Klionsky, D. (1996). Cytoplasm-to-vacuole targeting and autophagy employ the same machinery to deliver proteins to the yeast vacuole. *Proc Natl Acad Sci U S A* 93(22), 12304-12308.
- Shintani, T., Mizushima, N., Ogawa, Y., Matsuura, A., Noda, T., and Ohsumi, Y. (1999). Apg10p, a novel protein-conjugating enzyme essential for autophagy in yeast. *EMBO J* 18, 5234-5241.

- Silva, E., Tsatskis, Y., Gardano, L., Tapon, N., and McNeill, H. (2006). The tumor-suppressor gene fat controls tissue growth upstream of expanded in the hippo signaling pathway. *Curr Biol* *16*, 2081-2089.
- Simmonds, A. J., Liu, X., Soanes, K. H., Krause, H. M., Irvine, K. D., and Bell, J. B. (1998). Molecular interactions between Vestigial and Scalloped promote wing formation in *Drosophila*. *Genes Dev* *12*, 3815-3820.
- Sliter, T. J., and Gilbert, L. I. (1992). Developmental arrest and ecdysteroid deficiency resulting from mutations at the *dre4* locus of *Drosophila*. *Genetics* *130*, 555-568.
- Song, Z., McCall, K., and Steller, H. (1997). DCP-1, a *Drosophila* cell death protease essential for development. *Science* *275*, 536-540.
- Srinivasula, S. M., Datta, P., Kobayashi, M., Wu, J. W., Fujioka, M., Hegde, R., Zhang, Z., Mukattash, R., Fernandes-Alnemri, T., Shi, Y., *et al.* (2002). *sickle*, a novel *Drosophila* death gene in the *reaper/hid/grim* region, encodes an IAP-inhibitory protein. *Curr Biol* *12*, 125-130.
- Stark, A., Brennecke, J., Russell, R. B., and Cohen, S. M. (2003). Identification of *Drosophila* MicroRNA targets. *PLoS Biol* *123*, 1133-1146.
- Stocker, H., Andjelkovic, M., Oldham, S., Laffargue, M., Wymann, M. P., Hemmings, B. A., and Hafen, E. (2002). Living with lethal PIP3 levels: viability of flies lacking PTEN restored by a PH domain mutation in Akt/PKB. *Science* *295*, 2088-2091.
- Sulis, M., and Parsons, R. (2003). PTEN: from pathology to biology. *Trends Cell Biol* *13(9)*, 478-483.
- Suzuki, K., Kirisako, T., Kamada, Y., Mizushima, N., Noda, T., and Y., O. (2001). The pre-autophagosomal structure organized by concerted functions of APG genes is essential for autophagosome formation. *EMBO J* *20*, 5971-5981.
- Tapon, N., Harvey, K. F., Bell, D. W., Wahrer, D. C., Schiripo, T. A., Haber, D. A., and Hariharan, I. K. (2002). *salvador* promotes both cell cycle exit and apoptosis in *Drosophila* and is mutated in human cancer cell lines. *Cell* *110*, 467-478.
- Thomas, H. E., Stunnenberg, H. G., and Stewart, A. F. (1993). Heterodimerization of the *Drosophila* ecdysone receptor with retinoid X receptor and *ultraspiracle*. *Nature* *362*, 471-475.
- Thompson, B. J., and Cohen, S. M. (2006). The Hippo pathway regulates the bantam microRNA to control cell proliferation and apoptosis in *Drosophila*. *Cell* *126*, 767-774.

- Thompson, C. B. (1995). Apoptosis in the pathogenesis and treatment of disease. *Science* 267, 1456-1462.
- Thumm, M., Egner, R., Koch, B., Schlumpberger, M., Straub, M., Veenhuis, M., and Wolf, D. H. (1994). Isolation of autophagocytosis mutants of *Saccharomyces cerevisiae*. *FEBS Lett* 349, 275-280.
- Thummel, C. S. (1995). From embryogenesis to metamorphosis: the regulation and function of *Drosophila* nuclear receptor superfamily members. *Cell* 83, 871-877.
- Thummel, C. S. (1996). Flies on steroids - *Drosophila* metamorphosis and the mechanisms of steroid hormone action. *Trends in Genetics* 12, 306-310.
- Tsukada, M., and Ohsumi, Y. (1993). Isolation and characterization of autophagy-defective mutants of *Saccharomyces cerevisiae*. *FEBS Lett* 1-2, 169-174.
- Udan, R. S., Kango-Singh, M., Nolo, R., Tao, C., and Halder, G. (2003). Hippo promotes proliferation arrest and apoptosis in the Salvador/Warts pathway. *Nat Cell Biol* 5, 914-920.
- Urness, L. D., and Thummel, C. S. (1995). Molecular analysis of a steroid-induced regulatory hierarchy: the *Drosophila* E74A protein directly regulates *L71-6* transcription. *EMBO J* 14, 6239-6246.
- Vaux, D. L., Weissman, I. L., and Kim, S. K. (1992). Prevention of programmed cell death in *Caenorhabditis elegans* by human bcl-2. *Science* 258, 1955-1957.
- Vernooy, S. Y., Copeland, J., Ghaboosi, N., Griffin, E. E., Yoo, S. J., and Hay, B. A. (2000). Cell death regulation in *Drosophila*: conservation of mechanism and unique insights. *J Cell Biol* 150, F69-F75.
- Villa, P., Kaufmann, S. H., and Earnshaw, W. C. (1997). Caspases and caspase inhibitors. *Trends Biochem Sci* 22, 388-393.
- White, K., Grether, M. E., Abrams, J. M., Young, L., Farrell, K., and Steller, H. (1994). Genetic control of programmed cell death in *Drosophila*. *Science* 264, 677-683.
- White, K., Tahaoglu, E., and Steller, H. (1996). Cell killing by the *Drosophila* gene *reaper*. *Science* 271, 805-807.
- Willecke, M., Hamaratoglu, F., Kango-Singh, M., Udan, R., Chen, C. L., Tao, C., Zhang, X., and Halder, G. (2006). The fat cadherin acts through the hippo tumor-suppressor pathway to regulate tissue size. *Curr Biol* 16, 2090-2100.

- Wood, L., Parsons, D., and Vogelstein, B. (2007). The genomic landscapes of human breast and colorectal cancers. *Science* *318*(5853), 1108-1113.
- Woodard, C. T., Baehrecke, E. H., and Thummel, C. S. (1994). A molecular mechanism for the stage-specificity of the *Drosophila* prepupal genetic response to ecdysone. *Cell* *79*, 607-615.
- Wu, G., Chai, J., Suber, T. L., Wu, J. W., Du, C., Wang, X., and Shi, Y. (2000). Structural basis of IAP recognition by Smac/DIABLO. *Nature* *408*, 1008-1012.
- Wu, S., Huang, J., Dong, J., and Pan, D. (2003). hippo encodes a Ste-20 family protein kinase that restricts cell proliferation and promotes apoptosis in conjunction with salvador and warts. *Cell* *114*, 445-456.
- Wu, S., Liu, Y., Zheng, Y., Dong, J., and Pan, D. (2008). The TEAD/TEF family protein Scalloped mediates transcriptional output of the Hippo growth-regulatory pathway. *Dev Cell* *14*, 388-398.
- Wullschleger, S., Loewith, R., and Hall, M. N. (2006). TOR signaling in growth and metabolism. *Cell* *124*, 471-484.
- Xu, T., Wang, W., Zhang, S., Stewart, R. A., and Yu, W. (1995). Identifying tumor suppressors in genetic mosaics: the *Drosophila* lats gene encodes a putative protein kinase. *Development* *121*, 1053-1063.
- Yagi, R., Chen, L., Shigesada, K., Murakami, Y., and Ito, Y. (1999). A WW domain-containing yes-associated protein (YAP) is a novel transcriptional co-activator. *EMBO J* *18*(9), 2551-2562.
- Yao, T.-P., Segraves, W. A., Oro, A. E., McKeown, M., and Evans, R. M. (1992). *Drosophila ultraspiracle* modulates ecdysone receptor function via heterodimer formation. *Cell* *71*, 63-72.
- Yin, V. P., Thummel, C. S., and Bashirullah, A. (2007). Down-regulation of inhibitor of apoptosis levels provides competence for steroid-triggered cell death. *J Cell Biol* *178*, 85-92.
- Yoo, S. J., Huh, J. R., Muro, I., Yu, H., Wang, L., Wang, S. L., Feldman, R. M., Clem, R. J., Muller, H. A., and Hay, B. A. (2002). Hid, Rpr and Grim negatively regulate DIAP1 levels through distinct mechanisms. *Nat Cell Biol* *4*, 416-424.
- Zhang, L., Ren, F., Zhang, Q., Chen, Y., Wang, B., and Jiang, J. (2008). The TEAD/TEF family of transcription factor Scalloped mediates Hippo signaling in organ size control. *Dev Cell* *14*, 377-387.

Zhou, L., Song, Z., Tittel, J., and Steller, H. (1999). HAC-1, a *Drosophila* homolog of APAF-1 and CED-4, functions in developmental and radiation-induced apoptosis. *Mol Cell* *4*, 745-755.

Zou, H., Henzel, W. J., Liu, X., Lutschg, A., and Wang, X. (1997). Apaf-1, a human protein homologous to *C. elegans* CED-4, participates in cytochrome c-dependent activation of caspase-3. *Cell* *90*, 405-413.